



Published in final edited form as:

J Med Chem. 2015 August 13; 58(15): 5863–5888. doi:10.1021/acs.jmedchem.5b00423.

Bicyclic [3.3.0]-Octahydrocyclopenta[*c*]pyrrolo Antagonists of Retinol Binding Protein 4: Potential Treatment of Atrophic Age-Related Macular Degeneration and Stargardt Disease

Christopher L. Cioffi^{†,*}, Boglarka Racz[§], Emily E. Freeman[†], Michael P. Conlon[†], Ping Chen[†], Douglas G. Stafford[†], Daniel M. C. Schwarz[†], Lei Zhu[‡], Douglas B. Kitchen[‡], Keith D. Barnes[†], Nicoleta Dobri[§], Enrique Michelotti[#], Charles L. Cywin[○], William H. Martin[⊥], Paul G. Pearson^{||}, Graham Johnson^{||}, and Konstantin Petrukhin^{§,*}

[†]Department of Medicinal Chemistry, University Place, Rensselaer, New York 12144, United States

[‡]Computer Assisted Drug Discovery, AMRI, East Campus, 3 University Place, Rensselaer, New York 12144, United States

[§]Department of Ophthalmology, Columbia University Medical Center, New York, New York 10032, United States

^{||}iCuraVision LLC, 31194 La Baya Drive, Suite 101, Westlake Village, California 91362, United States

[⊥]WHM Consulting LLC, 111 Sterling City Road, Lyme, Connecticut 06371, United States

[#]National Institute of Mental Health, National Institutes of Health, Bethesda, Maryland 20892, United States

[○]National Institute of Neurological Disorders and Stroke, National Institutes of Health, Bethesda, Maryland 20892, United States

Abstract

Antagonists of retinol-binding protein 4 (RBP4) impede ocular uptake of serum all-*trans* retinol (**1**) and have been shown to reduce cytotoxic bisretinoid formation in the retinal pigment epithelium (RPE), which is associated with the pathogenesis of both dry age-related macular degeneration (AMD) and Stargardt disease. Thus, these agents show promise as a potential pharmacotherapy by which to stem further neurodegeneration and concomitant vision loss associated with geographic atrophy of the macula. We previously disclosed the discovery of a novel series of nonretinoid RBP4 antagonists, represented by bicyclic [3.3.0]-

*Corresponding Authors. (C.L.C.) Phone: 518-512-2955. christopher.cioffi@amrigoal.com., (K.P.) Phone: 212-305-9040. kep4@cumc.columbia.edu.

ASSOCIATED CONTENT

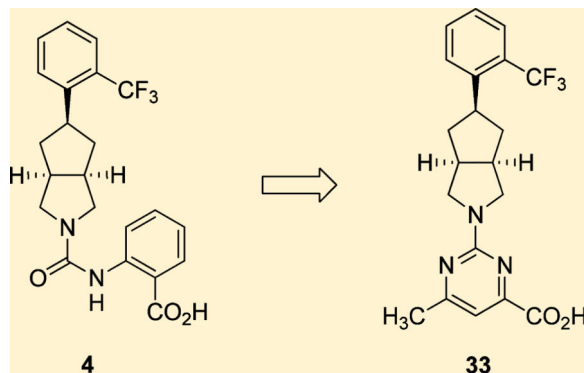
Supporting Information

In vivo protocols and ¹H NMR spectral data. The Supporting Information is available free of charge on the ACS Publications website at DOI: 10.1021/acs.jmedchem.5b00423.

The authors declare the following competing financial interest(s): C.L.C., N.D., E.E.F., M.P.C., P.C., L.Z., G.J., and K.P. are inventors on the patent applications for compounds disclosed in this paper that are assigned to The Trustees of Columbia University in the City of New York and licensed to iCura Vision. K.P., G.J., and P.G.P. are co-founders of iCura Vision.

octahydrocyclopenta[*c*]pyrrolo analogue **4**. We describe herein the utilization of a pyrimidine-4-carboxylic acid fragment as a suitable isostere for the anthranilic acid appendage of **4**, which led to the discovery of standout antagonist **33**. Analogue **33** possesses exquisite *in vitro* RBP4 binding affinity and favorable drug-like characteristics and was found to reduce circulating plasma RBP4 levels *in vivo* in a robust manner (>90%).

Graphical abstract



INTRODUCTION

Atrophic (dry) age-related macular degeneration (AMD) is a chronic and slowly progressing neurodegenerative ocular disorder that involves geographic atrophy of the central region of the retina called the macula.¹ Approximately 85% to 90% of reported cases of macular degeneration are of the atrophic form,¹ and this disorder is the leading cause of vision loss for individuals aged 60 years or older.² The dry AMD patient population is estimated at 11 million individuals in the US alone and is expected to double by 2020.³ Currently, there is no FDA-approved treatment available for patients suffering from this debilitating disease.

Accumulation of lipofuscin, a granular substance comprising cytotoxic bisretinoid fluorophores, in the retinal pigment epithelium (RPE) has been implicated as one of several pathogenic factors contributing to photoreceptor cell degeneration in the macula of dry AMD patients.⁴ In addition, dramatic retinal accumulation of lipofuscin is also believed to be the key etiological factor in autosomal recessive Stargardt disease, an untreatable and inherited form of juvenile-onset macular degeneration caused by genetic mutations in the *Abca4* gene. *Abca4* is a key component of the visual retinoid cycle, and this critical gene product loss is functionally recapitulated in the *Abca4*^{-/-} knockout mouse model.⁵ The best studied bisretinoid component of lipofuscin is *N*-retinide-*N*-retinylidene ethanolamine (A2E),⁴ⁱ a naturally occurring byproduct of the visual cycle derived from phosphatidylethanolamine and two molecules of all-*trans* retinal. A2E induces several toxic effects that may lead to the observed abnormalities in the dry AMD RPE.^{4h,6} Therefore, it is postulated that disruption or inhibition of *de novo* A2E formation in the RPE may provide a pharmacological intervention point by which to delay or retard the neurodegenerative processes associated with dry AMD and Stargardt disease.⁷ Currently, there are several agents in various stages of development that interfere with the visual cycle under clinical investigation for the treatment of dry AMD.^{3,8} We recently reported our initial efforts in this

field, which are based on the hypothesis that reduction of the ocular uptake of serum all-*trans* retinol (retinol, vitamin A) (**1**) (Figure 1) via reduction in circulating levels of serum retinol binding protein 4 (RBP4) can lead to a reduced rate of bisretinoid A2E accumulation in the retina.⁹

Retinol is transported systemically via a tertiary complex with RBP4 and transthyretin (TTR).¹⁰ Non-TTR complexed RBP4, a low molecular weight (21 kDa) lipocalin serum protein,¹¹ is rapidly cleared from the bloodstream through glomerular filtration. RBP4-TTR complexation is retinol dependent as apo-RBP4 interacts poorly with TTR.¹⁰ It was suggested that lower serum retinol levels achieved via inhibition of RBP4 would modulate the visual cycle, which is fueled by a constant delivery of retinol to the RPE by RBP4.¹² As a consequence of reduced retinol supply to fuel the visual cycle, the rate of bisretinoid formation in the RPE would be slowed or halted and the concomitant progression of geographic atrophy within the dry AMD retina would be retarded.^{7a} Indeed, this hypothesis is supported by preclinical and clinical data obtained for the retinoid-based RBP4 antagonist fenretinide (**2**). In preclinical studies, fenretinide also lowered circulating plasma RBP4 levels *in vivo*^{7a,13} and significantly reduced the accumulation of lipo-fuscin bisretinoids in the *Abca4*^{-/-} mouse model of enhanced retinal lipofuscinogenesis.^{7a} In extended clinical studies, fenretinide lowered serum RBP4 levels and reduced the rate of the geographic atrophy growth in a subset of the treated AMD patients wherein an approximate 70% (or greater) reduction in circulating serum RBP4 levels was achieved.¹⁴

We have shown that chronic oral administration of the nonretinoid RBP4 antagonist A1120 (**3**) (previously developed by Amgen for the potential treatment of diabetes)¹⁵ reduced the accumulation of lipofuscin bisretinoids by approximately 50% in the *Abca4*^{-/-} mouse model of enhanced retinal lipo-fuscinogenesis.¹⁶ This reduction was correlated with a 75% reduction in serum RBP4.¹⁶ In our more recent report,⁹ we described medicinal chemistry efforts conducted in the pursuit of designing novel nonretinoid RBP4 antagonists that utilized **3** as a rational design starting point. Compound **3** exhibits favorable RBP4 binding affinity and provided several key structural elements that allowed for rapid structure-activity relationship (SAR) exploration. However, the compound suffers from poor human liver microsomal (HLM) stability (~3% remaining after 30 min incubation), which was a major liability that needed to be addressed. Thus, our goal was to develop novel chemical matter with improved drug-like characteristics relative to **3**, and our efforts led to the discovery of the novel bicyclic [3.3.0]-octahydrocyclopenta[*c*]pyrrolo RBP4 antagonist **4**.⁹ Analogue **4** possesses a favorable balance of suitable *in vitro* RBP4 binding (scintillation proximity assay (SPA)) and functional RBP4-TTR interaction antagonist (HTRF) activity with significantly improved HLM stability (100% remaining after a 30 min incubation). Furthermore, **4** possesses good pharmacokinetic (PK) and pharmacodynamic (PD) properties, leading to robust and sustained lowering (>85%) of serum RBP4 levels in both acute and chronic rodent oral dosing studies.⁹

We sought to build upon our reported SAR efforts by further exploring the anthranilic acid appendage of **3** and compound **4**. Specifically, we wished to investigate whether a pyrimidine-4-carboxylic acid could provide a suitable isostere for the amide of **3** while still presenting the acid group as a favorable interaction. Pyrimidine reduces the number of

rotatable bonds and was expected to lead to improved RBP4 binding affinity (Figure 2). Our overarching goal was to further enhance the *in vitro* and *in vivo* RBP4 potency observed for **4** while maintaining its excellent microsomal stability and other favorable drug-like characteristics. Guided by our RBP4 computational docking models,⁹ we initially designed and synthesized illustrative examples containing alternative cores that link together the *ortho*-trifluoromethylphenyl moiety of **3** and **4** with the newly proposed 6-methylpyrimidine-4-carboxylic acid fragment. We subsequently explored the SAR of the pyrimidine-4-carboxylic acid appended to the bicyclic [3.3.0]-octahydrocyclopenta[*c*]-pyrrolo core featured in compound **4**. Lastly, we also included within our test set a focused series of bicyclic [3.3.0]-octa-hydrocyclopenta[*c*]pyrrolo core analogues bearing a 6-methylpyrimidine-4-carboxylic acid fragment in conjunction with variable aryl head groups.

CHEMISTRY

The synthesis of 6-methyl-2-(4-(2-(trifluoromethyl)phenyl)-piperidin-1-yl)pyrimidine-4-carboxylic acid (**10**) is presented in Scheme 1.^{9,17} Addition of the lithium salt of 1-bromo-2-(trifluoromethyl)benzene (**5**) to 1-benzylpiperidin-4-one gave tertiary alcohol **6**, which was readily dehydrated in the presence of thionyl chloride to furnish tetrahydropyridine **7**. Reduction of the olefin of **7** with concomitant *N*-benzyl deprotection using ammonium formate and 10% Pd/C followed by exposure to HCl provided piperidine hydrochloride salt **8**. Treatment of **8** with methyl 2-chloro-6-methylpyrimidine-4-carboxylate in the presence of *i*-Pr₂NEt in DMF at 60 °C afforded methyl ester **9**, which underwent facile saponification with LiOH·H₂O. Acidification afforded carboxylic acid **10** in good yield.

The synthesis of 6-methyl-2-(4-(2-(trifluoromethyl)phenyl)-piperazin-1-yl)pyrimidine-4-carboxylic acid (**14**) is highlighted in Scheme 2. A palladium-catalyzed amination reaction between 1-bromo-2-(trifluoromethyl)benzene (**5**) and *tert*-butyl piperazine-1-carboxylate afforded aryl piperazine **11**, which underwent smooth Boc-deprotection in the presence of HCl to provide piperazine hydrochloride **12**. Treatment of **12** with methyl 2-chloro-6-methylpyrimidine-4-carboxylate gave ester **13**, which underwent saponification in the presence of LiOH·H₂O to give upon acidification the desired carboxylic acid **14**.

The synthesis of 6-methyl-2-((3*aR*,6*aS*)-5-(2-(trifluoromethyl)-phenyl)hexahydropyrrolo[3,4-*c*]pyrrol-2(1*H*)-yl)pyrimidine-4-carboxylic acid (**18**) is depicted in Scheme 3. Palladium-catalyzed amination of 1-bromo-2-(trifluoromethyl)benzene (**5**) with (3*aR*,6*aS*)-*tert*-butyl hexahydropyrrolo[3,4-*c*]pyrrole-2(1*H*)-carboxylate provided intermediate **15**, which underwent HCl-mediated Boc-deprotection to give amine hydrochloride **16**. Treatment of **16** with methyl 2-chloro-6-methylpyrimidine-4-carboxylate gave the corresponding methyl ester **17**, which was hydrolyzed with LiOH·H₂O and then acidified to afford carboxylic acid **18** in good yield.

Construction of the [3.3.0]-octahydrocyclopenta[*c*]pyrrolo series of analogues **32–36** was achieved following our previously reported route (Scheme 4).^{9,18} LiAlH₄ reduction of commercially available dione **19** and subsequent *N*-Boc protection of the resulting secondary amine gave tetrahydroisoindole **20** in good yield. NaIO₄ and RuO₂·H₂O promoted oxidative cleavage of **20** gave ring-opened diacid **21**, which underwent Dieckman

condensation with concomitant decarboxylation in acetic anhydride at 120 °C to give ketone **22**. Ketone **22** was converted to the corresponding racemic triflate (\pm)-**23** in the presence of 1,1,1-trifluoro-*N*-phenyl-*N*-((trifluoromethyl)sulfonyl)methanesulfonamide. Intermediate (\pm)-**23** underwent facile Suzuki Pd-catalyzed cross-coupling with (2-(trifluoromethyl)phenyl)-boronic acid conversion to give styrene (\pm)-**24**. Catalytic reduction of (\pm)-**24** was conducted under 40 psi H₂ in the presence of 10% Pd/C in CH₃OH and exclusively provided *endo*-product **25**. HCl-induced Boc-deprotection of **25** followed by reaction with a corresponding 6-substituted 2-chloropyrimidine-4-carboxylic acid methyl ester afforded analogues **27–31**. Methyl esters **27–31** were subsequently hydrolyzed and acidified to the corresponding acids **32–36**.

The preparation of *exo*-analogue **40** was achieved via our previously reported route, which is shown in Scheme 5.^{9,18} Reduction of *des*-Boc olefin (\pm)-**37** provided a mixture of *endo*- and *exo*-isomers **38** and **39**, which were isolated via reversed phase column chromatography. Treatment of *exo*-amine **39** with methyl 2-chloro-5-methylpyrimidine-4-carboxylate followed by saponification with 2 N NaOH and subsequent acidification provided the desired *exo*-acid **40**.

Pyrimidine analogues **41–44** were accessed via intermediate **26** (Scheme 6). Compound **41** was furnished via a palladium-catalyzed amination of 2,4-dichloro-5,6-dimethylpyrimidine with **26**, followed by carbonylation with Mo(CO)₆ and subsequent saponification of the resulting methyl ester. Treatment of **26** with methyl 2-chloro-5-methylpyrimidine-4-carboxylate followed by hydrolysis and acidification gave acid **42**. Analogues **43** and **44** were prepared via treatment of **26** with either methyl 2-chloro-4-methylpyrimidine-5-carboxylate or methyl 2-chloro-5-methylpyrimidine-4-carboxylate followed by saponification and acidification of the corresponding methyl esters.

The preparation of the carboxylic acid isosteres carboxamide **46** and tetrazole **47** are depicted in Scheme 7. Treatment of **26** with 2-chloro-6-methylpyrimidine-4-carbonitrile provided nitrile intermediate **45**, which was hydrolyzed with LiOH·H₂O in THF and H₂O at 70 °C to provide carboxamide **46**. Nitrile **45** also underwent cycloaddition with NaN₃ to furnish tetrazole **47** in good yield.

A series of diverse analogues (**48–54**) designed to further explore pyrimidine carboxylic acid SAR is shown in Scheme 8. The corresponding substituted chloro or bromo-substituted picolinic, nicotinic, isonicotinic, or benzoic acid methyl esters were aminated with amine **26** using a combination of either Pd(OAc)₂ or Pd₂(dba)₃ and ligands XantPhos or JohnPhos in the presence of Cs₂CO₃ in refluxing toluene or 1,4-dioxane. The intermediary methyl esters were subsequently hydrolyzed and acidified to give the corresponding acid analogues **48–54**.

The syntheses of alternative heteroaromatic analogues **55–57** are highlighted in Scheme 9. Methyl 6-chloropyrazine-2-carboxylate, methyl 6-chloropyridazine-4-carboxylate, and methyl 2-chloro-5-methylthiazole-4-carboxylate were independently reacted with amine **26** in the presence of either Et₃N or *i*-Pr₂N₂Et in DMF at 60 °C followed by saponification of the resulting intermediary methyl esters with LiOH·H₂O and acidification to provide analogues **55**, **56**, and **57**, respectively.

The synthesis of a series of analogues possessing varied aryl head groups (**61–66**) is depicted in Scheme 10. Palladium-catalyzed Suzuki cross-coupling of triflate (\pm)-**23** with the appropriately substituted aryl boronic acids provided the corresponding styrene intermediates represented by (\pm)-**58a–f** in good yield. Hydrogenation of the olefins followed by HCl-promoted Boc-deprotection afforded the *endo*-amine hydrochloride intermediates **60a–f**. Treatment of these secondary amines with 2-methyl 2-chloro-6-methylpyrimidine-4-carboxylate followed by hydrolysis and acidification of the corresponding methyl esters provided the desired acids **61–66**.

RESULTS AND DISCUSSION

Computational docking of an initial proposed set of 6-methyl-pyrimidine-4-carboxylic acid ligands was conducted within our model derived from the cocrystal structure of **3** bound to RBP4 (PDB code: 3fmz)¹⁵ using standard precision (SP) mode. The docked poses were then refined using the extra precision (XP) mode of Glide (version 5.8, Schrödinger, LLC.). These docked poses of the proposed ligands were minimized within the binding site of the **3fmz** model. All molecular mechanics (MM) minimization used Impact (version 5.8, Schrodinger, LLC).

We modified the binding site by incorporating a structural water molecule within the anthranilic acid binding region of **3fmz**. Several reported RBP4 crystal structures show two water molecules (W1 and W2) housed within the anthranilic acid region of the RBP4 binding site, where they are engaged in H-bond interactions with Arg121, Gln98, and Tyr90. However, **3fmz** is devoid of these water molecules likely because the region is surface exposed, and the solvent is likely quite mobile. However, our docking and minimization procedures would be less accurate if a solvent hole were left in this fairly polar portion of the site. Therefore, to account for partially structured water molecules, we added structural waters from other RBP4 crystal structures. When the structural water W2 of *Ifel* (RBP4 cocrystallized with fenretinide) was minimized within **3fmz**, strong H-bond interactions among it, compound **3**, and Arg121 were observed (data not shown). This observation suggests that structural water W2 could be playing a critical role in the binding of **3** to RBP4. Therefore, we have incorporated this structural water within our **3fmz** docking model so as to ensure that any key differences with regard to critical H-bond interactions are observed for all newly proposed analogues and so that ligand poses do not fill a nonexistent hole.

As previously reported, the functional antagonist activity observed for **3** is attributed to conformational changes it induces in RBP4 loops β 3- β 4 and β 5- β 6.^{9,15} These changes block complex formation with TTR, leading to reduced RBP4 plasma levels as a result of increased glomerular excretion of the uncomplexed protein. The anthranilic carboxylic acid fragment of **3** is positioned at the opening of the RBP4 binding cavity where it is engaged in several key binding interactions; the carboxamido carbonyl oxygen atom of **3** accepts an H-bond from the backbone of Leu37, and the carboxylic acid forms a salt bridge with Arg121 and two H-bonds with Tyr90 and Gln98.^{9,15} These key interactions are potentially playing critical roles in inducing and stabilizing the conformational changes observed within the aforementioned RBP4 loops. To see if the 6-methylpyrimidine-4-carboxylic acid moiety

could provide a suitable isosteric replacement for the anthranilic acid, we initially conducted a *3fmz* docking overlay of **3** with proposed comparator **10**. Indeed, analogue **10** presented a similar docking geometry relative to that of **3** (Figure 3); both compounds are shown extending through the β -barrel core of the RBP4 binding cavity with their respective *ortho*-trifluoromethylphenyl fragments projecting into the internal lipophilic β -ionone pocket. The overlays also show the carboxylic acid moieties of both compounds positioned within close proximity to one another and engaged in the same key H-bond interactions with Arg121, Gln98, and Tyr90. It should be noted that the geometry of the pyrimidine moiety suggests the unexpected replacement of the H-bond donor amide with the H-bond acceptor pyrimidine. The geometry shown in Figure 3B likely induces some very interesting protonation states among the acid group, Tyr90, Arg121, the modeled water molecule, and the pyrimidine, likely stabilized by Gln98. The movement of Gln98 to this region appears to be a driving force for the blocking motion of loops β 3- β 4 and β 5- β 6. These conformations are significantly different (2.7 Å) from those in the fenretinide antagonist structure *Ifel*. Buoyed by the favorable geometric alignment observed in this docking experiment, we sought to synthesize compound **10** and other similar analogues that contain alternative cores linking together the *ortho*-trifluoro-methylphenyl and 6-methylpyrimidine-4-carboxylic acid fragments. Acknowledging our previous success with the bicyclic [3.3.0]-octahydrocyclopenta[*c*]pyrrole core used to generate the aforementioned RBP4 antagonist **4**,⁹ we ensured that this core scaffold was included within our initial sample set of analogues.

***In Vitro* Binding of Compounds to RBP4**

Analogue binding affinities for RBP4 were measured using our previously described scintillation proximity assay (SPA).¹⁶ Nonlinear regression analysis conducted following saturation binding of retinol to RBP4 revealed a K_d of 62.5 nM in our assay conditions, which is in line with the previously reported 70–190 nM range of values.^{10d,19} For compound characterization, we measured the competitive displacement of radiolabeled retinol added to the reaction mix at 10 nM which roughly corresponds to the generally recommended 1/10 of the K_d concentration of radioligand. The IC_{50} values were calculated from the 12-point compound titrations using a four-parameter logistic equation. Compounds with appreciable RBP4 binding potency (generally, with $IC_{50} < 150$ nM) were further assessed for the ability to antagonize the retinol-dependent RBP4-TTR interaction using the HTRF assay.¹⁶

Assessment of Antagonistic Activity in the HTRF RBP4-TTR Interaction Assay

The ability of an analogue to disrupt the retinol-induced interaction of RBP4 with TTR was examined using the previously described HTRF assay¹⁶ that probes retinol-dependent RBP4-TTR interaction. We used bacterially expressed maltose binding protein (MBP)-tagged RBP4 and commercially available TTR labeled directly with Eu^{3+} cryptate along with a d2-conjugated anti-MBP monoclonal antibody in order to implement this assay. Retinol added to the reaction mix at 1 μ M concentration stimulates RBP4-TTR interaction which brings europium in close proximity to the d2 dye with the following fluorescence energy transfer (FRET) to d2. The FRET signal, measured as a 668 nm emission, was normalized using the 620 nm europium emission to compensate for the pipetting and

dispensing errors. Following a 12-point dose titration (20 μ M-0.1 nM), the IC₅₀ values were calculated using a standard four parameter logistic nonlinear regression model equation. In order to monitor a correlation between the binding affinity of compounds for RBP4 and their potency as antagonists of the retinol-dependent RBP4-TTR interaction, we tracked a ratio of IC₅₀ values in the HTRF and SPA assays. Despite the difference in binding potency, for the majority of analogues, this ratio tended to be within the 5–20 range.

Structure–Activity Relationships

An initial series of analogues containing both the 6-methylpyrimidine-4-carboxylic acid and corresponding methyl ester moieties were prepared with the following core structures; piperidine (**9** and **10**), piperazine (**13** and **14**), bicyclic [3.3.0]-octahydropyrrolo[3,4-*c*]pyrrole (**17** and **18**), and bicyclic [3.3.0]-octahydrocyclopenta-*[c]*pyrrole (**28** and **33**). The RBP4 SPA binding affinity, HTRF functional antagonist activity, and microsomal stability data for these new analogues is shown in Table 1. Notably, the most direct comparator of **3**, analogue **10**, exhibited similar *in vitro* RBP4 binding affinity and functional antagonist activity (RBP4 SPA IC₅₀ = 35.3 nM; RBP4 HTRF IC₅₀ = 188 nM), verifying that the 6-methylpyrimidine-4-carboxylic acid fragment was indeed a suitable isostere for anthranilic acid. Interestingly, the pyrimidine-4-carboxylic acid of **10** also conferred the additional benefit of significantly improving human liver microsomal stability (68% remaining after 30 min incubation) relative to that of **3**. The corresponding methyl ester of **10** (**9**) was found to be ~3-fold more potent than **3**, and the remaining methyl esters **13**, **17**, and **28** also exhibited appreciable *in vitro* RBP4 potency in both assays. However, methyl esters **13** and **28** suffered from extensive degradation in the presence of human (HLM) and rat (RLM) liver microsomes. Piperazine acid analogue **14** was less potent than **3** (RBP4 SPA IC₅₀ = 89.5 nM; RBP4 HTRF IC₅₀ = 511 nM), and it presented only a modest improvement in HLM stability, whereas bicyclic [3.3.0]-octahydropyrrolo[3,4-*c*]pyrrole **18** was slightly more potent and exhibited better HLM stability. Incorporation of the bicyclic [3.3.0]-octahydrocyclopenta-*[c]*pyrrole core provided standout analogue **33**, which exhibited significantly improved *in vitro* RBP4 potency (RBP4 SPA IC₅₀ = 12.8 \pm 0.4 nM; RBP4 HTRF IC₅₀ = 43.6 \pm 10.5 nM) and excellent microsomal stability. Subsequent docking analysis of **33** revealed favorable alignment within the RBP4 binding cavity (Figure 4). The 6-methylpyrimidine-4-carboxylic acid appendage of **33** is engaged in key H-bond interactions as the bicyclic [3.3.0]-octahydrocyclopenta-*[c]*pyrrolo core extends through the β -barrel channel and projects the *ortho*-trifluoromethylphenyl ring slightly farther into the lipophilic hydrophobic β -ionone cavity than **3**. We postulate that the excellent RBP4 potency observed for **33** potentially results from two possible factors (or a combination thereof): (1) more favorable van der Waals interactions resulting from the deeper extension and optimal angle of projection of the *ortho*-trifluoromethylphenyl ring into the lipophilic β -ionone cavity and/or (2) more fortified key H-bond interactions due to increased rotational restriction of the 6-methylpyrimidine-4-carboxylic acid relative to the anthranilic acid of **3** and **4** (two fewer rotatable bonds). In addition, the *exo*-isomer **40** was also prepared and found to be devoid of RBP4 activity (SPA IC₅₀ > 3 μ M, data not shown). The RBP4 activity differences observed between potent *endo*-isomer **33** and inactive *exo*-isomer **40** were consistent with our previously reported findings for these geometric isomers of this scaffold

class.⁹ The results obtained from this initial sample set of probe compounds prompted us to further explore the SAR of analogue **33**.

The SAR of the 6-methylpyrimidine-4-carboxylic acid region of analogue **33** is summarized in Table 2. Initial efforts within Table 2 focused on examining the impact on potency of incorporating various chemotypes at the 6-position of the pyrimidine-4-carboxylic acid ring. Limited exploration of this region revealed that the size of the substituent was important and that *in vitro* binding affinity and functional antagonist activity trends do not generally correlate. For example, removal of the 6-methyl group of analogue **33** to furnish **32** led to a ~2-fold diminishment in potency in both the SPA (RBP4 SPA IC₅₀ = 20.8 ± 0.5 nM) and HTRF (RBP4 HTRF IC₅₀ = 79.7 nM) assays. However, when a trifluoromethyl group was introduced to the 6-position (**34**), the SPA binding affinity was recovered (RBP4 SPA IC₅₀ = 9.6 nM), yet HTRF potency remained roughly 2-fold lower (RBP4 HTRF IC₅₀ = 88.0 nM). Introduction of the larger isopropyl group (**36**) led to a significant diminishment in potency relative to that of **33**, which may be indicative of a size/steric tolerability limit in that region of the binding space. In addition, there was no differentiation between substituents possessing electron-donating or electron-withdrawing character, as trifluoromethyl analogue **34** and methoxy analogue **35** exhibited similar binding affinity. The incorporation of an additional methyl group at the 5-position to give 5,6-dimethyl analogue **41** resulted in a 5-fold decrease in potency, and monosubstitution of a methyl group at the 5-position (**42**) led to a further diminishment in potency. These data suggest that the most potent analogues of this series require one substituent of limited size to be positioned *meta* to the pyrimidine-4-carboxylic acid and that substitution *ortho* to the carboxylic acid is disfavored. We also examined the impact of repositioning the carboxylic acid of **33** from the 4- to the 5-position on the pyrimidine ring. Interestingly, analogues **43** and **44** were tolerated and exhibited appreciable binding affinity (RBP4 SPA IC₅₀ = 40.8 nM and 171 nM, respectively); however, both analogues were significantly less potent than **33** in the HTRF assay (RBP4 HTRF IC₅₀ = 523 nM and 1864 nM, respectively). Lastly, primary carboxamide **46** and tetrazole **47** served as suitable carboxylic acid isosteres within this series as both compounds displayed RBP4 binding affinities comparable to that of **33**. However, **46** and **47** were found to be significantly less potent in the HTRF assay (RBP4 HTRF IC₅₀ = 248 nM and 175 nM, respectively).

In parallel, we evaluated replacing the pyrimidine-4-carboxylic acid of **33** with picolinic, isonicotinic, nicotinic, and benzoic acid moieties (Table 3). 4-Methyl picolinic acid **48** and 2-methyl isonicotinic acid **49** exhibited binding affinities within a 5-fold range of **33**; however, they were both nearly 10-fold less potent in the HTRF assay (RBP4 HTRF IC₅₀ = 295 nM and 228 nM, respectively). In contrast, 3-methyl picolinic acid **50** was significantly less potent in both assays and the unsubstituted nicotinic acid **51** was devoid of RBP4 activity. Removal of all nitrogen atoms to furnish benzoic acid **52** provided an analogue with appreciable binding affinity yet was very weakly potent in the HTRF assay (RBP4 SPA IC₅₀ = 83.2 nM; RBP4 HTRF IC₅₀ = 3956 nM). These data suggest that while the methyl-substituted pyridine congeners of **33** (**48** and **49**) exhibit good binding affinity, both nitrogen atoms of pyrimidine **33** appear to be required for optimal functional antagonist activity in the HTRF assay. In addition, the positioning of a methyl group *ortho* to the carboxylic acid

within this pyridine series (**50**) had the same deleterious effect on SPA binding and HTRF potency that was observed for 5-methyl substituted pyrimidine analogue **42**. We next investigated the effect of repositioning the carboxylic acid adjacent to the bicyclic [3.3.0]-octahydrocyclopenta[*c*]pyrrolo core, as docking of nicotinic acid analogue **54** indicated favorable geometric alignment within the RBP4 binding cavity (Figure 5). Indeed, analogues **53** and **54** were tolerated and exhibited comparable SPA binding affinities relative to one another (RBP4 SPA IC₅₀ = 68.4 nM and 43.8 nM, respectively); however, **54** was found to be 5-fold more potent than **53** in the HTRF assay. Interestingly, the HTRF trend observed between nicotinic acids **53** and **54** suggests that substitution on this heteroaromatic system in a manner analogous to the 6-methyl group of pyrimidine **33** is not favorable with regard to functional antagonist activity. Lastly, we also pursued alternative heteroaromatic analogues pyrazine **55**, pyridazine **56**, and thiazole **57**. Of this set, pyridazine **56** and thiazole **57** were found to possess good binding affinity (RBP4 SPA IC₅₀ = 23.0 nM and 29.3 nM, respectively); however, both analogues were significantly less potent than benchmark **33** in the HTRF assay (RBP4 HTRF IC₅₀ = 437 nM and 495 nM, respectively).

We also probed the SAR associated with the aryl headgroup region of compound **33** with a focused set of substituted aromatic and heteroaromatic analogues that are shown in Table 4. 5-Fluoro-2-(trifluoromethyl)phenyl analogue **61** exhibited potency comparable to that of parent **33** (RBP4 SPA IC₅₀ = 46.3 ± 1.1 nM; RBP4 HTRF IC₅₀ = 33.4 ± 1.8 nM). In contrast, incorporation of a fluorine *ortho* to the trifluoromethyl group to give 3-fluoro-2-(trifluoromethyl)phenyl analogue **62** was not well tolerated and led to a 20-fold loss in SPA binding potency (RBP4 SPA IC₅₀ = 196 nM). Replacing the *ortho*-trifluoromethyl group of **61** and **62** with chlorine to give analogues **63** and **64** led to a precipitous drop in potency (SPA IC₅₀ = 532 ± 198 nM and 137 nM; HTRF IC₅₀ = 347 nM and 504 nM, respectively). Lastly, introduction of polarity by means of pyridine analogues **65** and **66** yielded appreciable SPA binding affinity; however, the compounds were weakly potent in the HTRF assay.

In light of the excellent RBP4 potency and robust microsomal stability observed for analogue **33**, the compound was selected for further *in vitro* and *in vivo* evaluation. The *in vitro* pharmacological profile is presented in Table 5. Compound **33** exhibited excellent kinetic solubility in phosphate buffered saline (PBS) (pH 7.4) and was classified as highly permeable in the MDR1-MDCK permeability assay. The observed CL_{int} values suggest very low predicted hepatic clearance, and the % plasma protein binding (PPB) data indicate low unbound fractions. Interestingly, unlike previously reported anthranilic acid analogue **4**, which exhibited significant CYP2C9 inhibitory activity (IC₅₀ = 340 nM),⁹ **33** was found to be clean in a standard CYP panel (all CYP IC₅₀ values >34 μM). Additional selectivity profiling revealed no significant off-target activity at the hERG channel or within a standard screening panel of fifty-five GPCRs, enzymes, ion channels, and transporters (data not shown). Lastly, **33** did not induce human PXR activation (data not shown).

***In Vivo* Activity: PK Characteristics of 33 in Rats**

Single dose PK studies conducted with Sprague–Dawley rats at 5.1 μmol/kg (2 mg/kg) IV and 18.2 μmol/kg (5 mg/kg) PO doses showed very low plasma clearance (5.06 mL/min/kg)

and a very long half-life of 22 h (Table 6). The compound was well absorbed and slowly eliminated from plasma after oral administration with an observed C_{\max} of 62.2 μM and corresponding T_{\max} at 2.67 h. Very high exposures were observed (AUC_{INF} was 3636 $\mu\text{M}\cdot\text{h}$) and the estimated % F exceeded 100%. The greater than 100% oral bioavailability may be related to the very low plasma clearance of **33** and some nonlinear pharmacokinetics over the 5.1 to 12.7 $\mu\text{mol}/\text{kg}$ dose range.

We also conducted a subsequent 7-day, subchronic rodent oral dosing PK–PD study with **33** (Figure 6). Sprague–Dawley rats received either a single 18.2 $\mu\text{mol}/\text{kg}$ (5 mg/kg) oral dose or a once daily (QD) 18.2 $\mu\text{mol}/\text{kg}$ oral dose of **33** over a period of 7-days. Blood was collected from the single dose-treated rats (Group 1) at predose, 15 and 30 min, and 1, 2, 4, 8, 12, 24, 36, and 48 h post dose on Day 1. Blood was collected from the 7-day QD dose-treated rats (Group 3) at predose (Days 1–6; for RBP4 biomarker analysis only) and predose, 15 and 30 min, and 1, 2, 4, 8, 12, 24, 36, and 48 h post-last dose on Day 7. A vehicle dose group (Group 2) was also included in the study and blood was collected on Days 1 and 7 as a control group for RBP4 biomarker analysis. The plasma exposure levels of **33** were high in all samples of Groups 1 and 3. On Day 1, compound **33** reached the peak concentration rapidly after dose administration and declined slowly thereafter (Figure 6, A). Mean plasma levels of **33** were approximately 20 μM at the 48 h time-point. As a result of the slow clearance of **33** from plasma, the mean predose plasma concentration on Day 7 was $148.1 \pm 58.2 \mu\text{M}$ (Figure 6B). After the administration of the seventh daily dose, the mean plasma level increased to $178.9 \pm 59.4 \mu\text{M}$ at the 4 h time-point (Figure 6A). At 48 h after this dose, the mean concentration of compound **33** remained high at $97.1 \pm 48.6 \mu\text{M}$. The PK parameters for the single and 7-day doses were also determined. The observed C_{\max} values were $66.5 \pm 23.6 \mu\text{M}$ with a T_{\max} of $2.75 \pm 2.17 \text{ h}$ and $183.1 \pm 55.2 \mu\text{M}$ with a T_{\max} of $2.17 \pm 1.76 \text{ h}$ on Days 1 and 7, respectively. Exposure levels based on AUC_{last} were $1697 \pm 279 \mu\text{M}\cdot\text{h}$ on Day 1 and $6385 \pm 2501 \mu\text{M}\cdot\text{h}$ on Day 7. The elimination phase $t_{1/2}$ values were calculated to be $31.9 \pm 17.7 \text{ h}$ and $49.4 \pm 17.7 \text{ h}$ for Day 1 and Day 7, respectively. Notably, plasma collected before the administration of the final dose on Day 7 contained approximately 150 μM of **33**, which is consistent with the observed long $t_{1/2}$ and suggests that steady state levels were achieved after 6 to 7 days of QD oral administration (Figure 6, B).

In Vivo Activity: PK–PD Correlations of Analogue 33

In order to establish the *in vivo* target engagement, provide proof of *in vivo* activity, and document PK–PD correlations, we studied the effect of single and 7-day dosing of **33** on the level of plasma RBP4 in rats. Aliquots of plasma samples collected during the PK experiments were used to analyze plasma RBP4 concentrations. After a single 18.2 $\mu\text{mol}/\text{kg}$ (5 mg/kg) oral dose of **33**, a maximum of 85% decrease in plasma RBP4 was observed (Figure 7, A), while the 7-day QD oral administration in rats at 18.2 $\mu\text{mol}/\text{kg}$ induced an approximately 95% reduction in plasma RBP4 (Figure 7, A). Comparison of the dynamics of RBP4 lowering in the compound **33**-treated animals with that of the vehicle-treated rats over 7 days of QD dosing confirmed the magnitude of the compound effect on the level of plasma RBP4 (Figure 7, B). The extent of the RBP4 lowering (Figure 7) shows a clear correlation with plasma compound levels (Figure 6). With regard to this effect, even though

the plasma protein binding of **33** is significant (rat 99.4%, Table 5), the high circulating plasma levels, long exposure, and very low clearance mean that the projected plasma free drug concentration of **33** significantly exceeds that required to antagonize RBP4/TTR interaction measured by either the SPA or HTRF binding assays (Table 4). Antagonists of the RBP4-TTR interaction from different structural classes had previously established the correlation among RBP4 lowering, serum retinol lowering, and bisretinoid reduction in the *Abca4*^{-/-} mouse model of Stargardt disease.^{7a,15} While we did not measure retinol lowering by **33** in our *in vivo* studies, it seemed reasonable to expect that **33** would reduce serum retinol and show the desired preclinical chronic efficacy in the *Abca4*^{-/-} mice given its pronounced RBP4-lowering activity (Figure 7) and the established correlations between levels of serum RBP4 and serum retinol.^{7a,15,20} This and additional data describing the nonrodent pharmacology of compound **33** will be published elsewhere.

CONCLUSIONS

We sought to investigate whether a 6-methylpyrimidine-4-carboxylic acid fragment could serve as a suitable isostere for the anthranilic acid moiety of **3** and the previously reported bicyclic [3.3.0]-octahydrocyclopenta[*c*]pyrrolo RBP4 antagonist **4** with the goal of further improving RBP4 potency and druglike characteristics. We initially investigated probe analogues (**10**, **14**, **18**, and **33**) that featured diverse cores in which the *ortho*-trifluoromethylphenyl headgroup of **3** and **4** was retained. Of this focused sample set of compounds, bicyclic [3.3.0]-octahydrocyclopenta[*c*]pyrrolo **33** emerged as a standout analogue exhibiting exquisite *in vitro* RBP4 potency (SPA IC₅₀ = 12.8 ± 0.4 nM and HTRF IC₅₀ = 43.6 ± 10.5 nM) and excellent *in vitro* microsomal stability. Follow-up analogues of **33** that explored the 6-methylpyrimidine-4-carboxylic acid region of the scaffold were subsequently pursued. Although these analogues displayed intriguing SAR trends, none of them proved to be better than **33** in terms of *in vitro* RBP4 potency. Concurrent with this campaign, SAR exploration of the aryl headgroup of **33** was also conducted. Similar to the aforementioned 6-methylpyrimidine-4-carboxylic acid SAR effort, the aryl headgroup campaign did not yield a more potent compound than **33**.

Analogue **33** was further evaluated *in vitro* and *in vivo* and was found to possess a favorable ADME profile, no limiting off-target *in vitro* pharmacology, and excellent PK characteristics. In addition, the compound induced a robust and sustained lowering (>90%) of serum RBP4 levels upon 7-day QD oral dosing studies conducted in rats. Taken collectively, these data suggest that compound **33** shows particular promise as a potential oral treatment for dry AMD and Stargardt disease.

EXPERIMENTAL SECTION

General Chemistry

All reactions were performed under a dry atmosphere of nitrogen unless otherwise specified. Indicated reaction temperatures refer to the reaction bath, while room temperature (rt) is noted as 25 °C. Commercial grade reagents and anhydrous solvents were used as received from vendors, and no attempts were made to purify or dry these components further. Removal of solvents under reduced pressure was accomplished with a Buchi rotary

evaporator at approximately 28 mmHg pressure using a Teflon-linked KNF vacuum pump. Thin layer chromatography was performed using 1" × 3" AnalTech No. 02521 silica gel plates with fluorescent indicator. Visualization of TLC plates was made by observation with short wave UV light (254 nm lamp), 10% phosphomolybdic acid in ethanol, or in iodine vapors. Preparative thin layer chromatography was performed using Analtech, 20 × 20 cm, 1000 μm preparative TLC plates. Flash column chromatography was carried out using a Teledyne Isco CombiFlash Companion Unit with RediSep Rf silica gel columns. If needed, products were purified by reverse phase chromatography, using a Teledyne Isco CombiFlash Companion Unit with RediSep Gold C18 reverse phase column. Proton NMR spectra were obtained either on a 300 MHz Bruker Nuclear Magnetic Resonance Spectrometer or on 500 MHz Bruker Nuclear Magnetic Resonance Spectrometer, and chemical shifts (δ) are reported in parts per million (ppm). Coupling constant (J) values are given in Hz, with the following spectral pattern designations: s, singlet; d, doublet; t, triplet; q, quartet; dd, doublet of doublets; m, multiplet; and br, broad. Tetramethylsilane was used as an internal reference. Melting points are uncorrected and were obtained using a MEL-TEMP electrothermal melting point apparatus. Mass spectroscopic analyses were performed using positive mode electron spray ionization (ESI) on a Varian ProStar LC-MS with a 1200L quadrupole mass spectrometer. High pressure liquid chromatography (HPLC) purity analysis was performed using a Varian Pro Star HPLC system with a binary solvent system A and B using gradient elution [A, H₂O with 0.05% trifluoroacetic acid (TFA); B, CH₃CN with 0.05% TFA] and a flow rate = 1 mL/min, with UV detection at 223 nm. All final compounds were purified to 95% purity, and these purity levels were measured by a Varian Pro Star HPLC system. The following Varian Pro Star HPLC methods were used to establish compound purity: (A) Phenomenex C18(2) column (3.0 × 250 mm); mobile phase, A = H₂O with 0.05% TFA and B = CH₃CN with 0.05% TFA; gradient, 0–90% B (0.0–20.0 min); UV detection at 254 nm. (B) Phenomenex C18(2) column (3.0 × 250 mm); mobile phase, A = H₂O with 0.05% TFA and B = CH₃CN with 0.05% TFA; gradient, 0–100% B (0.0–20 min); UV detection at 254 nm.

6-Methyl-2-(4-(2-(trifluoromethyl)phenyl)piperidin-1-yl)-pyrimidine-4-carboxylic Acid (10)

Step A: To a solution of 1-bromo-2-(trifluoromethyl)benzene (5, 35.0 g, 156 mmol) in THF (350 mL) cooled to –78 °C was slowly added a solution of *n*-BuLi (70.4 mL, 2.5 M in THF, 176 mmol) over a period of 15 min. The mixture stirred at –78 °C for 40 min was allowed to warm to 0 °C and then cooled back down to –78 °C. To this was added a solution of 1-benzylpiperidin-4-one (22.1 g, 117 mmol) in THF (80 mL) over a period of 10 min. The resulting mixture continued to stir at –78 °C for 2 h. The reaction was carefully quenched with aqueous, saturated aq NH₄Cl solution (500 mL), and the mixture was extracted with EtOAc (300 mL). The organic extract was washed with H₂O, brine, dried over Na₂SO₄, filtered, and concentrated under reduced pressure. The resulting residue was chromatographed over silica gel (Isco CombiFlash Companion unit, 330 g RediSep column, 0–30% EtOAc in hexanes) to give 1-benzyl-4-(2-(trifluoromethyl)phenyl)piperidin-4-ol (**6**) as a light-yellow oil (29.2 g, 74%): ¹H NMR (500 MHz, CDCl₃) δ 7.78 (d, J = 1.6 Hz, 1H), 7.59 (m, 1H), 7.47 (m, 1H), 7.36 (m, 5H), 7.31 (m, 2H), 3.58 (s, 2H), 2.80 (m, 2H), 2.55 (m, 2H), 2.27 (m, 2H), 1.88 (m, 2H); MS (ESI+) m/z 336 [M + H]⁺.

Step B: A 0 °C cooled solution of 1-benzyl-4-(2-(trifluoromethyl)-phenyl)piperidin-4-ol (**6**, 29.2 g, 87.1 mmol) in SOCl₂ (60 mL) was stirred for 2 h and was then diluted with CH₂Cl₂ (250 mL). The mixture was carefully poured into a saturated aq NaHCO₃ solution (200 mL). The biphasic mixture was separated, and the aqueous layer was further extracted with CH₂Cl₂ (400 mL). The combined organic layers were washed with brine, dried over Na₂SO₄, filtered, and concentrated. The resulting residue was chromatographed over silica gel (Isco CombiFlash Companion unit, 330 g RediSep column, 0–30% EtOAc in hexanes) to give 1-benzyl-4-(2-(trifluoromethyl)phenyl)-1,2,3,6-tetrahydropyridine (**7**) as a light-yellow oil (13.5 g, 49%): ¹H NMR (500 MHz, CDCl₃) δ 7.63 (d, *J* = 1.6 Hz, 1H), 7.48 (m, 1H), 7.39 (m, 5H), 7.28 (m, 2H), 5.56 (s, 1H), 0.68 (s, 2H), 3.14 (m, 2H), 2.70 (m, 2H), 2.39 (m, 2H); MS (ESI+) *m/z* 318 [M + H]⁺.

Step C: A mixture of 1-benzyl-4-(2-(trifluoromethyl)phenyl)-1,2,3,6-tetrahydropyridine (**7**, 13.6 g, 42.5 mmol), 10% Pd/C (3.0 g), and ammonium formate (26.8 g, 425 mmol) in CH₃OH (800 mL) was heated at reflux for 2 h. The mixture was cooled to rt and was filtered over Celite. The filtrate was concentrated, and the resulting residue was chromatographed over silica gel (Isco CombiFlash Companion unit, 330 g RediSep column, 0–10% CH₃OH with 1% NH₄OH in CH₂Cl₂) to give 4-(2-(trifluoromethyl)phenyl)piperidine as a colorless oil (2.0 g, 21%): ¹H NMR (500 MHz, CDCl₃) δ 7.61 (d, *J* = 1.7 Hz, 1H), 7.52 (m, 2H), 7.29 (m, 1H), 3.21 (m, 2H), 3.07 (m, 1H), 2.80 (m, 2H), 2.33 (bs, 1H), 1.77 (m, 4H); MS (ESI+) *m/z* 230 [M + H]⁺. To a solution of 4-(2-(trifluoromethyl)phenyl)piperidine (5.6 g, 24.5 mmol) in CH₃CN (30 mL) was added a 4 M solution of HCl in 1,4-dioxane (6.1 mL, 24.5 mmol) at rt. The mixture was stirred for 2 h and was then concentrated under reduced pressure to give 4-(2-(trifluoromethyl)-phenyl)piperidine hydrochloride (**8**) as a white solid (6.4 g, >99%): MS (ESI+) *m/z* 230 [M + H]⁺.

Step D: A mixture of 4-(2-(trifluoromethyl)phenyl)piperidine hydrochloride (**8**, 0.050 g, 0.19 mmol), methyl 2-chloro-6-methylpyr-imidine-4-carboxylate (0.046 g, 0.21 mmol), and *i*-Pr₂N⁺Et⁻ (0.04 mL, 0.23 mmol) in DMF (2 mL) was heated at 60 °C for 16 h. The reaction was concentrated under reduced pressure, and the resulting residue was chromatographed over silica gel (0% to 100% EtOAc in hexanes) to give methyl 6-methyl-2-(4-(2-(trifluoromethyl)phenyl)-piperidin-1-yl)pyrimidine-4-carboxylate (**9**) as an off-white solid (0.049 g, 68%): mp 109–112 °C; ¹H NMR (500 MHz, CDCl₃) δ 7.70–7.61 (m, 3H), 7.43 (m, 1H), 7.02 (s, 1H), 4.94 (m, 2H), 3.85 (s, 3H), 3.16 (m, 1H), 2.99 (m, 2H), 2.38 (s, 3H), 1.79–1.68 (m, 4H); MS (ESI+) *m/z* 380 [M + H]⁺; HPLC >99% (AUC), (Method A), *t*_R = 16.8 min.

Step E: A solution of methyl 6-methyl-2-(4-(2-(trifluoromethyl)-phenyl)piperidin-1-yl)pyrimidine-4-carboxylate (**9**, 0.049 g, 0.13 mmol) and LiOH·H₂O (0.030 g, 0.72 mmol) in THF (2 mL) and H₂O (2 mL) was stirred at rt for 16 h. The mixture was acidified to pH 5 with 2 N aq HCl and extracted with CH₂Cl₂ (3 × 10 mL). The combined organic extracts were washed with brine, dried over Na₂SO₄, filtered, and concentrated under reduced pressure to give 6-methyl-2-(4-(2-(trifluoromethyl)phenyl)piperidin-1-yl)pyrimidine-4-carboxylic acid (**10**) as an off-white solid (0.043 g, 91%): mp 166–169 °C; ¹H NMR (300 MHz, DMSO-*d*₆) δ 13.27 (bs, 1H), 7.70–7.61 (m, 3H), 7.43 (m, 1H), 6.99 (s, 1H), 4.98 (m,

2H), 3.13 (m, 1H), 2.98 (m, 2H), 2.37 (s, 3H), 1.75–1.72 (m, 4H); MS (ESI+) m/z 366 [M + H]⁺; HPLC >99% (AUC), (Method A), t_R = 15.1 min.

6-Methyl-2-(4-(2-(trifluoromethyl)phenyl)piperazin-1-yl)pyrimidine-4-carboxylic Acid (14)

Step A: To a mixture of *tert*-butyl piperazine-1-carboxylate (1.0 g, 5.37 mmol), 1-bromo-2-(trifluoromethyl)-benzene (5, 1.0 mL, 7.34 mmol), BINAP (0.135 g, 0.22 mmol), and NaO*t*-Bu (0.670 g, 6.57 mmol) in toluene (20 mL) was added Pd(OAc)₂ (0.024 g, 0.11 mmol). The mixture was heated at 110 °C for 16 h then allowed to cool to rt. The mixture was filtered over Celite, and the filter cake was washed with EtOAc. The filtrate was concentrated under reduced pressure, and the resulting residue was purified by flash column chromatography (Isco CombiFlash Rf unit, 40 g Gold RediSep column, 0%-100% EtOAc in hexanes) to give *tert*-butyl 4-(2-(trifluoromethyl)-phenyl)piperazine-1-carboxylate (**11**) as an off-white solid (1.63 g, 92%): ¹H NMR (300 MHz, CDCl₃) δ 7.64 (m, 1H), 7.55 (m, 1H), 7.33 (m, 1H), 7.21 (m, 1H), 3.57 (m, 4H), 2.88 (m, 4H), 1.48 (s, 9H); MS (ESI+) m/z 331 [M + H]⁺.

Step B: A solution of *tert*-butyl 4-(2-(trifluoromethyl)phenyl)-piperazine-1-carboxylate (**11**, 1.63 g, 4.93 mmol) and 2.0 M HCl in Et₂O (10 mL, 20 mmol) in CH₂Cl₂ (10 mL) was stirred at rt for 3 h. The mixture was concentrated under reduced pressure to provide 1-(2-(trifluoromethyl)phenyl)piperazine hydrochloride (**12**) as an off-white solid (1.23 g, 94%): ¹H NMR (300 MHz, DMSO-*d*₆) δ 9.18 (bs, 1H), 7.74 (m, 2H), 7.55 (m, 1H), 7.38 (m, 1H), 3.36 (m, 4H), 3.07 (m, 4H); MS (ESI+) m/z 231 [M + H]⁺.

Step C: A mixture of 1-(2-(trifluoromethyl)phenyl)piperazine hydrochloride (**12**, 0.100 g, 0.37 mmol), methyl 2-chloro-6-methyl-pyrimidine-4-carboxylate (0.076 g, 0.41 mmol), and *i*-Pr₂NEt (0.15 mL, 0.86 mmol) in DMF (3 mL) was heated at 60 °C for 16 h. The reaction was concentrated under reduced pressure, and the resulting residue was chromatographed over silica gel (0% to 100% EtOAc in hexanes) to give methyl 6-methyl-2-(4-(2-(trifluoromethyl)phenyl)piperazin-1-yl)pyrimidine-4-carboxylate (**13**) as an off-white solid (0.089 g, 63%): mp 103–106 °C; ¹H NMR (300 MHz, DMSO-*d*₆) δ 7.71–7.57 (m, 3H), 7.39 (m, 1H), 7.06 (s, 1H), 3.90 (m, 4H), 3.85 (s, 3H), 2.94 (m, 4H), 2.39 (s, 3H); MS (ESI+) m/z 381 [M + H]⁺; HPLC 98.9% (AUC), (Method A), t_R = 16.5 min.

Step D: A mixture of methyl 6-methyl-2-(4-(2-(trifluoromethyl)-phenyl)piperazin-1-yl)pyrimidine-4-carboxylate (**13**, 0.080 g 0.21 mmol) and LiOH·H₂O (0.050 g, 1.19 mmol) in THF (2 mL) and H₂O (2 mL) was stirred at rt for 16 h. The mixture was acidified to pH 5 with 2 N aq HCl and extracted with CH₂Cl₂ (3 × 10 mL). The combined organic extracts were washed with brine, dried over Na₂SO₄, filtered, and concentrated under reduced pressure to give 6-methyl-2-(4-(2-(trifluoromethyl)-phenyl)piperazin-1-yl)pyrimidine-4-carboxylic acid (**14**) as an off-white solid (0.043 g, 91%): ¹H NMR (300 MHz, DMSO-*d*₆) δ 13.53 (bs, 1H), 7.91–7.80 (m, 3H), 7.58 (m, 1H), 7.01 (s, 1H), 4.12 (m, 4H), 2.70 (m, 4H), 2.37 (s, 3H); MS (ESI+) m/z 367 [M + H]⁺; HPLC >99% (AUC), (Method A), t_R = 14.8 min.

6-Methyl-2-((3aR,6aS)-5-(2-(trifluoromethyl)phenyl)hexahydropyrrolo[3,4-c]pyrrol-2(1H)-yl)pyrimidine-4-carboxylic Acid (18)

Step A: To a mixture of (3aR,6aS)-tert-butyl hexahydropyrrolo[3,4-c]-pyrrole-2(1H)-carboxylate (1.0 g, 4.70 mmol), 1-bromo-2-(trifluoro-methyl)benzene (**5**, 1.0 mL, 7.34 mmol), BINAP (0.117 g, 0.19 mmol), and NaO*t*-Bu (0.587 g, 6.11 mmol) in toluene (10 mL) was added Pd(OAc)₂ (0.021 g, 0.10 mmol). The mixture was heated at 110 °C for 16 h then allowed to cool to rt. The mixture was filtered over Celite, and the filter cake was washed with EtOAc. The filtrate was concentrated under reduced pressure, and the resulting residue was purified by flash column chromatography (Isco CombiFlash Rf unit, 40 g Gold RediSep column, 0%-100% EtOAc in hexanes) to give (3aR,6aS)-tert-butyl 5-(2-(trifluoromethyl)phenyl)hexahydropyrrolo[3,4-c]pyrrole-2(1H)-carboxylate (**15**) as an off-white solid (1.35 g, 81%): ¹H NMR (300 MHz, CDCl₃) δ 7.61 (m, 1H), 7.46 (m, 1H), 7.17 (m, 1H), 7.02 (m, 1H), 3.70 (m, 2H), 3.38–3.28 (m, 4H), 3.14 (m, 2H), 2.93 (m, 2H); MS (ESI+) *m/z* 357 [M + H]⁺.

Step B: A solution of (3aR,6aS)-tert-butyl 5-(2-(trifluoromethyl)phenyl)hexahydropyrrolo[3,4-c]pyrrole-2(1H)-carboxylate (**15**, 1.37 g, 3.84 mmol) and 2.0 M HCl in Et₂O (10 mL, 20 mmol) in CH₂Cl₂ (10 mL) was stirred at rt for 3 h. The mixture was concentrated under reduced pressure to provide (3aR,6aS)-2-(2-(trifluoromethyl)phenyl)-octahydropyrrolo[3,4-c]pyrrole hydrochloride (**16**) as an off-white solid (0.968 g, 86%): ¹H NMR (300 MHz, CDCl₃) δ 9.18 (bs, 1H), 10.08 (bs, 1H), 9.56 (bs, 1H), 7.64 (m, 1H), 7.53 (m, 1H), 7.43 (m, 1H), 7.21 (m, 1H), 3.72 (m, 2H), 3.12 (m, 8H); MS (ESI+) *m/z* 257 [M + H]⁺.

Step C: A mixture of (3aR,6aS)-2-(2-(trifluoromethyl)phenyl)-octahydropyrrolo[3,4-c]pyrrole hydrochloride (**16**, 0.100 g, 0.34 mmol), methyl 2-chloro-6-methylpyrimidine-4-carboxylate (0.070 g, 0.38 mmol), and *i*-Pr₂NEt (0.1 mL, 0.46 mmol) in DMF (4 mL) was heated at 60 °C for 16 h. The reaction was concentrated under reduced pressure, and the resulting residue was chromatographed over silica gel (0% to 10% CH₃OH in CH₂Cl₂) to give methyl 6-methyl-2-((3aR,6aS)-5-(2-(trifluoromethyl)phenyl)hexahydropyrrolo[3,4-c]pyrrol-2(1H)-yl)-pyrimidine-4-carboxylate (**17**) as an off-white solid (0.039 g, 28%): ¹H NMR (300 MHz, DMSO-*d*₆) δ 7.60–7.51 (m, 3H), 7.34 (m, 1H), 7.08 (s, 1H), 3.87 (m, 5H), 3.47–3.38 (m, 4H), 3.14–3.07 (m, 4H), 2.37 (s, 3H); MS (ESI+) *m/z* 407 [M + H]⁺; HPLC >99% (AUC), (Method A), *t*_R = 19.1 min.

Step D: A mixture of 6-methyl-2-((3aR,6aS)-5-(2-(trifluoromethyl)phenyl)hexahydropyrrolo[3,4-c]pyrrol-2(1H)-yl)pyrimidine-4-carboxylate (**17**, 0.031 g, 0.076 mmol) and LiOH · H₂O (0.031 g, 0.74 mmol) in THF (2 mL) and H₂O (1 mL) was stirred at rt for 16 h. The mixture was acidified to pH 5 with 2 N aq HCl and extracted with CH₂Cl₂ (3 × 10 mL). The combined organic extracts were washed with brine, dried over Na₂SO₄, filtered, and concentrated under reduced pressure to give 6-methyl-2-(4-(2-(trifluoromethyl)phenyl)-piperazin-1-yl)pyrimidine-4-carboxylic acid (**18**) as an off-white solid (0.043 g, 91%): ¹H NMR (300 MHz, DMSO-*d*₆) δ 13.53 (bs, 1H), 7.61–7.58 (m, 2H), 7.34 (m, 1H), 7.10 (m, 1H), 6.99 (s, 1H), 3.86 (m, 2H), 3.47–3.35 (m, 4H), 3.14 (m, 4H),

2.36 (s, 3H); MS (ESI+) m/z 393 [M + H]⁺; HPLC 97.6% (AUC), (Method A), t_R = 16.8 min.

(3aR,5r,6aS)-5-(2-(Trifluoromethyl)phenyl)octahydrocyclopenta-[c]pyrrole Hydrochloride (26)

Step A (i): To a 0 °C cooled solution of LiAlH₄ in THF (1.0 M, 800 mL, 800 mmol) in THF (800 mL) was carefully added (3aR,7aS)-3a,4,7,7a-tetrahydro-1H-isoindole-1,3(2H)-dione (**19**, 53.7 g, 0.35 mol) portion-wise. An exotherm of ~5 °C occurred upon each addition of **19**. Upon complete addition, the mixture was allowed to warm to rt followed by heating at 70 °C for 16 h. The mixture was allowed to cool back to rt and then further cooled to 0 °C. The reaction was carefully quenched by slow addition of H₂O (30 mL), 15% aq NaOH solution (30 mL), followed by another bolus of H₂O (90 mL). The rate of quenching was done carefully so as to maintain an internal temperature below 25 °C. The mixture was stirred for 1 h and was filtered through Celite. The aqueous filtrate was extracted with Et₂O (2 × 100 mL), and the organic extracts were combined and concentrated under reduced pressure. The resulting residue was purified using a Kugelrohr distillation apparatus to give (3aR,7aS)-2,3,3a,4,7,7a-hexahydro-1H-isoindole as a clear, colorless oil (19.45 g, 44%): ¹H NMR (500 MHz, CDCl₃) δ 5.29 (s, 2H), 3.88 (bs, 1H), 3.26 (m, 2H), 2.82 (m, 2H), 2.41–2.19 (m, 4H), 1.96 (m, 2H).

Step B: To a 0 °C cooled solution of (3aR,7aS)-2,3,3a,4,7,7a-hexahydro-1H-isoindole (11.5 g, 93.5 mmol) in CH₂Cl₂ (200 mL) was added Boc₂O (24.5 g, 112 mmol) and the mixture stirred at rt for 16 h. The mixture was washed with H₂O (100 mL), brine (100 mL), dried over Na₂SO₄, filtered, and concentrated under reduced pressure. The residue was purified by flash column chromatography (Isco CombiFlash Rf unit, 330 g RediSep column, 0% to 30% EtOAc in hexanes) to give (3aR,7aS)-*tert*-butyl 3a,4,7,7a-tetrahydro-1H-isoindole-2(3H)-carboxylate (**20**) as an oil (20.10 g, 49%): ¹H NMR (500 MHz, CDCl₃) δ 5.64 (s, 2H), 3.39 (m, 2H), 3.20 (m, 2H), 3.15 (m, 2H), 2.23–2.19 (m, 4H), 1.97 (m, 2H), 1.57 (s, 9H).

Step C: To a 0 °C cooled mixture of (3aR,7aS)-*tert*-butyl 3a,4,7,7a-tetrahydro-1H-isoindole-2(3H)-carboxylate (**20**, 66.78 g, 224 mmol) in CH₃CN (600 mL), CCl₄ (400 mL), and H₂O (800 mL) was added NaIO₄ (192.3 g, 899 mmol) followed by RuO₂·H₂O (1.19 g, 8.94 mmol). The mixture was stirred at rt for 24 h with mechanical stirring and then filtered through Celite. The filter cake was washed with 10% CH₃OH in CH₂Cl₂ (200 mL), and the biphasic mother liquor was separated. The aqueous phase was further extracted with CH₂Cl₂ (3 × 150 mL), and the combined organic extracts were washed with H₂O (100 mL), brine (100 mL), dried over Na₂SO₄, filtered, and concentrated under reduced pressure. The residue was filtered through a plug of silica gel using a CH₃OH/CH₂Cl₂ eluent system (2%-10% CH₃OH in CH₂Cl₂). The filtrate was concentrated under reduced pressure to give 2,2'-((3S,4R)-1-(*tert*-butoxycarbonyl)pyrrolidine-3,4-diyl)diacetic acid (**21**) as a solid (46.75 g, 72%): ¹H NMR (500 MHz, DMSO-*d*₆) δ 12.2 (s, 2H), 3.38 (m, 2H), 3.02 (m, 2H), 2.49 (m, 2H), 2.32 (m, 2H), 2.29 (m, 2H), 1.42 (s, 9H).

Step D: To a suspension of 2,2'-((3S,4R)-1-(*tert*-butoxycarbonyl)-pyrrolidine-3,4-diyl)diacetic acid (**21**, 6.97 g, 24.31 mmol) in Ac₂O (50 mL) was added NaOAc (1.99 g,

24.31 mmol), and the mixture was heated at 120 °C for 3 h. The mixture was allowed to cool to rt and filtered through Celite. The filter cake was washed with Et₂O (5 × 50 mL), and the mother liquor was concentrated under reduced pressure. The resulting residue was purified by flash column chromatography (Isco CombiFlash Rf unit, 120 g RediSep column, 0%-30% EtOAc in hexanes) to give (3*aR*,6*aS*)-*tert*-butyl 5-oxohexahydro-cyclopenta[*c*]pyrrole-2(1*H*)-carboxylate (**22**) as a white foam (2.17 g, 40%): ¹H NMR (500 MHz, CDCl₃) δ 3.69 (m, 2H), 3.22 (m, 2H), 2.91 (m, 2H), 2.50 (m, 2H), 2.17 (m, 2H), 1.46 (s, 9H).

Step E: To a -78 °C cooled solution of (3*aR*,6*aS*)-*tert*-butyl 5-oxohexahydrocyclopenta[*c*]pyrrole-2(1*H*)-carboxylate (**22**, 22.35 g, 99.2 mmol) in THF (500 mL) was slowly added a solution of LiHMDS in THF (1.0 M, 129 mL). The mixture continued to stir at -78 °C for 30 min, then a solution of 1,1,1-trifluoro-*N*-phenyl-*N*-((trifluoromethyl)sulfonyl)methanesulfonamide (49.65 g, 139 mmol) in THF (150 mL) was slowly added. The mixture was stirred for an additional 1 h at -78 °C and was then allowed to stir at rt for 2 h. The mixture was concentrated under reduced pressure, and the residue was purified by flash column chromatography (Isco CombiFlash Rf unit, 330 g RediSep column, 0%-50% EtOAc in hexanes) to give (±)-(3*aS*,6*aS*)-*tert*-butyl 5-(((trifluoromethyl)sulfonyl)oxy)-3,3*a*,6,6*a*-tetrahydrocyclopenta[*c*]pyrrole-2(1*H*)-carboxylate ((±)-**23**) as a clear, viscous oil (1.56 g, quantitative): ¹H NMR (500 MHz, CDCl₃) δ 5.58 (s, 1H), 3.62 (m, 1H), 3.53 (m, 1H), 3.46 (m, 2H), 3.19 (m, 1H), 2.95 (m, 2H), 2.46 (m, 1H), 1.47 (s, 9H).

Step F: To an N₂ degassed mixture of (±)-(3*aS*,6*aS*)-*tert*-butyl 5-(((trifluoromethyl)sulfonyl)oxy)-3,3*a*,6,6*a*-tetrahydrocyclopenta[*c*]pyrrole-2(1*H*)-carboxylate ((±)-**23**, 14.79 g, 41.4 mmol), 2-trifluoromethylphenylboronic acid (19.70 g, 104 mmol), and a 2 M aqueous solution of Na₂CO₃ (250 mL) in DME (500 mL) was added Pd(PPh₃)₄ (4.80 g, 4.16 mmol). The mixture was heated at 80 °C for 6 h, then cooled to rt, and diluted with H₂O (500 mL). The aqueous mixture was extracted with EtOAc (2 × 200 mL), and the combined organic extracts were washed with H₂O (200 mL), brine (200 mL), dried over Na₂SO₄, filtered, and concentrated under reduced pressure. The residue was purified by flash column chromatography (Isco CombiFlash Rf unit, 330 g RediSep column, 0%-10% EtOAc in hexanes) to give (±)-(3*aR*,6*aS*)-*tert*-butyl 5-(2-(trifluoromethyl)-phenyl)-3,3*a*,6,6*a*-tetrahydrocyclopenta[*c*]pyrrole-2(1*H*)-carboxylate ((±)-**24**) as a clear, viscous oil (13.70 g, 94%): ¹H NMR (500 MHz, CDCl₃) δ 7.65 (m, 1H), 7.47 (m, 2H), 7.25 (m, 1H), 5.58 (s, 1H), 3.85–3.42 (m, 4H), 3.23 (m, 1H), 2.98 (m, 2H), 2.49 (m, 1H), 1.47 (s, 9H).

Step G: A mixture of (±)-(3*aR*,6*aS*)-*tert*-butyl 5-(2-(trifluoromethyl)-phenyl)-3,3*a*,6,6*a*-tetrahydrocyclopenta[*c*]pyrrole-2(1*H*)-carboxylate ((±)-**24**, 8.63 g, 24.41 mmol) and 10% Pd/C (1.57 g, wet, 10% w/w) in CH₃OH (50 mL) was subjected to an atmosphere of H₂ gas (40 psi) using a Parr Shaker apparatus at rt for 16 h. The mixture was filtered through Celite, and the filtrate was concentrated under reduced pressure. The resulting residue was purified by flash column chromatography (Isco CombiFlash Rf unit, 40 g RediSep column, 0%-30% EtOAc in hexanes) to give (3*aR*,5*r*,6*aS*)-*tert*-butyl 5-(2-(trifluoromethyl)-

phenyl)hexahydrocyclopenta[*c*]pyrrole-2(1*H*)-carboxylate (**25**) as a clear, viscous oil (0.910 g, 85%): ¹H NMR (500 MHz, CDCl₃) δ 7.69 (m, 1H), 7.51 (m, 2H), 7.25 (m, 1H), 3.49 (m, 5H), 2.75 (m, 2H), 2.92 (m, 2H), 1.52 (m, 2H), 1.48 (s, 9H).

Step H: To a 0 °C cooled solution of (3*aR*,5*r*,6*aS*)-*tert*-butyl 5-(2-(trifluoromethyl)phenyl)hexahydrocyclopenta[*c*]pyrrole-2(1*H*)-carboxylate (**25**, 7.94 g, 22.32 mmol) in CH₂Cl₂ (60 mL) was added a 2.0 M HCl solution in Et₂O (60 mL), and the mixture was allowed to stir at rt for 24 h. The mixture was diluted with Et₂O (200 mL), and the precipitated product was filtered to give (3*aR*,5*r*,6*aS*)-5-(2-(trifluoromethyl)phenyl)octahydrocyclopenta[*c*]pyrrole hydrochloride (**26**) as a white solid (5.90 g, 91%): ¹H NMR (500 MHz, CDCl₃) δ 10.17 (bs, 1H), 8.06 (m, 1H), 7.59 (m, 1H), 7.53 (m, 1H), 7.27 (m, 1H), 3.42 (m, 2H), 3.38 (m, 3H), 3.01 (m, 2H), 2.36 (m, 2H), 1.96 (m, 2H); MS (ESI+) *m/z* 256 [M + H]⁺.

Methyl 2-((3*aR*,5*r*,6*aS*)-5-(2-(trifluoromethyl)phenyl)hexahydrocyclopenta[*c*]pyrrol-2(1*H*)-yl)pyrimidine-4-carboxylate (27**)**

Step A: To a solution of (3*aR*,5*R*,6*aS*)-5-(2-(trifluoromethyl)phenyl)octahydrocyclopenta[*c*]pyrrole hydrochloride (**26**, 0.050 g, 0.17 mmol) and Et₃N (0.05 mL, 0.51 mmol) in DMF (10 mL) was added methyl 2-chloropyrimidine-4-carboxylate (0.029 g, 0.17 mmol), and the resulting solution was stirred at 60 °C for 16 h. The reaction was diluted with H₂O (200 mL) and extracted with EtOAc (3 × 100 mL). The combined organic extracts were washed with H₂O (3 × 100 mL), brine (100 mL), dried over Na₂SO₄, filtered, and concentrated under reduced pressure. The resulting residue was chromatographed over silica gel (0% to 30% EtOAc in hexanes) to give methyl 2-((3*aR*,5*r*,6*aS*)-5-(2-(trifluoromethyl)phenyl)hexahydrocyclopenta[*c*]pyrrol-2(1*H*)-yl)pyrimidine-4-carboxylate (**27**) as an off-white solid (0.055 g, 77%): MS (ESI+) *m/z* 392 [M + H]⁺.

Methyl 6-Methyl-2-((3*aR*,5*r*,6*aS*)-5-(2-(trifluoromethyl)phenyl)hexahydrocyclopenta[*c*]pyrrol-2(1*H*)-yl)pyrimidine-4-carboxylate (28**)**

Compound **28** was prepared according to a similar procedure described for the synthesis of **27**. ¹H NMR (300 MHz, CDCl₃) δ 7.61 (m, 1H), 7.58 (m, 2H), 7.23 (m, 1H), 7.05 (s, 1H), 3.95 (s, 3H), 3.82 (m, 4H), 3.59 (m, 1H), 2.92 (m, 2H), 2.44 (s, 3H), 2.40 (m, 2H), 1.69 (m, 2H); MS (ESI+) *m/z* 406 [M + H]⁺; HPLC >99% purity (Method C), *t*_R = 16.3 min.

Methyl 6-(trifluoromethyl)-2-((3*aR*,5*r*,6*aS*)-5-(2-(trifluoromethyl)phenyl)hexahydrocyclopenta[*c*]pyrrol-2(1*H*)-yl)pyrimidine-4-carboxylate (29**)**

Compound **29** was prepared according to a similar procedure described for the synthesis of **27**. MS (ESI+) *m/z* 460 [M + H]⁺.

Methyl 6-methoxy-2-((3*aR*,5*r*,6*aS*)-5-(2-(trifluoromethyl)phenyl)hexahydrocyclopenta[*c*]pyrrol-2(1*H*)-yl)pyrimidine-4-carboxylate (30**)**

Compound **30** was prepared according to a similar procedure described for the synthesis of **27**. MS (ESI+) *m/z* 422 [M + H]⁺.

Methyl 6-isopropyl-2-((3aR,5r,6aS)-5-(2-(trifluoromethyl)phenyl)-hexahydrocyclopenta[c]pyrrol-2(1H)-yl)pyrimidine-4-carboxylate (31)—

Compound **31** was prepared according to a similar procedure described for the synthesis of **27**. MS (ESI+) m/z 434 [M + H]⁺.

2-((3aR,5r,6aS)-5-(2-(Trifluoromethyl)phenyl)hexahydrocyclopenta[c]pyrrol-2(1H)-yl)pyrimidine-4-carboxylic Acid (32)

Step A: A solution of methyl 2-((3aR,5r,6aS)-5-(2-(trifluoromethyl)-phenyl)hexahydrocyclopenta[c]pyrrol-2(1H)-yl)pyrimidine-4-carboxylate (**27**, 0.050 g, 0.12 mmol) and 2 N aq NaOH (5 mL) in a 1:1 mixture of CH₃OH/THF (10 mL) stirred at rt for 16 h. The mixture was neutralized at 0 °C with 2 N aq HCl and extracted with CH₂Cl₂ (3 × 10 mL). The combined organic extracts were washed with brine, dried over Na₂SO₄, filtered, and concentrated under reduced pressure. The resulting residue was chromatographed over silica gel (0% to 10% CH₃OH in CH₂Cl₂) to give 2-((3aR,5r,6aS)-5-(2-(trifluoromethyl)-phenyl)hexahydrocyclopenta[c]pyrrol-2(1H)-yl)pyrimidine-4-carboxylic acid (**32**) as an off-white solid (0.044 g, 92%): mp 183–187 °C; ¹H NMR (300 MHz, DMSO-*d*₆) δ 8.56 (s, 1H), 7.71 (m, 1H), 7.65 (m, 2H), 7.39 (m, 1H), 7.06 (s, 1H), 3.73 (m, 2H), 3.64 (m, 2H), 3.43 (m, 1H), 2.86 (m, 2H), 2.30 (m, 2H), 1.64 (m, 2H); MS (ESI+) m/z 378 [M + H]⁺; HPLC >99% purity (Method A), t_R = 10.5 min.

6-Methyl-2-((3aR,5r,6aS)-5-(2-(trifluoromethyl)phenyl)-hexahydrocyclopenta[c]pyrrol-2(1H)-yl)pyrimidine-4-carboxylic Acid (33)—

Compound **33** was prepared according to a similar procedure described for the synthesis of **32**. Mp 129–131 °C; ¹H NMR (300 MHz, DMSO-*d*₆) δ 7.73 (m, 1H), 7.64 (m, 2H), 7.36 (m, 1H), 6.51 (s, 1H), 3.90 (s, 3H), 3.76 (m, 2H), 3.72 (m, 2H), 2.88 (m, 2H), 2.22 (m, 2H), 1.67 (m, 2H); ¹³C NMR (300 MHz, DMSO-*d*₆) δ 169.02, 166.47, 160.56, 157.04, 142.84, 132.72, 128.29, 127.09, 126.71, 126.34, 125.28, 125.19, 122.80, 107.82, 52.08, 42.65, 42.28, 41.19, 23.94; MS (ESI+) m/z 408 [M + H]⁺; HRMS (ESI+) for C₂₀H₂₁F₃N₃O₂ [M + H]⁺ calcd 392.1586, found 392.1570; HPLC >99% purity (Method A), t_R = 14.3 min.

6-(Trifluoromethyl)-2-((3aR,5r,6aS)-5-(2-(trifluoromethyl)phenyl)-hexahydrocyclopenta[c]pyrrol-2(1H)-yl)pyrimidine-4-carboxylic Acid (34)—

Compound **34** was prepared according to a similar procedure described for the synthesis of **32**. Mp 155–156 °C; ¹H NMR (500 MHz, DMSO-*d*₆) δ 13.92 (bs, 1H), 7.57 (m, 1H), 7.65 (m, 1H), 7.59 (m, 1H), 7.40 (m, 1H), 7.33 (s, 1H), 3.78 (m, 2H), 3.68 (m, 2H), 3.30 (m, 1H), 2.93 (m, 2H), 2.29 (m, 2H), 1.64 (m, 2H); MS (ESI+) m/z 446 [M + H]⁺; HPLC >99% purity (Method A), t_R = 12.9 min.

6-Methoxy-2-((3aR,5r,6aS)-5-(2-(trifluoromethyl)phenyl)-hexahydrocyclopenta[c]pyrrol-2(1H)-yl)pyrimidine-4-carboxylic Acid (35)—

Compound **35** was prepared according to a similar procedure described for the synthesis of **32**. Mp 171–174 °C; ¹H NMR (300 MHz, CDCl₃) δ 7.73 (m, 1H), 7.64 (m, 2H), 7.36 (m, 1H), 6.51 (s, 1H), 3.90 (s, 3H), 3.76 (m, 2H), 3.72 (m, 2H), 2.88 (m, 2H), 2.22 (m, 2H),

1.67 (m, 2H); MS (ESI+) m/z 408 [M + H]⁺; HPLC >99% purity (Method A), t_R = 16.2 min.

6-Isopropyl-2-((3aR,5r,6aS)-5-(2-(trifluoromethyl)phenyl)-hexahydrocyclopenta[c]pyrrol-2(1H)-yl)pyrimidine-4-carboxylic Acid (36)—

Compound **36** was prepared according to a similar procedure described for the synthesis of **32**. ¹H NMR (300 MHz, DMSO-*d*₆) δ 13.21 (bs, 1H), 7.72 (m, 1H), 7.65, (m, 2H), 7.39 (m, 2H), 7.01, (s, 1H), 3.75 (m, 2H), 3.71, (m, 2H), 3.42 (m, 1H), 2.90, (m, 3H), 2.49 (m, 2H), 1.66 (m, 2H), 1.23 (s, 6H); MS (ESI+) m/z 420 [M + H]⁺; HPLC >99% purity (Method A), t_R = 13.9 min.

6-Methyl-2-((3aR,5s,6aS)-5-(2-(trifluoromethyl)phenyl)-hexahydrocyclopenta[c]pyrrol-2(1H)-yl)pyrimidine-4-carboxylic Acid (40)

Step A: To a solution of (±)-(3a*R*,6a*S*)-*tert*-butyl 5-(2-(trifluoromethyl)phenyl)-3,3a,6,6a-tetrahydrocyclopenta[*c*]pyrrole-2(1*H*)-carboxylate ((±)-24, 120 mg, 0.34 mmol) in CH₂Cl₂ (3 mL) was added TFA (3 mL) and the resulting solution stirred at rt for 3 h. The residue was dissolved in CH₂Cl₂ (25 mL) and washed with saturated aq NaHCO₃ solution (25 mL), brine (25 mL), dried over Na₂SO₄, filtered, and concentrated under reduced pressure to provide (±)-(3a*S*,6a*R*)-5-(2-(trifluoromethyl)phenyl)-1,2,3,3a,4,6a-hexahydrocyclopenta[*c*]pyrrole ((±)-37) as an off-white solid (0.146 mg, > 99%): ¹H NMR (300 MHz, CDCl₃) δ 9.21 (br s, 1H), 8.18 (br s, 1H), 7.67 (d, *J* = 7.8 Hz, 1H), 7.51–7.34 (m, 3H), 5.57 (s, 1H), 3.82 (br s, 1H), 3.62–3.54 (m, 2H), 3.39–3.09 (m, 4H), 2.62–2.56 (m, 1H).

Step B: To a solution of (±)-(3a*S*,6a*R*)-5-(2-(trifluoromethyl)-phenyl)-1,2,3,3a,4,6a-hexahydrocyclopenta[*c*]pyrrole ((±)-37, 0.680 g, 1.92 mmol) in CH₃OH (25 mL) was added Pd/C (10% w/w, Degussa type E101 NE/W, 0.140 g). The mixture was subjected to an atmosphere of H₂ (50 psi) at rt for 6 h and was filtered through Celite. The filtrate was concentrated under reduced pressure, and the resulting residue was purified by reversed phase column chromatography (Isco C18 Reversed Phase Gold column, 10%-30% CH₃CN in H₂O with 0.05% TFA). The resulting material was dissolved in CH₂Cl₂ and washed with saturated aqueous NaHCO₃, dried over Na₂SO₄, filtered, and concentrated under reduced pressure to give (3a*R*,5*S*,6a*S*)-5-(2-(trifluoromethyl)phenyl)octahydrocyclopenta[*c*]pyrrole (**39**) as a white solid (0.070 g, 14%): ¹H NMR (300 MHz, CDCl₃) δ 7.61 (d, *J* = 7.8 Hz, 1H), 7.50 (m, 2H), 7.30–7.24 (m, 1H), 3.54–3.42 (m, 1H), 3.32–3.26 (m, 2H), 2.81–2.68 (m, 2H), 2.51–2.46 (m, 2H), 1.84–1.76 (m, 4H); MS (ESI+) m/z 256 [M + H]⁺.

Step C: To a solution of (3a*R*,5*S*,6a*S*)-5-(2-(trifluoromethyl)-phenyl)octahydrocyclopenta[*c*]pyrrole (**39**, 0.100 g, 0.39 mmol) and Et₃N (0.16 mL, 1.17 mmol) in DMF (10 mL) was added methyl 2-chloropyrimidine-4-carboxylate (0.067 g, 0.39 mmol), and the resulting solution was stirred at 60 °C for 16 h. The reaction was diluted with H₂O (200 mL) and extracted with EtOAc (3 × 100 mL). The combined organic extracts were washed with H₂O (3 × 100 mL), brine (100 mL), dried over Na₂SO₄, filtered, and concentrated under reduced pressure. The resulting residue was chromatographed over silica gel (0% to 30% EtOAc in hexanes) to give methyl 6-methyl-2-((3a*R*,5*S*,6a*S*)-5-(2-

(trifluoromethyl)phenyl)hexahydrocyclopenta[*c*]-pyrrol-2(*1H*)-yl)pyrimidine-4-carboxylate as an off-white solid (0.123 g, 78%): MS (ESI+) *m/z* 406 [M + H]⁺.

Step D: A solution of methyl 6-methyl-2-((3*aR*,5*s*,6*aS*)-5-(2-(trifluoromethyl)phenyl)hexahydrocyclopenta[*c*]pyrrol-2(*1H*)-yl)-pyrimidine-4-carboxylate (0.100 g, 0.24 mmol) and 2 N aq NaOH (5 mL) in a 1:1 mixture of CH₃OH/THF (10 mL) stirred at room temperature for 16 h. The mixture was carefully at 0 °C with 2 N aq HCl and extracted with CH₂Cl₂ (3 × 10 mL). The combined organic extracts were washed with brine, dried over Na₂SO₄, filtered, and concentrated under reduced pressure. The resulting residue was chromatographed over silica gel (0% to 10% CH₃OH in CH₂Cl₂) to give 6-methyl-2-((3*aR*,5*s*,6*aS*)-5-(2-(trifluoromethyl)phenyl)hexahydro-cyclopenta[*c*]pyrrol-2(*1H*)-yl)pyrimidine-4-carboxylic acid (**40**) as an off-white solid (0.089 g, 93%): mp 175–178 °C; ¹H NMR (300 MHz, CDCl₃) δ 7.68–7.45 (m, 3H), 7.29 (m, 1H), 7.15 (s, 1H), 4.00 (m, 2H), 3.75 (m, 1H), 3.46 (m, 2H), 3.17 (m, 2H), 2.48 (s, 3H), 2.17–1.90 (m, 4H); MS (ESI+) *m/z* 392 [M + H]⁺; HPLC >99% purity (Method A), *t*_R = 14.2 min.

5,6-Dimethyl-2-((3*aR*,5*r*,6*aS*)-5-(2-(trifluoromethyl)phenyl)-hexahydrocyclopenta[*c*]pyrrol-2(*1H*)-yl)pyrimidine-4-carboxylic Acid (**41**)

Step A: To a mixture of (3*aR*,5*r*,6*aS*)-5-(2-(trifluoromethyl)-phenyl)octahydrocyclopenta[*c*]pyrrole hydrochloride (**26**, 0.400 g, 1.37 mmol), 2,4-dichloro-5,6-dimethylpyrimidine (0.242 g 1.37 mmol), JohnPhos (0.048 g, 0.137 mmol), and Cs₂CO₃ (1.34 g, 4.11 mmol) in toluene (10 mL) was added Pd(OAc)₂ (0.015 g, 0.068 mmol). The mixture was heated at reflux for 16 h then allowed to cool to rt. The mixture was filtered over Celite, and the filter cake was washed with EtOAc. The filtrate was concentrated under reduced pressure, and the resulting residue was purified by flash column chromatography (Isco CombiFlash Rf unit, 40 g Gold RediSep column, 0%-15% EtOAc in hexanes) to give (3*aR*,5*r*,6*aS*)-2-(4-chloro-5,6-dimethylpyrimidin-2-yl)-5-(2-(trifluoromethyl)phenyl)octahydrocyclopenta[*c*]pyrrole as a white solid (0.271 g, 50%): MS (ESI+) *m/z* 396 [M + H]⁺.

Step B: To a mixture of (3*aR*,5*r*,6*aS*)-5-(2-(trifluoromethyl)phenyl)-octahydrocyclopenta[*c*]pyrrole hydrochloride (**26**, 0.200 g, 0.50 mmol), Mo(CO)₆ (0.160 g, 0.60 mmol), and BINAP (0.009 g, 0.05 mmol) in CH₃OH (10 mL), and CH₃CN (10 mL) was added Pd(OAc)₂ (0.005 g, 0.024 mmol). The mixture was heated at 80 °C for 16 h then allowed to cool to rt. The mixture was filtered over Celite, and the filter cake was washed with EtOAc. The filtrate was concentrated under reduced pressure, and the resulting residue was purified by flash column chromatography (Isco CombiFlash Rf unit, 40 g Gold RediSep column, 0%-15% EtOAc in hexanes) to give methyl 5,6-dimethyl-2-((3*aR*,5*r*,6*aS*)-5-(2-(trifluoromethyl)phenyl)hexahydrocyclopenta[*c*]pyrrol-2(*1H*)-yl)pyrimidine-4-carboxylate as a white solid (0.132 g, 63%): MS (ESI+) *m/z* 420 [M + H]⁺.

Step C: A mixture of 5,6-dimethyl-2-((3*aR*,5*r*,6*aS*)-5-(2-(trifluoromethyl)phenyl)hexahydrocyclopenta[*c*]pyrrol-2(*1H*)-yl)pyrimidine-4-carboxylate (0.130 g 0.309 mmol) and LiOH·H₂O (0.038 g, 0.929 mmol) in THF (4 mL), CH₃OH (4 mL), and H₂O (4 mL) stirred at rt for 16 h. The mixture was acidified to pH 6 via the addition of 2 N

aq HCl and then extracted with CH₂Cl₂ (3 × 50 mL). The combined organic extracts were washed with brine, dried over Na₂SO₄, filtered, and concentrated under reduced pressure. The resulting residue was purified by flash column chromatography (Isco CombiFlash Rf unit, 40 g RediSep column, 0%-8% CH₃OH in CH₂Cl₂) to give 5,6-dimethyl-2-((3*aR*,5*r*,6*aS*)-5-(2-(trifluoromethyl)phenyl)hexahydrocyclopenta[*c*]pyrrol-2(1*H*)-yl)-pyrimidine-4-carboxylic acid (**41**) as a white solid (0.115 g, 92%): mp 140–142 °C; ¹H NMR (300 MHz, DMSO-*d*₆) δ 7.72 (m, 3H), 7.32 (m, 1H), 3.62 (m, 4H), 2.89 (m, 2H), 2.43 (s, 3H), 2.23 (m, 2H), 2.09 (s, 3H), 1.66 (m, 2H); MS (ESI+) *m/z* 406 [M + H]⁺; HPLC >99% (AUC), (Method A), *t*_R = 13.3 min.

5-Methyl-2-((3*aR*,5*r*,6*aS*)-5-(2-(trifluoromethyl)phenyl)-hexahydrocyclopenta[*c*]pyrrol-2(1*H*)-yl)pyrimidine-4-carboxylic Acid (42**)**

Step A: To a solution of (3*aR*,5*R*,6*aS*)-5-(2-(trifluoromethyl)-phenyl)octahydrocyclopenta[*c*]pyrrole hydrochloride (**26**, 0.050 g, 0.17 mmol) and Et₃N (0.05 mL, 0.51 mmol) in DMF (10 mL) was added methyl 2-chloro-5-methylpyrimidine-4-carboxylate (0.031 g, 0.17 mmol), and the resulting solution was stirred at 60 °C for 16 h. The reaction was allowed to cool to rt and then diluted with H₂O (200 mL). The aqueous mixture was extracted with EtOAc (3 × 100 mL), and the combined organic extracts were washed with H₂O (3 × 100 mL), brine (100 mL), dried over Na₂SO₄, filtered, and concentrated under reduced pressure. The resulting residue was chromatographed over silica gel (0% to 30% EtOAc in hexanes) to give methyl 5-methyl-2-((3*aR*,5*r*,6*aS*)-5-(2-(trifluoromethyl)phenyl)hexahydrocyclopenta[*c*]pyrrol-2(1*H*)-yl)pyrimidine-4-carboxylate as an off-white solid (0.015 g, 22%): MS (ESI+) *m/z* 406 [M + H]⁺.

Step B: A solution of methyl 5-methyl-2-((3*aR*,5*r*,6*aS*)-5-(2-(trifluoromethyl)phenyl)hexahydrocyclopenta[*c*]pyrrol-2(1*H*)-yl)-pyrimidine-4-carboxylate (0.015 g, 0.04 mmol) and 2 N aq NaOH (5 mL) in a 1:1 mixture of CH₃OH/THF (10 mL) stirred at rt for 16 h. The mixture was carefully neutralized at 0 °C with 2 N aq HCl and extracted with CH₂Cl₂ (3 × 10 mL). The combined organic extracts were washed with brine, dried over Na₂SO₄, filtered, and concentrated under reduced pressure. The resulting residue was chromatographed over silica gel (0% to 10% CH₃OH in CH₂Cl₂) to 5-methyl-2-((3*aR*,5*r*,6*aS*)-5-(2-(trifluoromethyl)phenyl)hexahydro-cyclopenta[*c*]pyrrol-2(1*H*)-yl)pyrimidine-4-carboxylic acid (**42**) as an off-white solid (0.013 g, 92%): ¹H NMR (300 MHz, CD₃OD) δ 8.12 (s, 1H), 7.67–7.78 (m, 3H), 7.31 (m, 1H), 3.41–3.61 (m, 5H), 2.91 (m, 2H), 2.34 (m, 4H), 2.15 (s, 3H), 1.67 (m, 2H); MS (ESI+) *m/z* 392 [M + H]⁺; HPLC >99% (AUC), (Method A), *t*_R = 14.2 min.

4-Methyl-2-((3*aR*,5*r*,6*aS*)-5-(2-(trifluoromethyl)phenyl)-hexahydrocyclopenta[*c*]pyrrol-2(1*H*)-yl)pyrimidine-5-carboxylic Acid (43**)**

Step A: A solution of (3*aR*,6*aS*)-5-(2-(trifluoromethyl)-phenyl)octahydrocyclopenta[*c*]pyrrole hydrochloride (**26**, 0.100 g, 0.340 mmol), ethyl 2-chloro-6-methylpyrimidine-5-carboxylate (76 mg, 0.38 mmol), and *i*-Pr₂NEt (0.15 mL, 0.86 mmol) in DMF (5 mL) was heated at 70 °C for 90 min via microwave irradiation. The mixture was allowed to cool to rt then concentrated under reduced pressure. The resulting residue was chromatographed over silica gel (Isco CombiFlash Companion unit, 12 g

Redisepp column, 0–100% EtOAc in hexanes) to provide methyl 4-methyl-2-((3a*R*,6a*S*)-5-(2-(trifluoro-methyl)phenyl)hexahydrocyclopenta[*c*]pyrrole-2(1*H*)-yl)pyrimidine-5-carboxylate as a colorless semisolid (99 mg, 69%): ¹H NMR (300 MHz, CDCl₃) δ 8.87 (s, 1H), 7.61 (dd, *J* = 7.8 Hz, 1H), 7.50–7.48 (m, 2H), 4.36–4.29 (m, 2H) 3.88–3.77 (m, 4H), 3.59–3.56 (m, 1H), 3.06–2.94 (m, 2H), 2.71 (s, 3H), 2.44–2.35 (m, 2H), 1.69–1.56 (m, 3H), 1.39–1.35 (m, 3H); MS (ESI+) *m/z* 420 [M + H]⁺.

Step B: A mixture of methyl 4-methyl-2-((3a*R*,6a*S*)-5-(2-(trifluoromethyl)phenyl)hexahydro cyclopenta[*c*]pyrrole-2(1*H*)-yl)-pyrimidine-5-carboxylate (0.099 g, 0.241 mmol) and LiOH·H₂O (0.100 g, 2.38 mmol) in THF (4 mL) and H₂O (2 mL) stirred at rt for 18 h and was then heated at 40 °C for 7 h. The mixture was allowed to cool to rt and was diluted with H₂O (4 mL) and acidified with 2 N aq HCl to pH 6. The mixture was extracted with EtOAc (3 × 10 mL), and the combined extracts were dried over Na₂SO₄, filtered, and concentrated under reduced pressure to provide 4-methyl-2-((3a*R*,6a*S*)-5-(2-(trifluoromethyl)phenyl)hexahydrocyclopenta[*c*]pyrrol-2(1*H*)-yl)-pyrimidine-5-carboxylic acid (**43**) as a white solid (0.020 g, 21%): mp 82–85 °C; ¹H NMR (300 MHz, DMSO-*d*₆) δ 12.57 (br s, 1H), 8.73 (s, 1H), 7.73–7.61 (m, 3H), 7.41–7.38 (m, 1H), 3.82–3.62 (m, 4H), 2.86 (br s, 2H), 2.58 (s, 3H), 2.26 (br s, 2H), 1.63 (br s, 2H); MS (ESI+) *m/z* 392 [M + H]⁺; HPLC 98.5% purity (Method H), *t*_R = 17.4 min.

2-((3a*R*,5*r*,6a*S*)-5-(2-(Trifluoromethyl)phenyl)hexahydrocyclopenta[*c*]pyrrol-2(1*H*)-yl)pyrimidine-5-carboxylic Acid (44**)**

Step A: A mixture of (3a*R*,5*R*,6a*S*)-5-(2-(trifluoromethyl)phenyl)-octahydrocyclopenta[*c*]pyrrole hydrochloride (**26**, 0.050 g, 0.172 mmol) methyl 2-chloropyrimidine-5-carboxylate (0.029 g, 0.17 mmol), and Et₃N (0.05 mL, 0.51 mmol) in DMF (5 mL) was heated at 70 °C for 16 h. The mixture was allowed to cool to rt and was diluted with H₂O (20 mL). The aqueous mixture was extracted with EtOAc (3 × 20 mL), and the combined organic extracts were washed with H₂O (3 × 100 mL), brine (100 mL), dried over Na₂SO₄, filtered, and concentrated under reduced pressure. The resulting residue was chromatographed over silica gel (0% to 30% EtOAc in hexanes) to give methyl 2-((3a*R*,5*r*,6a*S*)-5-(2-(trifluoromethyl)phenyl)hexahydro-cyclopenta[*c*]pyrrol-2(1*H*)-yl)pyrimidine-5-carboxylate as an off-white solid (0.035 g, 52%): MS (ESI+) *m/z* 392 [M + H]⁺.

Step B: A solution of methyl 2-((3a*R*,5*r*,6a*S*)-5-(2-(trifluoromethyl)phenyl)hexahydrocyclopenta[*c*]pyrrol-2(1*H*)-yl)pyrimidine-5-carboxylate (0.030 g, 0.071 mmol) and 2 N aq NaOH (5 mL) in a 1:1 mixture of CH₃OH/THF (10 mL) stirred at room temperature for 16 h. The mixture was carefully neutralized at 0 °C with 2 N HCl and extracted with CH₂Cl₂ (3 × 10 mL). The combined organic extracts were washed with brine, dried over Na₂SO₄, filtered, and concentrated under reduced pressure. The resulting residue was chromatographed over silica gel (0% to 10% CH₃OH in CH₂Cl₂) to 2-((3a*R*,5*r*,6a*S*)-5-(2-(trifluoromethyl)phenyl)hexahydrocyclopenta[*c*]pyrrol-2(1*H*)-yl)-pyrimidine-5-carboxylic acid (**44**) as an off-white solid (0.026 g, 91%): mp 218–222 °C; ¹H NMR (500 MHz, CDCl₃) δ 8.90 (bs, 1H), 7.32–7.51 (m, 3H), 7.21 (m, 3H), 3.41–3.91 (m, 5H), 2.89

(m, 2H), 2.32 (m, 2H), 1.64 (m, 2H); MS (ESI+) m/z 378 [M + H]⁺; HPLC >99% (AUC), (Method A), t_R = 17.6 min.

6-Methyl-2-((3aR,5r,6aS)-5-(2-(trifluoromethyl)phenyl)-hexahydrocyclopenta[c]pyrrol-2(1H)-yl)pyrimidine-4-carboxamide (46)

Step A: A mixture of 5-(2-(trifluoromethyl)phenyl)octahydrocyclopenta[c]pyrrole hydrochloride (**26**, 0.068 g, 0.355 mmol), 2-chloro-6-methylpyrimidine-4-carbonitrile (0.054 g, 0.352 mmol), and *i*-Pr₂NEt (0.14 mL, 1.05 mmol) in DMF (2 mL) was heated at 60 °C for 16 h. The mixture was allowed to cool to rt and then poured into brine (50 mL). The aqueous mixture was extracted with EtOAc (3 × 50 mL), and the combined organic extracts were washed with saturated NaHCO₃ (3 × 50 mL), dried over Na₂SO₄, filtered, and concentrated under reduced pressure. The resulting residue was chromatographed over silica gel (0–50% EtOAc in hexanes) to afford 6-methyl-2-((3aR,5r,6aS)-5-(2-(trifluoromethyl)phenyl)hexahydrocyclopenta[c]pyrrol-2(1H)-yl)pyrimidine-4-carbonitrile (**45**) as an off-white solid (0.072 g, 55%): ESI MS m/z 373 [M + H]⁺.

Step B: A mixture of 6-methyl-2-((3aR,5r,6aS)-5-(2-(trifluoromethyl)phenyl)hexahydrocyclopenta[c]pyrrol-2(1H)-yl)pyrimidine-4-carbonitrile (**45**, 0.049 g, 0.133 mmol) LiOH·H₂O (0.030 g, 0.665 mmol) in THF (4 mL) and H₂O (2 mL) was heated at 70 °C for 18 h. The mixture was allowed to cool to rt and was then acidified to pH 6 with 2 N aq HCl. The aqueous mixture was extracted with CH₂Cl₂ (3 × 50 mL), and the combined organics were dried over Na₂SO₄, filtered, and concentrated under reduced pressure. The residue was chromatographed over silica gel (0–5% methanol in CH₂Cl₂) to yield 6-methyl-2-((3aR,5r,6aS)-5-(2-(trifluoromethyl)phenyl)hexahydrocyclopenta[c]pyrrol-2(1H)-yl)pyrimidine-4-carboxamide (**46**) as an off-white solid (0.041 g, 78%): mp 183–187 °C; ¹H NMR (300 MHz, CDCl₃) δ 7.77 (s, 1H), 7.66–7.58 (m, 1H), 7.58–7.41 (m, 2H), 7.20 (s, 1H), 5.57 (s, 1H), 3.85–3.64 (m, 4H) 3.64–3.45 (m, 1H), 3.01–3.85 (m, 2H), 2.46 (s, 3H), 2.45–2.32 (m, 2H), 1.72–1.56 (m, 2H), aromatic CH obscured by residual peak; ESI MS m/z : 254.1 [M + H]⁺; HPLC >99% (AUC), (Method B), t_R = 17.5 min.

(3aR,5r,6aS)-2-(4-Methyl-6-(1H-tetrazol-5-yl)pyrimidin-2-yl)-5-(2-(trifluoromethyl)phenyl)octahydrocyclopenta[c]pyrrole (47)

Step A: A mixture of 6-methyl-2-((3aR,5r,6aS)-5-(2-(trifluoromethyl)phenyl)hexahydrocyclopenta[c]pyrrol-2(1H)-yl)pyrimidine-4-carbonitrile (**45**, 0.093 g, 0.250 mmol), NaN₃ (0.195 g, 3.0 mmol), and NH₄Cl (0.160 g, 3.0 mmol) in DMF (5 mL) was heated at 130 °C in a sealed tube via microwave irradiation for 1 h. The mixture was allowed to cool to rt and then diluted with H₂O (50 mL). The aqueous mixture was extracted with EtOAc (3 × 50 mL), and the combined organic extracts were washed with H₂O (3 × 50 mL) and brine. The organic layer was dried over Na₂SO₄, filtered, and concentrated under reduced pressure. The resulting residue was purified by reversed phase column chromatography (Isco RediSep 12 g Gold C18 reverse phase column, 0%–100% CH₃CN in H₂O) to provide (3aR,5r,6aS)-2-(4-methyl-6-(1H-tetrazol-5-yl)pyrimidin-2-yl)-5-(2-(trifluoromethyl)phenyl)octahydrocyclopenta[c]pyrrole (**47**) as a white solid (0.074 g, 71%): mp 150–158 °C; ¹H NMR (500 MHz, DMSO-*d*₆) δ 7.71–7.59 (m, 3H), 7.41 (m, 1H),

7.21 (s, 1H), 3.85–3.65 (m, 4H), 3.49 (m, 1H), 2.98 (m, 2H), 2.42 (s, 3H), 2.32 (m, 2H), 1.62 (m, 2H); MS (ESI+) m/z 416 [M + H]⁺; HPLC 98.3% (AUC), (Method A), t_R = 18.0 min.

4-Methyl-6-((3aR,5r,6aS)-5-(2-(trifluoromethyl)phenyl)-hexahydrocyclopenta[c]pyrrol-2(1H)-yl)picolinic Acid (48)

Step A: A mixture of (3aR,5R,6aS)-5-(2-(trifluoromethyl)phenyl)octahydrocyclopenta[c]pyrrole hydrochloride (**26**, 0.158 g, 0.54 mmol), methyl 2-chloro-4-methylnicotinate (0.100 g, 0.54 mmol), Pd(OAc)₂ (0.011 g, 0.05 mmol), Xantphos (0.011 g), and Cs₂CO₃ (0.050 g, 0.15 mmol) in toluene (10 mL) was heated at 110 °C for 16 h. The reaction was allowed to cool to rt then diluted with H₂O (200 mL) and extracted with EtOAc (3 × 100 mL). The combined organic extracts were washed with H₂O (3 × 100 mL), brine (100 mL), dried over Na₂SO₄, filtered, and concentrated under reduced pressure. The resulting residue was chromatographed over silica gel (0% to 30% EtOAc in hexanes) to give methyl 4-methyl-6-((3aR,5r,6aS)-5-(2-(trifluoromethyl)phenyl)-hexahydrocyclopenta[c]pyrrol-2(1H)-yl)picolinate as an off-white solid (0.129 g, 59%).

Step B: A solution of methyl 4-methyl-6-((3aR,5r,6aS)-5-(2-(trifluoromethyl)phenyl)hexahydrocyclopenta[c]pyrrol-2(1H)-yl)picolinate (0.129 g, 0.07 mmol) and 2 N aq NaOH (10 mL) in a 1:1 mixture of CH₃OH/THF (20 mL) stirred at room temperature for 16 h. The mixture was carefully neutralized at 0 °C with 2 N aq HCl and extracted with CH₂Cl₂ (3 × 10 mL). The combined organic extracts were washed with brine, dried over Na₂SO₄, filtered, and concentrated under reduced pressure. The resulting residue was chromatographed over silica gel (0% to 10% CH₃OH in CH₂Cl₂) to give 4-methyl-6-((3aR,5r,6aS)-5-(2-(trifluoromethyl)phenyl)hexahydrocyclopenta[c]-pyrrol-2(1H)-yl)picolinic acid (**48**) as an off-white solid (0.106 g, 88%): mp 152–155 °C; ¹H NMR (500 MHz, DMSO-*d*₆) δ 12.51 (bs, 1H), 7.71 (m, 3H), 7.61 (m, 1H), 7.14 (s, 1H), 6.62 (s, 1H), 3.55 (m, 4H), 3.34 (m, 4H), 2.88 (m, 2H), 2.29 (m, 5H), 1.62 (m, 2H); MS (ESI+) m/z 391 [M + H]⁺; HPLC >99% (AUC), (Method A), t_R = 13.4 min.

2-Methyl-6-((3aR,5r,6aS)-5-(2-(trifluoromethyl)phenyl)-hexahydrocyclopenta[c]pyrrol-2(1H)-yl)isonicotinic Acid (49)

Step A: A mixture of (3aR,5R,6aS)-5-(2-(trifluoromethyl)phenyl)octahydrocyclopenta[c]pyrrole hydrochloride (**26**, 0.160 g, 0.55 mmol), methyl 2-chloro-6-methylisonicotinate (0.101 g, 0.55 mmol), Pd(OAc)₂ (0.011 g, 0.05 mmol), Xantphos (0.011 g), and Cs₂CO₃ (0.050 g, 0.15 mmol) in toluene (10 mL) was stirred at 110 °C for 16 h. The reaction was allowed to cool to rt and diluted with H₂O (200 mL) and extracted with EtOAc (3 × 100 mL). The combined organic extracts were washed with H₂O (3 × 100 mL), brine (100 mL), dried over Na₂SO₄, filtered, and concentrated under reduced pressure. The resulting residue was chromatographed over silica gel (0% to 30% EtOAc in hexanes) to give methyl 2-methyl-6-((3aR,5r,6aS)-5-(2-(trifluoromethyl)phenyl)hexahydrocyclopenta[c]pyrrol-2(1H)-yl)isonicotinate as an off-white solid (0.140 g, 63%).

Step B: A solution of methyl 2-methyl-6-((3a*R*,5*r*,6a*S*)-5-(2-(trifluoromethyl)phenyl)hexahydrocyclopenta[*c*]pyrrol-2(1*H*)-yl)-isonicotinate (0.140 g, 0.08 mmol) and 2 N aq NaOH (10 mL) in a 1:1 mixture of CH₃OH/THF (20 mL) was stirred at room temperature for 16 h. The mixture was carefully neutralized at 0 °C with 2 N aq HCl and extracted with CH₂Cl₂ (3 × 10 mL). The combined organic extracts were washed with brine, dried over Na₂SO₄, filtered, and concentrated under reduced pressure. The resulting residue was chromatographed over silica gel (0% to 10% CH₃OH in CH₂Cl₂) to give 2-methyl-6-((3a*R*,5*r*,6a*S*)-5-(2-(trifluoromethyl)phenyl)-hexahydrocyclopenta[*c*]pyrrol-2(1*H*)-yl)isonicotinic acid (**49**) as an off-white solid (0.124 g, 86%): mp 121–124 °C; ¹H NMR (500 MHz, DMSO-*d*₆) δ 12.81 (bs, 1H), 7.77 (s, 1H), 7.66 (m, 3H), 7.40 (m, 1H), 6.60 (s, 1H), 3.52 (m, 4H), 3.45 (m, 1H), 2.80 (m, 2H), 2.36 (s, 3H), 2.24 (m, 2H), 1.60 (m, 2H); MS (ESI+) *m/z* 391 [M + H]⁺; HPLC >99% (AUC), (Method A), *t*_R = 10.1 min.

3-Methyl-6-((3a*R*,5*r*,6a*S*)-5-(2-(trifluoromethyl)phenyl)-hexahydrocyclopenta[*c*]pyrrol-2(1*H*)-yl)picolinic Acid (**50**)

Step A: To a mixture of (3a*R*,5*r*,6a*S*)-5-(2-(trifluoromethyl)phenyl)octahydrocyclopenta[*c*]pyrrole hydrochloride (**26**, 0.400 g, 1.37 mmol), 6-chloro-3-methylpicolinic acid (0.254 g, 1.37 mmol), JohnPhos (0.048 g, 0.137 mmol), and Cs₂CO₃ (1.34 g, 4.11 mmol) in toluene (7 mL) was added Pd(OAc)₂ (0.015 g, 0.068 mmol). The mixture was heated at reflux for 14 h then allowed to cool to rt. The mixture was filtered over Celite, and the filter cake was washed with EtOAc. The filtrate was concentrated under reduced pressure, and the resulting residue was purified by flash column chromatography (Isco CombiFlash Rf unit, 40 g Gold RediSep column, 0%-15% EtOAc in hexanes) to give methyl 3-methyl-6-((3a*R*,5*r*,6a*S*)-5-(2-(trifluoromethyl)phenyl)-hexahydrocyclopenta[*c*]pyrrol-2(1*H*)-yl)picolinic acid as a white solid (0.366 g, 66%): MS (ESI+) *m/z* 405 [M + H]⁺.

Step B: A mixture of methyl 3-methyl-6-((3a*R*,5*r*,6a*S*)-5-(2-(trifluoromethyl)phenyl)hexahydrocyclopenta[*c*]pyrrol-2(1*H*)-yl)picolinic acid (0.366 g, 0.905 mmol) and LiOH·H₂O (0.114 g, 2.71 mmol) in THF (4 mL), CH₃OH (4 mL), and H₂O (4 mL) was stirred at rt for 72 h. The mixture was acidified to pH 6 via the addition of 2 N aq HCl and then extracted with CH₂Cl₂ (3 × 50 mL). The combined organic extracts were washed with brine, dried over Na₂SO₄, filtered, and concentrated under reduced pressure. The resulting residue was purified by flash column chromatography (Isco CombiFlash Rf unit, 40 g RediSep column, 0%-8% CH₃OH in CH₂Cl₂) to give 3-methyl-6-((3a*R*,5*r*,6a*S*)-5-(2-(trifluoromethyl)phenyl)hexahydrocyclopenta[*c*]pyrrol-2(1*H*)-yl)picolinic acid (**50**) as a white solid (0.337 g, 95%): mp 148–150 °C; ¹H NMR (500 MHz, CDCl₃) δ 11.97 (bs, 1H), 7.67 (s, 1H), 7.59–7.50 (m, 3H), 7.27 (m, 1H), 6.65 (s, 1H), 3.70–3.44 (m, 5H), 2.94 (m, 2H), 2.61 (s, 3H), 1.70 (m, 2H), 1.50 (m, 2H); MS (ESI+) *m/z* 391 [M + H]⁺; HPLC >99% (AUC), (Method A), *t*_R = 11.8 min.

5-((3aR,5r,6aS)-5-(2-(trifluoromethyl)phenyl)hexahydrocyclopenta[c]pyrrol-2(1H)-yl)nicotinic Acid (51)

Step A: To a mixture of (3aR,5r,6aS)-5-(2-(trifluoromethyl)phenyl)octahydrocyclopenta[c]pyrrole hydrochloride (**26**, 0.153 g, 0.524 mmol), methyl 5-bromonicotinate (0.103 g, 0.477 mmol), XantPhos (0.083 g, 0.140 mmol), and Cs₂CO₃ (0.465 g, 1.43 mmol) in 1,4-dioxane (8 mL) was added Pd₂(dba)₃ (0.043 g, 0.047 mmol). The mixture was heated at reflux for 16 h, then allowed to cool to rt. The mixture was concentrated under reduced pressure, and the resulting residue was purified by flash column chromatography (Isco CombiFlash Rf unit, 40 g Gold RediSep column, 0%-25% CH₃OH in CH₂Cl₂) to give methyl 5-((3aR,5r,6aS)-5-(2-(trifluoromethyl)phenyl)hexahydrocyclopenta[c]pyrrol-2(1H)-yl)-nicotinate as a yellow film (0.077 g, 41%): ¹H NMR (500 MHz, CDCl₃) δ 8.59 (s, 1H), 7.62 (s, 1H), 7.53 (m, 1H), 7.48 (m, 3H), 7.29 (m, 1H), 3.94 (s, 3H), 3.52 (m, 1H), 3.43 (m, 4H), 2.98 (m, 2H), 2.45 (m, 2H), 1.67 (m, 2H); MS (ESI+) *m/z* 391 [M + H]⁺.

Step B: A mixture of methyl 5-((3aR,5r,6aS)-5-(2-(trifluoromethyl)phenyl)hexahydrocyclopenta[c]pyrrol-2(1H)-yl)nicotinate (0.076 g, 0.194 mmol) and LiOH·H₂O (0.081 g, 1.94 mmol) in THF (4 mL), CH₃OH (2 mL), and H₂O (1 mL) was stirred at rt for 4 h. The mixture was acidified to pH 2 via the addition of 2 N aq HCl and then diluted with H₂O (40 mL). The aqueous mixture was extracted with CH₂Cl₂ (3 × 50 mL), and the combined organic extracts were washed with brine, dried over Na₂SO₄, filtered, and concentrated under reduced pressure to provide 5-((3aR,5r,6aS)-5-(2-(trifluoromethyl)phenyl)-hexahydrocyclopenta[c]pyrrol-2(1H)-yl)nicotinic acid (**51**) as a yellow solid (0.063 g, 88%): mp 302–304 °C; ¹H NMR (500 MHz, DMSO-*d*₆) δ 13.17 (bs, 1H), 8.39 (s, 1H), 8.23 (s, 1H), 7.72–7.59 (m, 3H), 7.38 (m, 2H), 3.44 (m, 5H), 2.94 (m, 2H), 2.30 (m, 2H), 1.65 (m, 2H); MS (ESI+) *m/z* 377 [M + H]⁺; HPLC >99% (AUC), (Method B), *t*_R = 7.8 min.

3-((3aR,5r,6aS)-5-(2-(trifluoromethyl)phenyl)hexahydrocyclopenta[c]pyrrol-2(1H)-yl)benzoic Acid (52)

Step A: To a mixture of (3aR,5r,6aS)-5-(2-(trifluoromethyl)phenyl)octahydrocyclopenta[c]pyrrole hydrochloride (**26**, 0.250 g, 0.86 mmol), NaO*t*-Bu (0.180 g, 0.89 mmol), and BINAP (0.105 g, 0.17 mmol) in toluene (10 mL) was added Pd(OAc)₂ (0.020 g, 0.089 mmol). The mixture was heated at 110 °C for 16 h, then allowed to cool to rt. The mixture was filtered over Celite, and the filter cake was washed with EtOAc. The filtrate was concentrated under reduced pressure, and the resulting residue was purified by flash column chromatography (Isco CombiFlash Rf unit, 40 g Gold RediSep column, 0%-15% EtOAc in hexanes) to give methyl 3-((3aR,5r,6aS)-5-(2-(trifluoromethyl)phenyl)hexahydrocyclopenta[c]pyrrol-2(1H)-yl)benzoate as a white solid (0.132 g, 63%): MS (ESI+) *m/z* 390 [M + H]⁺.

Step B: A mixture of methyl 3-((3aR,5r,6aS)-5-(2-(trifluoromethyl)phenyl)hexahydrocyclopenta[c]pyrrol-2(1H)-yl)benzoate (0.396 g, 0.95 mmol) and LiOH·H₂O (0.400 g, 9.5 mmol) in THF (4 mL), CH₃OH (2 mL), and H₂O (1 mL) stirred at rt for 16 h. The mixture was acidified to pH 2 via the addition of 2 N aq HCl and then

diluted with H₂O (40 mL). The aqueous mixture was extracted with CH₂Cl₂ (3 × 50 mL), and the combined organic extracts were washed with brine, dried over Na₂SO₄, filtered, and concentrated under reduced pressure to provide 3-((3*aR*,5*r*,6*aS*)-5-(2-(trifluoromethyl)phenyl)-hexahydrocyclopenta[*c*]pyrrol-2(1*H*)-yl)benzoic acid (**52**) as a yellow solid (0.026 g, 18%): ¹H NMR (300 MHz, DMSO-*d*₆) δ 12.72 (bs, 1H), 7.72–7.63 (m, 3H), 7.41 (m, 1H), 7.30–7.20 (m, 3H), 6.89 (m, 1H), 3.40 (m, 5H), 2.91 (m, 2H), 2.31 (m, 2H), 1.64 (m, 2H); MS (ESI+) *m/z* 376 [M + H]⁺; HPLC 98.8% (AUC), (Method B), *t*_R = 18.6 min.

6-Methyl-2-((3*aR*,5*r*,6*aS*)-5-(2-(trifluoromethyl)phenyl)-hexahydrocyclopenta[*c*]pyrrol-2(1*H*)-yl)nicotinic Acid (53**)**

Step A: To a mixture of (3*aR*,5*r*,6*aS*)-5-(2-(trifluoromethyl)phenyl)octahydrocyclopenta[*c*]pyrrole hydrochloride (**26**, 0.250 g, 0.857 mmol), methyl 2-chloro-6-methylnicotinate (0.146 g, 0.787 mmol), XantPhos (0.135 g, 0.233 mmol), and Cs₂CO₃ (0.647 g, 1.98 mmol) in toluene (25 mL) was added Pd₂(dba)₃ (0.071 g, 0.077 mmol). The mixture was heated at 100 °C for 16 h, then allowed to cool to rt. The mixture was concentrated under reduced pressure, and the resulting residue was purified by flash column chromatography (Isco CombiFlash Rf unit, 24 g Gold RediSep column, 0%-25% CH₃OH in CH₂Cl₂) to give methyl 6-methyl-2-((3*aR*,5*r*,6*aS*)-5-(2-(trifluoromethyl)phenyl)hexahydrocyclopenta[*c*]pyrrol-2(1*H*)-yl)nicotinate as a crude yellow film (0.036 g).

Step B: A mixture of methyl 6-methyl-2-((3*aR*,5*r*,6*aS*)-5-(2-(trifluoromethyl)phenyl)hexahydrocyclopenta[*c*]pyrrol-2(1*H*)-yl)nicotinate (0.036 g, 0.089 mmol) and LiOH·H₂O (0.037 g, 0.89 mmol) in THF (4 mL), CH₃OH (4 mL), and H₂O (1 mL) stirred at 50 °C for 30 min. The mixture was acidified to pH 2 via the addition of 2 N aq HCl and then diluted with H₂O (40 mL). The aqueous mixture was extracted with CH₂Cl₂ (3 × 20 mL), and the combined organic extracts were washed with brine, dried over Na₂SO₄, filtered, and concentrated under reduced pressure. The resulting residue was purified by reversed phase column chromatography (Isco RediSep 12 g Gold C18 reverse phase column, 0%-100% CH₃CN in H₂O) to provide 6-methyl-2-((3*aR*,5*r*,6*aS*)-5-(2-(trifluoromethyl)phenyl)-hexahydrocyclopenta[*c*]pyrrol-2(1*H*)-yl)nicotinic acid (**53**) as a white solid (0.007 g, 20% over two steps): mp 156–157 °C; ¹H NMR (500 MHz, DMSO-*d*₆) δ 13.28 (bs, 1H), 7.71–7.59 (m, 3H), 7.38 (m, 1H), 6.87 (s, 1H), 6.74 (s, 1H), 3.55 (m, 4H), 3.41 (m, 1H), 2.89 (m, 2H), 2.35 (s, 3H), 2.27 (m, 2H), 1.65 (m, 2H); MS (ESI+) *m/z* 391 [M + H]⁺; HPLC 98.6% (AUC), (Method A), *t*_R = 8.4 min.

2-((3*aR*,5*r*,6*aS*)-5-(2-(Trifluoromethyl)phenyl)hexahydrocyclopenta[*c*]pyrrol-2(1*H*)-yl)nicotinic Acid (54**)**

Step A: A mixture of (3*aR*,5*r*,6*aS*)-5-(2-(trifluoromethyl)phenyl)octahydrocyclopenta[*c*]pyrrole hydrochloride (**26**, 0.160 g, 0.55 mmol), methyl 2-chloronicotinate (0.071 g, 0.41 mmol), Pd(OAc)₂ (0.011 g, 0.05 mmol), Xantphos (0.011 g), and Cs₂CO₃ (0.050 g, 0.15 mmol) in toluene (10 mL) was stirred at 110 °C for 16 h. The reaction was diluted with H₂O (200 mL) and extracted with EtOAc (3 × 100 mL). The combined organic extracts were washed with H₂O (3 × 100 mL), brine (100 mL), dried over Na₂SO₄, filtered, and

concentrated under reduced pressure. The resulting residue was chromatographed over silica gel (0% to 30% EtOAc in hexanes) to give methyl 2-((3*aR*,5*r*,6*aS*)-5-(2-(trifluoromethyl)phenyl)hexahydrocyclopenta[*c*]pyrrol-2(1*H*)-yl)nicotinate as an off-white solid (0.07 g, 33%).

Step B: A solution of 2-((3*aR*,5*r*,6*aS*)-5-(2-(trifluoromethyl)phenyl)hexahydrocyclopenta[*c*]pyrrol-2(1*H*)-yl)nicotinate (0.70 g, 0.18 mmol) and 2 N aq NaOH (10 mL) in a 1:1 mixture of CH₃OH/THF (20 mL) was stirred at room temperature for 16 h. The mixture was carefully neutralized at 0 °C with 2 N HCl and extracted with CH₂Cl₂ (3 × 10 mL). The combined organic extracts were washed with brine, dried over Na₂SO₄, filtered, and concentrated under reduced pressure. The resulting residue was chromatographed over silica gel (0% to 10% CH₃OH in CH₂Cl₂) to give 2-((3*aR*,5*r*,6*aS*)-5-(2-(trifluoromethyl)phenyl)hexahydrocyclopenta[*c*]pyrrol-2(1*H*)-yl)nicotinic acid (**54**) as an off-white solid (0.057 g, 85%): mp 158–160 °C; ¹H NMR (500 MHz, DMSO-*d*₆) δ 8.20 (s, 1H), 7.79 (m, 1H), 7.63 (m, 3H), 7.39 (m, 1H), 6.71 (s, 1H), 3.53 (m, 4H), 3.48 (m, 1H), 2.80 (m, 2H), 2.24 (m, 2H), 1.61 (m, 2H); MS (ESI+) *m/z* 377 [M + H]⁺; HPLC >99% (AUC), (Method A), *t*_R = 10.4 min.

6-((3*aR*,5*r*,6*aS*)-5-(2-(Trifluoromethyl)phenyl)hexahydrocyclopenta[*c*]pyrrol-2(1*H*)-yl)pyrazine-2-carboxylic Acid (55**)**

Step A: A mixture of 5-(2-(trifluoromethyl)phenyl)octahydrocyclopenta[*c*]pyrrole hydrochloride (**26**, 0.057 g, 0.29 mmol), methyl 2-chloro-pyrazine-6-carboxylate (0.051 g, 0.29 mmol), and *i*-Pr₂NEt (0.14 mL, 1.09 mmol) in DMF (10 mL) was heated at 60 °C for 16 h. The mixture was allowed to cool to rt and poured into brine (50 mL). The aqueous mixture was extracted with EtOAc (3 × 50 mL), and the combined organic extracts were washed with a saturated NaHCO₃ (3 × 50 mL), dried over Na₂SO₄, and concentrated under reduced pressure. The resulting residue was chromatographed over silica gel (0–50% EtOAc in hexanes) to afford methyl 6-((3*aR*,5*r*,6*aS*)-5-(2-(trifluoromethyl)phenyl)hexahydrocyclopenta[*c*]pyrrol-2(1*H*)-yl)-pyrazine-2-carboxylate (66 mg, 57%): ¹H NMR (300 MHz, CDCl₃) δ 8.53 (s, 1H), 8.10 (s, 1H), 7.66–7.56 (m, 1H), 7.56–7.42 (m, 2H), 3.99 (s, 3H), 3.81–3.48 (m, 5H) 3.07–2.92 (m, 2H), 2.51–2.34 (m, 2H), 1.75–1.61 (m, 2H), aromatic CH obscured by a residual peak; ESI MS *m/z* 392 [M + H]⁺.

Step B: A mixture of methyl 6-((3*aR*,5*r*,6*aS*)-5-(2-(trifluoromethyl)phenyl)hexahydrocyclopenta[*c*]pyrrol-2(1*H*)-yl)pyrazine-2-carboxylate (66.0 mg, 0.169 mmol) and LiOH·H₂O (0.027 g, 0.64 mmol) in THF (4 mL), CH₃OH (4 mL), and H₂O (1 mL) was stirred at rt for 30 min. The mixture was acidified to pH 6 using 2 N aq HCl and extracted with CH₂Cl₂ (3 × 20 mL), and the combined organic extracts were washed with brine, dried over Na₂SO₄, filtered, and concentrated under reduced pressure. The resulting residue was purified by reversed phase column chromatography (Isco RediSep 12 g Gold C18 reverse phase column, 0%–100% CH₃CN in H₂O) to provide 2-((3*aR*,5*r*,6*aS*)-5-(2-(trifluoromethyl)phenyl)hexahydro-cyclopenta[*c*]pyrrol-2(1*H*)-yl)nicotinic acid (**55**) as a white solid (0.015 g, 24%). mp 182–185 °C; ¹H NMR: (300 MHz, CDCl₃) δ 8.60 (s, 1H), 8.29–8.00 (br s, 1H), 7.74–7.55 (m, 1H), 7.55–7.39 (m, 2H), 3.93–3.40 (m, 5H), 2.79–2.54

(m, 2H) 2.50–2.22 (m, 2H), 1.80–1.44 (m, 2H); ESI MS m/z : 378 [M + H]⁺; HPLC 98.7% (AUC), (Method B), t_R = 14.0 min.

6-((3aR,5r,6aS)-5-(2-(trifluoromethyl)phenyl)hexahydrocyclopenta[c]pyrrol-2(1H)-yl)pyridazine-4-carboxylic Acid (56)

Step A: A mixture of (3aR,5r,6aS)-5-(2-(trifluoromethyl)phenyl)octahydrocyclopenta[c]pyrrole hydrochloride (**26**, 0.500 g, 1.71 mmol), methyl 3-chloropyridazine-5-carboxylate (0.295 g, 1.71 mmol), and Et₃N (0.71 mL, 5.15 mmol) in DMF (10 mL) was heated at 60 °C for 16 h. The mixture was then allowed to cool to rt and diluted with H₂O (50 mL). The aqueous mixture was extracted with EtOAc (3 × 50 mL), and the combined organic extracts were washed with H₂O (3 × 50 mL) and brine. The organic layer was dried over Na₂SO₄, filtered, and concentrated under reduced pressure. The resulting residue was purified by flash column chromatography (Isco CombiFlash Rf unit, 40 g RediSep column, 0%-50% EtOAc in hexanes) to give methyl 6-((3aR,5r,6aS)-5-(2-(trifluoromethyl)phenyl)hexahydrocyclopenta[c]-pyrrol-2(1H)-yl)pyridazine-4-carboxylate as an oil (0.069 g, 10%): MS (ESI+) m/z 392 [M + H]⁺.

Step B: A mixture of methyl 6-((3aR,5r,6aS)-5-(2-(trifluoromethyl)phenyl)hexahydrocyclopenta[c]pyrrol-2(1H)-yl)pyridazine-4-carboxylate (0.060 g, 0.153 mmol) and LiOH·H₂O (0.020 g, 0.477 mmol) in THF (5 mL) and H₂O (5 mL) was stirred at rt for 16 h. The mixture was acidified to pH 6 via the addition of 2 N aq HCl and then extracted with CH₂Cl₂ (3 × 20 mL). The combined organic extracts were washed with brine, dried over Na₂SO₄, filtered, and concentrated under reduced pressure to provide 6-((3aR,5r,6aS)-5-(2-(trifluoro-methyl)phenyl)hexahydrocyclopenta[c]pyrrol-2(1H)-yl)pyridazine-4-carboxylic acid (**56**) as a light-yellow solid (0.054 g, 95%): ¹H NMR (300 MHz, DMSO-*d*₆) δ 13.92 (bs, 1H), 8.82 (s, 1H), 7.75–7.62 (m, 3H), 7.38 (m, 1H), 7.22, (s, 1H), 3.72–3.66 (m, 4H), 3.44 (m, 1H), 2.94 (m, 2H), 2.29 (m, 2H), 1.67 (m, 2H); MS (ESI+) m/z 378 [M + H]⁺; HPLC 97.4% (AUC), (Method A), t_R = 12.8 min.

5-Methyl-2-((3aR,5r,6aS)-5-(2-(trifluoromethyl)phenyl)hexahydrocyclopenta[c]pyrrol-2(1H)-yl)thiazole-4-carboxylic Acid (57)

Step A: To a solution of (3aR,5r,6aS)-5-(2-(trifluoromethyl)phenyl)hexahydrocyclopenta[c]pyrrole-2(1H)-carbonyl chloride (0.300 g, 1.03 mmol) in DMSO (8 mL) and ethyl 2-chloro-5-methyl-thiazole-4-carboxylate (0.211 g, 1.03 mmol) was added *i*-Pr₂NEt (0.40 g, 3.09 mmol). The resulting solution was heated at 110 °C for 24 h. The reaction was allowed to cooled to rt and diluted with H₂O (30 mL) and extracted with EtOAc (3 × 30 mL). The combined organic extracts were washed with brine (2 × 30 mL), dried over Na₂SO₄, filtered, and concentrated under reduced pressure. The resulting residue was chromatographed over silica gel (Isco CombiFlash Rf unit, 12 g RediSep column, 0–30% EtOAc in hexanes) to give ethyl 5-methyl-2-((3aR,5r,6aS)-5-(2-(trifluoromethyl)phenyl)hexahydrocyclopenta[c]-pyrrol-2(1H)-yl)thiazole-4-carboxylate as an off-white solid (0.042 g, 9%): ¹H NMR (300 MHz, DMSO-*d*₆) δ 7.76–7.70 (m, 1H), 7.68–7.54 (m, 2H), 7.42–7.35 (m, 1H), 4.22 (q, *J* = 6.9 Hz, 2H), 3.55–3.42 (m, 2H), 3.42–

3.35 (m, 2H), 2.97–2.83 (m, $J = 2$ Hz), 2.55 (s, 3H), 2.32–2.18 (m, 3H), 1.74–1.53 (m, 2H), 1.27 (t, $J = 6.9$ Hz, 3H); MS (ESI+) m/z 425 $[M + H]^+$.

Step B: A mixture of ethyl 5-methyl-2-((3*aR*,5*r*,6*aS*)-5-(2-(trifluoromethyl)phenyl)hexahydrocyclopenta[*c*]pyrrol-2(1*H*)-yl)-thiazole-4-carboxylate (0.040 g, 0.094 mmol) and LiOH·H₂O (0.039 g, 0.94 mmol) in THF (2 mL), CH₃OH (1 mL), and H₂O (0.5 mL) was stirred at rt for 16 h. The mixture was then acidified to pH 5 with 2 N aq HCl and diluted with H₂O (50 mL). The resulting solids were collected by filtration to provide 5-methyl-2-((3*aR*,5*r*,6*aS*)-5-(2-(trifluoromethyl)phenyl)hexahydrocyclopenta[*c*]pyrrol-2(1*H*)-yl)-thiazole-4-carboxylic acid (**57**) as a white solid (0.030 g, 81%): mp 166–170 °C; ¹H NMR (500 MHz, DMSO-*d*₆) δ 12.41 (br s, 1H), 7.72 (d, $J = 8.0$ Hz, 1H), 7.67–7.58 (m, 2H), 7.42–7.36 (m, 1H), 3.51–3.45 (m, 2H), 3.42–3.32 (m, 3H), 2.95–2.85 (m, 2H), 2.53 (s, 3H), 2.30–2.22 (m, 2H), 1.66–1.57 (m, 2H); MS (ESI+) m/z 397 $[M + H]^+$; HPLC >99% (AUC), (Method B), $t_R = 14.5$ min.

2-((3*aR*,5*r*,6*aS*)-5-(5-Fluoro-2-(trifluoromethyl)phenyl)-hexahydrocyclopenta[*c*]pyrrol-2(1*H*)-yl)-6-methylpyrimidine-4-carboxylic Acid (**61**)

Step A: To a N₂ degassed mixture of (3*aS*,6*aS*)-*tert*-butyl 5-(((trifluoromethyl)sulfonyl)oxy)-3,3*a*,6,6*a*-tetrahydro-cyclopenta[*c*]pyrrole-2(1*H*)-carboxylate ((±)-**23**, 5.0 g, 14.0 mmol), (5-fluoro-2-(trifluoromethyl)phenyl)boronic acid (2.91 g, 14.0 mmol), and aqueous 2 M Na₂CO₃ (100 mL) in DME (200 mL) was added Pd(PPh₃)₄ (0.500 g, 1.4 mmol). The mixture was heated at 80 °C for 6 h, then allowed to cool to rt and diluted with H₂O (500 mL). The aqueous mixture was extracted with EtOAc (2 × 200 mL), and the combined organic extracts were washed with H₂O (200 mL) and brine (200 mL), dried over Na₂SO₄, filtered, and concentrated under reduced pressure. The residue was purified by flash column chromatography (Isco CombiFlash Rf unit, 330 g Rediseq column, 0% to 10% EtOAc in hexanes) to give (3*aR*,6*aS*)-*tert*-butyl 5-(5-fluoro-2-(trifluoromethyl)phenyl)-3,3*a*,6,6*a*-tetrahydrocyclopenta[*c*]pyrrole-2(1*H*)-carboxylate (**58a**) as a clear, viscous oil (4.88 g, 94%).

Step B: A mixture of 5-(5-fluoro-2-(trifluoromethyl)phenyl)-3,3*a*,6,6*a*-tetrahydrocyclopenta[*c*]pyrrole-2(1*H*)-carboxylate (4.8 g, 12.9 mmol) and 10% Pd/C (1.57 g wet, 10% w/w) in CH₃OH (50 mL) was subjected to an atmosphere of H₂ gas (40 psi) using a Parr Shaker apparatus for 16 h at rt. The mixture was filtered through Celite, and the filtrate was concentrated under reduced pressure. The resulting residue was purified by flash column chromatography (Isco CombiFlash Rf unit, 40 g Rediseq column, 0% to 30% EtOAc in hexanes) to give (3*aR*,5*r*,6*aS*)-*tert*-butyl 5-(5-fluoro-2-(trifluoromethyl)phenyl)hexahydrocyclopenta[*c*]pyrrole-2(1*H*)-carboxylate (**59a**) as a clear, viscous oil (4.5 g 95%).

Step C: To a 0 °C cooled solution of (3*aR*,5*r*,6*aS*)-*tert*-butyl 5-(5-fluoro-2-(trifluoromethyl)phenyl)hexahydrocyclopenta[*c*]pyrrole-2(1*H*)-carboxylate (4.50 g, 12.1 mmol) in CH₂Cl₂ (60 mL) was added a 2.0 M HCl solution in Et₂O (100 mL), and the mixture was allowed to stir at rt for 24 h. The mixture was diluted with Et₂O (200 mL), and the precipitated product was filtered to give (3*aR*,5*r*,6*aS*)-5-(5-fluoro-2-

(trifluoromethyl)phenyl)octahydrocyclopenta[*c*]pyrrole hydrochloride (**60a**) as a white solid (3.45 g, 92%): MS (ESI+) m/z 274 [M + H]⁺.

Step D: To a solution of (3*aR*,5*r*,6*aS*)-5-(5-fluoro-2-(trifluoromethyl)phenyl)octahydrocyclopenta[*c*]pyrrole hydrochloride (1.0 g, 3.23 mmol) and Et₃N (1.43 mL, 10.29 mmol) in DMF (50 mL) was added a methyl 2-chloropyrimidine-4-carboxylate (0.641 g, 3.43 mmol), and the resulting solution was stirred at 60 °C for 16 h. The reaction was diluted with H₂O (200 mL) and extracted with EtOAc (3 × 100 mL). The combined organic extracts were washed with H₂O (3 × 100 mL) and brine (100 mL), dried over Na₂SO₄, filtered, and concentrated under reduced pressure. The resulting residue was chromatographed over silica gel (0% to 30% EtOAc in hexanes) to give methyl 2-((3*aR*,5*r*,6*aS*)-5-(5-fluoro-2-(trifluoromethyl)phenyl)-hexahydrocyclopenta[*c*]pyrrol-2(1*H*)-yl)-6-methylpyrimidine-4-carboxylate as an off-white solid (1.14 g, 84%): MS (ESI+) m/z 424 [M + H]⁺.

Step E: A solution of methyl 2-((3*aR*,5*r*,6*aS*)-5-(5-fluoro-2-(trifluoromethyl)phenyl)hexahydrocyclopenta[*c*]pyrrol-2(1*H*)-yl)-6-methylpyrimidine-4-carboxylate (1.0 g, 2.36 mmol) and 2 N aq NaOH (20 mL) in a 1:1 mixture of CH₃OH/THF (40 mL) was stirred at room temperature for 16 h. The mixture was carefully neutralized at 0 °C with 2 N aq HCl and extracted with CH₂Cl₂ (3 × 10 mL). The combined organic extracts were washed with brine, dried over Na₂SO₄, filtered, and concentrated under reduced pressure. The resulting residue was chromatographed over silica gel (0% to 10% CH₃OH in CH₂Cl₂) to give 2-((3*aR*,5*r*,6*aS*)-5-(5-fluoro-2-(trifluoromethyl)phenyl)hexahydrocyclopenta[*c*]pyrrol-2(1*H*)-yl)-6-methylpyrimidine-4-carboxylic acid (**61**) as an off-white solid (0.831 g, 86%): ¹H NMR (500 MHz, DMSO-*d*₆) δ 7.74 (m, 1H), 7.54 (m, 1H), 7.24 (m, 1H), 6.63 (s, 1H), 3.63 (m, 4H), 3.58 (m, 1H), 2.82 (m, 2H), 2.36 (m, 2H), 2.27 (s, 3H), 1.61 (m, 2H); MS (ESI+) m/z 410 [M + H]⁺; HPLC >99% (AUC) (Method B), *t*_R = 10.8 min.

2-((3*aR*,5*r*,6*aS*)-5-(3-Fluoro-2-(trifluoromethyl)phenyl)-hexahydrocyclopenta[*c*]pyrrol-2(1*H*)-yl)-6-methylpyrimidine-4-carboxylic Acid (62**)**—Compound **62** was prepared according to a similar procedure described for the synthesis of **61**. ¹H NMR (300 MHz, DMSO-*d*₆) δ 7.52–7.44 (m, 1H), 7.02–6.99 (d, *J* = 8.4 Hz, 1H), 6.89–6.84 (m, 2H), 3.80–3.73 (m, 2H), 3.46–3.42 (m, 4H), 3.14–3.04 (m, 4H); ESI MS m/z 411 [M + H]⁺; HPLC >99.0% purity (Method B), *t*_R = 16.8 min.

2-((3*aR*,5*r*,6*aS*)-5-(2-Chloro-5-fluorophenyl)hexahydrocyclopenta[*c*]pyrrol-2(1*H*)-yl)-6-methylpyrimidine-4-carboxylic Acid (63**)**—Compound **63** was prepared according to a similar procedure described for the synthesis of **61**. Mp 183–185 °C; ¹H NMR (500 MHz, DMSO-*d*₆) δ 13.22 (br s, 1H), 7.44 (dd, *J* = 9.0, 5.5 Hz, 1H), 7.34 (dd, *J* = 10.5, 3.0 Hz, 1H), 7.10–7.05 (m, 1H), 6.99 (s, 1H), 3.70–3.64 (m, 2H), 3.62–3.57 (m, 2H), 3.50–3.41 (m, 1H), 2.92–2.81 (m, 2H), 2.36 (s, 3H), 2.34–2.25 (m, 2H), 1.57–1.47 (m, 2H); MS (ESI+) m/z 376 [M + H]⁺; HPLC >99% purity (Method B), *t*_R = 12.7 min.

2-((3aR,5r,6aS)-5-(2-Chloro-3-fluorophenyl)hexahydrocyclopenta[c]pyrrol-2(1H)-yl)-6-methylpyrimidine-4-carboxylic Acid (64)—Compound **64** was prepared according to a similar procedure described for the synthesis of **61**. ¹H NMR (300 MHz, DMSO-*d*₆) δ 7.35–7.28 (m, 2H), 7.28–7.19 (m, 1H), 6.68 (s, 1H), 3.62–3.54 (m, 4H), 3.53–3.41 (m, 1H), 2.91–2.76 (m, 2H), 2.40–2.26 (m, 2H), 2.33 (s, 3H), 1.56–1.41 (m, 2H); MS (ESI+) *m/z* 376 [M + H]⁺; HPLC >99% purity (Method B), *t*_R = 10.9 min.

2-((3aR,5r,6aS)-5-(2-Chloro-3-fluorophenyl)hexahydrocyclopenta[c]pyrrol-2(1H)-yl)-6-methylpyrimidine-4-carboxylic Acid (65)—Compound **65** was prepared according to a similar procedure described for the synthesis of **61**. Mp 176–180 °C; ¹H NMR (300 MHz, DMSO-*d*₆) δ 13.31 (br s, 1H), 8.99 (s, 1H), 8.65 (d, *J* = 5.1 Hz, 1H), 7.65 (d, *J* = 5.1 Hz, 1H), 6.99 (s, 1H), 3.75–3.62 (m, 4H), 3.41–3.35 (m, 1H), 2.91–2.90 (m, 2H), 2.37 (s, 3H), 2.32–2.27 (m, 2H), 1.80–1.74 (m, 2H); MS (ESI+) *m/z* 393 [M + H]⁺; HPLC 98.3% purity (Method H), *t*_R = 13.8 min.

2-((3aR,5r,6aS)-5-(2-Chloro-3-fluorophenyl)hexahydrocyclopenta[c]pyrrol-2(1H)-yl)-6-methylpyrimidine-4-carboxylic Acid (66)—Compound **66** was prepared according to a similar procedure described for the synthesis of **61**. Mp 161 – 165 °C; ¹H NMR (300 MHz, DMSO-*d*₆) δ 13.31 (br s, 1H), 8.55–8.53 (m, 1H), 8.22 (d, *J* = 8.1 Hz, 1H), 7.67–7.62 (m, 1H), 7.00 (s, 1H), 3.71–3.61 (m, 4H), 3.44–3.38 (m, 1H), 2.91–2.89 (m, 2H), 2.37 (s, 3H), 2.31–2.23 (m, 2H), 1.67–1.57 (m, 2H); MS (ESI+) *m/z* 393 [M + H]⁺; HPLC >99.0% purity (Method B), *t*_R = 14.7 min.

Supplementary Material

Refer to Web version on PubMed Central for supplementary material.

Acknowledgments

This study was supported by NIH Grants U01 NS074476 (to K.P.), P30 EY019007 (Core Support for Vision Research), and unrestricted funds from Research to Prevent Blindness (New York, NY) to the Department of Ophthalmology, Columbia University. We thank The Burch Family Foundation, the Mary Jaharis-John Catsimatidis Scholarship Fund, the Kaplen Foundation, and the Eye Surgery Fund for gifts supporting this study. This project has also been funded in whole or in part with Federal funds from the National Institute of Neurological Disorders and Stroke, the National Eye Institute, the NIH Blueprint Neurotherapeutics Network, Blueprint for Neuro-science Research Program, National Institutes of Health, Department of Health and Human Services, under Contract No. HHSN271201100013C.

ABBREVIATIONS USED

AMD	age-related macular degeneration
A2E	<i>N</i> -retinide- <i>N</i> -retinylidene ethanolamine
SPA	scintillation proximity assay
HTRF	homogeneous time-resolved fluorescence assay

HLM	human liver microsomes
RLM	rat liver microsomes
<i>n</i>-BuLi	<i>n</i> -butyl lithium
THF	tetrahydrofuran
DMF	<i>N,N</i> -dimethylformamide
DME	dimethoxyethane
Et₂O	diethyl ether
EtOAc	ethyl acetate
CH₃OH	methyl alcohol
EtOH	ethyl alcohol
Boc₂O	di- <i>tert</i> -butyl dicarbonate
TFA	trifluoroacetic acid
Pd(OAc)₂	palladium(II) acetate
Pd₂(dba)₃	tris-(dibenzylideneacetone) dipalladium(0)
BINAP	2,2'-bis-(diphenylphosphino)-1,1'-binaphthalene
XantPhos	4,5-bis-(diphenylphosphino)-9,9-dimethylxanthene
JohnPhos	(2-biphenyl)di- <i>tert</i> -butylphosphine
Ac₂O	acetic anhydride
NaOAc	sodium acetate
LiHMDS	lithium bis(trimethylsilyl)amide
<i>i</i>-Pr₂NEt	<i>N,N</i> -diisopropylethylamine
Et₃N	triethylamine
LiOH·H₂O	lithium hydroxide monohydrate
NaOH	sodium hydroxide
SOCl₂	thionyl chloride
Pd(PPh₃)₄	tetrakis(triphenylphosphine)palladium(0)
PhN(SO₂CF₃)₂	1,1,1-trifluoro- <i>N</i> -phenyl- <i>N</i> -((trifluoromethyl)sulfonyl)-methanesulfonamide
LiAlH₄	lithium aluminum hydride

Gly	glycine
Tyr	tyrosine
Arg	arginine
Gln	glutamine
Leu	leucine
Phe	phenylalanine
CYP	cytochrome P450
CYP2C9	cytochrome P450 2C9
CYP2C19	cytochrome P450 2C19
CYP2D6	cytochrome P450 2D6
CYP3A4	cytochrome P450 3A4
GPCR	G-protein coupled receptor
hERG	human ether-à-go-go-related gene
PK	pharmacokinetics
PD	pharmacodynamics
iv	intravenous
po	oral
qd	once daily
Cl	clearance
V_{ss}	volume of distribution at steady state
AUC	area under the curve
% F	% bioavailability
SAR	structure–activity relationship
SPR	structure–property relationship
ADME	absorption, distribution, metabolism, elimination
PPB	plasma protein binding
THF	tetrahydrofuran
DME	dimethoxyethane
CH₂Cl₂	dichloromethane

CH₃CN	acetonitrile
aq	aqueous

REFERENCES

- Petrukhin K. New therapeutic targets in atrophic age-related macular degeneration. *Expert Opin. Ther. Targets.* 2007; 11(5):625–639. [PubMed: 17465722]
- Hubschman JP, Reddy S, Schwartz SD. Age-related macular degeneration: current treatments. *Clin. Ophthalmol.* 2009; 3:155–166. [PubMed: 19668560]
- [accessed June 10, 2015] Macular Degeneration Facts and Statistics. <http://www.brightfocus.org/macular/about/understanding/facts.html>
- (a) Young RW. Pathophysiology of age-related macular degeneration. *Surv. Ophthalmol.* 1987; 31(5):291–306. [PubMed: 3299827] (b) Dorey CK, Wu G, Ebenstein D, Garsd A, Weiter JJ. Cell loss in the aging retina. Relationship to lipofuscin accumulation and macular degeneration. *Invest. Ophthalmol. Visual Sci.* 1989; 30(8):1691–1699. [PubMed: 2759786] (c) Holz FG, Bellman C, Staudt S, Schutt F, Volcker HE. Fundus autofluorescence and development of geographic atrophy in age-related macular degeneration. *Invest. Ophthalmol. Visual Sci.* 2001; 42(5):1051–1056. [PubMed: 11274085] (d) Holz FG, Bellmann C, Margaritidis M, Schutt F, Otto TP, Volcker HE. Patterns of increased in vivo fundus autofluorescence in the junctional zone of geographic atrophy of the retinal pigment epithelium associated with age-related macular degeneration. *Graefe's Arch. Clin. Exp. Ophthalmol.* 1999; 237(2):145–152. [PubMed: 9987631] (e) Holz FG, Bindewald-Wittich A, Fleckenstein M, Dreyhaupt J, Scholl HP, Schmitz-Valckenberg S. Progression of geographic atrophy and impact of fundus autofluorescence patterns in age-related macular degeneration. *Am. J. Ophthalmol.* 2007; 143(3):463–472. [PubMed: 17239336] (f) Schmitz-Valckenberg S, Fleckenstein M, Scholl HP, Holz FG. Fundus autofluorescence and progression of age-related macular degeneration. *Surv. Ophthalmol.* 2009; 54(1):96–117. [PubMed: 19171212] (g) Finnemann SC, Leung LW, Rodriguez-Boulan E. The lipofuscin component A2E selectively inhibits phagolysosomal degradation of photoreceptor phospholipid by the retinal pigment epithelium. *Proc. Natl. Acad. Sci. U. S. A.* 2002; 99(6):3842–3847. [PubMed: 11904436] (h) Suter M, Reme C, Grimm C, Wenzel A, Jaattela M, Esser P, Kociok N, Leist M, Richter C. Age-related macular degeneration. The lipofuscin component N-retinyl-N-retinylidene ethanolamine detaches proapoptotic proteins from mitochondria and induces apoptosis in mammalian retinal pigment epithelial cells. *J. Biol. Chem.* 2000; 275(50):39625–39630. [PubMed: 11006290] (i) Sparrow JR, Fishkin N, Zhou J, Cai B, Jang YP, Krane S, Itagaki Y, Nakanishi K. A2E, a byproduct of the visual cycle. *Vision Res.* 2003; 43(28):2983–2990. [PubMed: 14611934] (j) Sparrow JR, Gregory-Roberts E, Yamamoto K, Blonska A, Ghosh SK, Ueda K, Zhou J. The bisretinoids of retinal pigment epithelium. *Prog. Retinal Eye Res.* 2012; 31(2):121–135. (k) Delori, FC. RPE Lipofuscin in Ageing and Age-Related Macular Degeneration. In: Coscas, G.; Piccolino, FC., editors. *Retinal Pigment Epithelium and Macular Diseases (Documenta Ophthalmologica)*. Vol. 62. Dordrecht, The Netherlands: Kluwer Academic Publishers; 1995. p. 37-45.
- Weng J, Mata NL, Azarian SM, Tzekov RT, Birch DG, Travis GH. Insights into the function of Rim protein in photoreceptors and etiology of Stargardt's disease from the phenotype in abcr knockout mice. *Cell (Cambridge, MA, U. S.)*. 1999; 98(1):13–23.
- (a) Sparrow JR, Cai B. Blue light-induced apoptosis of A2E-containing RPE: involvement of caspase-3 and protection by Bcl-2. *Invest. Ophthalmol. Visual Sci.* 2001; 42(6):1356–1362. [PubMed: 11328751] (b) Bergmann M, Schutt F, Holz FG, Kopitz J. Inhibition of the ATP-driven proton pump in RPE lysosomes by the major lipofuscin fluorophore A2-E may contribute to the pathogenesis of age-related macular degeneration. *FASEB J.* 2004; 18(3):562–564. [PubMed: 14715704] (c) Sparrow JR, Parish CA, Hashimoto M, Nakanishi K. A2E, a lipofuscin fluorophore, in human retinal pigmented epithelial cells in culture. *Invest. Ophthalmol. Visual Sci.* 1999; 40(12): 2988–2995. [PubMed: 10549662] (d) De S, Sakmar TP. Interaction of A2E with model membranes. Implications to the pathogenesis of age-related macular degeneration. *J. Gen. Physiol.* 2002; 120(2): 147–157. [PubMed: 12149277] (e) Vives-Bauza C, Anand M, Shirazi AK, Magrane J, Gao J, Vollmer-Snarr HR, Manfredi G, Finnemann SC. The age lipid A2E and mitochondrial dysfunction synergistically impair phagocytosis by retinal pigment epithelial cells. *J. Biol. Chem.* 2008;

- 283(36):24770–24780. [PubMed: 18621729] (f) Zhou J, Jang YP, Kim SR, Sparrow JR. Complement activation by photooxidation products of A2E, a lipofuscin constituent of the retinal pigment epithelium. *Proc. Natl. Acad. Sci. U. S. A.* 2006; 103(44):16182–16187. [PubMed: 17060630] (g) Radu RA, Hu J, Yuan Q, Welch DL, Makshanoff J, Lloyd M, McMullen S, Travis GH, Bok D. Complement system dysregulation and inflammation in the retinal pigment epithelium of a mouse model for Stargardt macular degeneration. *J. Biol. Chem.* 2011; 286(21):18593–18601. [PubMed: 21464132] (h) Ben-Shabat S, Parish CA, Vollmer HR, Itagaki Y, Fishkin N, Nakanishi K, Sparrow JR. Biosynthetic studies of A2E, a major fluorophore of retinal pigment epithelial lipofuscin. *J. Biol. Chem.* 2002; 277(9):7183–7190. [PubMed: 11756445] (i) Rozanowska M, Jarvis-Evans J, Korytowski W, Boulton ME, Burke JM, Sarna T. Blue light-induced reactivity of retinal age pigment. In vitro generation of oxygen-reactive species. *J. Biol. Chem.* 1995; 270(32):18825–18830. [PubMed: 7642534] (j) Sparrow JR, Zhou J, Ben-Shabat S, Vollmer H, Itagaki Y, Nakanishi K. Involvement of oxidative mechanisms in blue-light-induced damage to A2E-laden RPE. *Invest. Ophthalmol. Visual Sci.* 2002; 43(4):1222–1227. [PubMed: 11923269] (k) Dontsov AE, Sakina NL, Golubkov AM, Ostrovsky MA. Light-induced release of A2E photooxidation toxic products from lipofuscin granules of human retinal pigment epithelium. *Dokl. Biochem. Biophys.* 2009; 425:98–101. [PubMed: 19496332]
7. (a) Radu RA, Han Y, Bui TV, Nusinowitz S, Bok D, Lichter J, Widder K, Travis GH, Mata NL. Reductions in serum vitamin A arrest accumulation of toxic retinal fluorophores: a potential therapy for treatment of lipofuscin-based retinal diseases. *Invest. Ophthalmol. Visual Sci.* 2005; 46(12):4393–4401. [PubMed: 16303925] (b) Radu RA, Mata NL, Nusinowitz S, Liu X, Sieving PA, Travis GH. Treatment with isotretinoin inhibits lipofuscin accumulation in a mouse model of recessive Stargardt's macular degeneration. *Proc. Natl. Acad. Sci. U. S. A.* 2003; 100(8):4742–4747. [PubMed: 12671074] (c) Maeda A, Maeda T, Golczak M, Imanishi Y, Leahy P, Kubota R, Palczewski K. Effects of potent inhibitors of the retinoid cycle on visual function and photoreceptor protection from light damage in mice. *Mol. Pharmacol.* 2006; 70(4):1220–1229. [PubMed: 16837623] (d) Palczewski K. Retinoids for treatment of retinal diseases. *Trends Pharmacol. Sci.* 2010; 31(6):284–295. [PubMed: 20435355]
8. Petrukhin K. Pharmacological inhibition of lipofuscin accumulation in the retina as a therapeutic strategy for dry AMD treatment. *Drug Discovery Today: Ther. Strategies.* 2013; 10(1):e11–e20.
9. Cioffi CL, Dobri N, Freeman EE, Conlon MP, Chen P, Stafford DG, Schwarz DMC, Golden KC, Zhu L, Kitchen DB, Barnes KD, Racz B, Qin Q, Michelotti E, Cywin CL, Martin WH, Pearson PG, Johnson G, Petrukhin K. Design, Synthesis, and Evaluation of Nonretinoid Retinol Binding Protein 4 Antagonists for the Potential Treatment of Atrophic Age-Related Macular Degeneration and Stargardt Disease. *J. Med. Chem.* 2014; 57(18):7731–7757. [PubMed: 25210858]
10. (a) Kanai M, Raz A, Goodman DS. Retinol-binding protein: the transport protein for vitamin A in human plasma. *J. Clin. Invest.* 1968; 47(9):2025–2044. [PubMed: 5675424] (b) Naylor HM, Newcomer ME. The structure of human retinol-binding protein (RBP) with its carrier protein transthyretin reveals an interaction with the carboxy terminus of RBP. *Biochemistry.* 1999; 38(9):2647–2653. [PubMed: 10052934] (c) Noy N, Slosberg E, Scarlata S. Interactions of retinol with binding proteins: studies with retinol-binding protein and with transthyretin. *Biochemistry.* 1992; 31(45):11118–11124. [PubMed: 1445851] (d) Noy N, Xu ZJ. Interactions of retinol with binding proteins: implications for the mechanism of uptake by cells. *Biochemistry.* 1990; 29(16):3878–3883. [PubMed: 2354158] (e) Monaco HL. The transthyretin-retinol-binding protein complex. *Biochim Biophys. Acta, Protein Struct. Mol. Enzymol.* 2000; 1482(1–2):65–72. (f) Monaco HL. Three-dimensional structure of the transthyretin-retinol-binding protein complex. *Clin. Chem. Lab. Med.* 2002; 40(12):1229–1236. [PubMed: 12553423] (g) Monaco HL, Rizzi M, Coda A. Structure of a complex of two plasma proteins: transthyretin and retinol-binding protein. *Science.* 1995; 268(5213):1039–1041. [PubMed: 7754382]
11. Schlehner S, Skerra A. Lipocalins in drug discovery: from natural ligand-binding proteins to "anticalins". *Drug Discovery Today.* 2005; 10(1):23–33. [PubMed: 15676296]
12. Wolf G. Multiple functions of vitamin A. *Physiol. Rev.* 1984; 64(3):873–937. [PubMed: 6377341]
13. (a) Berni R, Formelli F. In vitro interaction of fenretinide with plasma retinol-binding protein and its functional consequences. *FEBS Lett.* 1992; 308(1):43–45. [PubMed: 1386578] (b) Adams WR, Smith JE, Green MH. Effects of N-(4-hydroxyphenyl)retinamide on vitamin A metabolism in rats. *Exp. Biol. Med.* 1995; 208(2):178–185.

14. Mata NL, Lichter JB, Vogel R, Han Y, Bui TV, Singerman LJ. Investigation of Oral Fenretinide for Treatment of Geographic Atrophy in Age-Related Macular Degeneration. *Retina*. 2013; 33(3): 498–507. [PubMed: 23023528]
15. Motani A, Wang Z, Conn M, Siegler K, Zhang Y, Liu Q, Johnstone S, Xu H, Thibault S, Wang Y, Fan P, Connors R, Le H, Xu G, Walker N, Shan B, Coward P. Identification and characterization of a non-retinoid ligand for retinol-binding protein 4 which lowers serum retinol-binding protein 4 levels in vivo. *J. Biol. Chem.* 2009; 284(12):7673–7680. [PubMed: 19147488]
16. Dobri N, Qin Q, Kong J, Yamamoto K, Liu Z, Moiseyev G, Ma J-X, Allikmets R, Sparrow JR, Petrukhin K. A1120, a Nonretinoid RBP4 Antagonist, Inhibits Formation of Cytotoxic Bisretinoids in the Animal Model of Enhanced Retinal Lipofuscinogenesis. *Invest. Ophthalmol. Visual Sci.* 2013; 54(1):85–95. [PubMed: 23211825]
17. Swanson DM, Dubin AE, Shah C, Nasser N, Chang L, Dax SL, Jetter M, Breitenbucher JG, Liu C, Mazur C, Lord B, Gonzales L, Hoey K, Rizzolio M, Bogenstaetter M, Codd EE, Lee DH, Zhang SP, Chaplan SR, Carruthers NI. Identification and biological evaluation of 4-(3-trifluoromethylpyridin-2-yl)-piperazine-1-carboxylic acid (5-trifluoromethylpyridin-2-yl)amide, a high affinity TRPV1 (VR1) vanilloid receptor antagonist. *J. Med. Chem.* 2005; 48(6):1857–1872. [PubMed: 15771431]
18. (a) Dart MJ, Searle XB, Tietje KR, Toupençe RB. Azabicyclic Compounds Are Central Nervous System Active Agents. PCT Int. Appl. WO2004016604 A2. Google Patents. 2004(b) Lauffer D, Li P, Waal N, McGinty K, Tang Q, Ronkin S, Farmer L, Shannon D, Jacobs D. C-Met Protein Kinase Inhibitors. PCT Int. Appl. WO2009045992 A2. Google Patents. 2009(c) Guillemont JEG, Lancois DFA, Motte MMS, Koul A, Balemans WMA, Arnoult EPA. Antibacterial Cyclopenta[c]pyrrole Substituted 3,4-Dihydro-1H-[1,8]naphthyridinones. PCT Int. Appl. WO2013021054 A1. Google Patents. 2013
19. Cogan U, Kopelman M, Mokady S, Shinitzky M. Binding affinities of retinol and related compounds to retinol binding proteins. *Eur. J. Biochem.* 1976; 65(1):71–78. [PubMed: 945163]
20. Gamble MV, Ramakrishnan R, Palafox NA, Briand K, Berglund L, Blaner WS. Retinol binding protein as a surrogate measure for serum retinol: studies in vitamin A-deficient children from the Republic of the Marshall Islands. *Am. J. Clin. Nutr.* 2001; 73(3):594–601. [PubMed: 11237937]

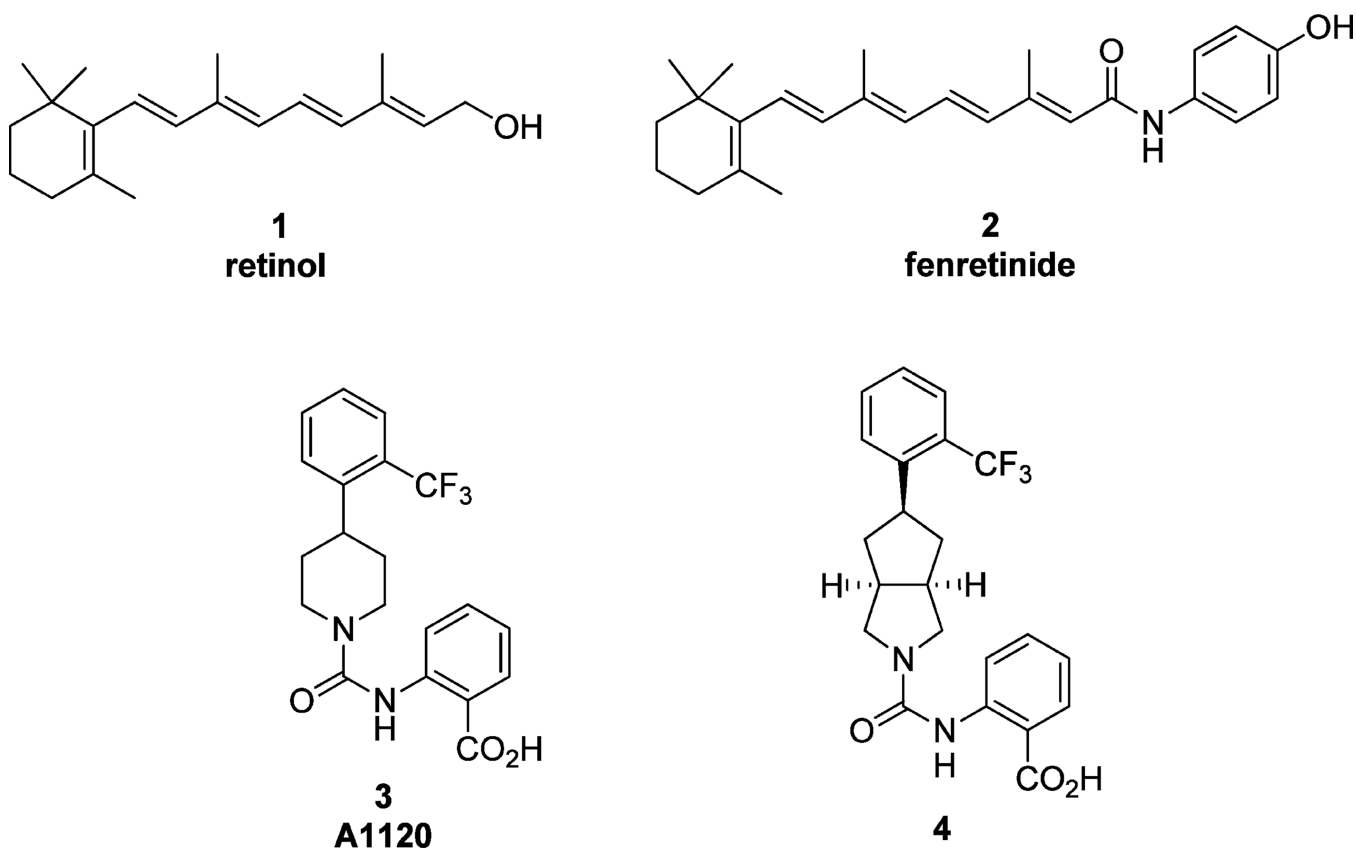


Figure 1. Retinol (**1**), fenretinide (**2**), A1120 (**3**), and 2-((3aR,5r,6aS)-5-(2-(trifluoromethyl)phenyl)octahydrocyclopenta[*c*]pyrrole-2-carboxamido)benzoic acid (**4**).

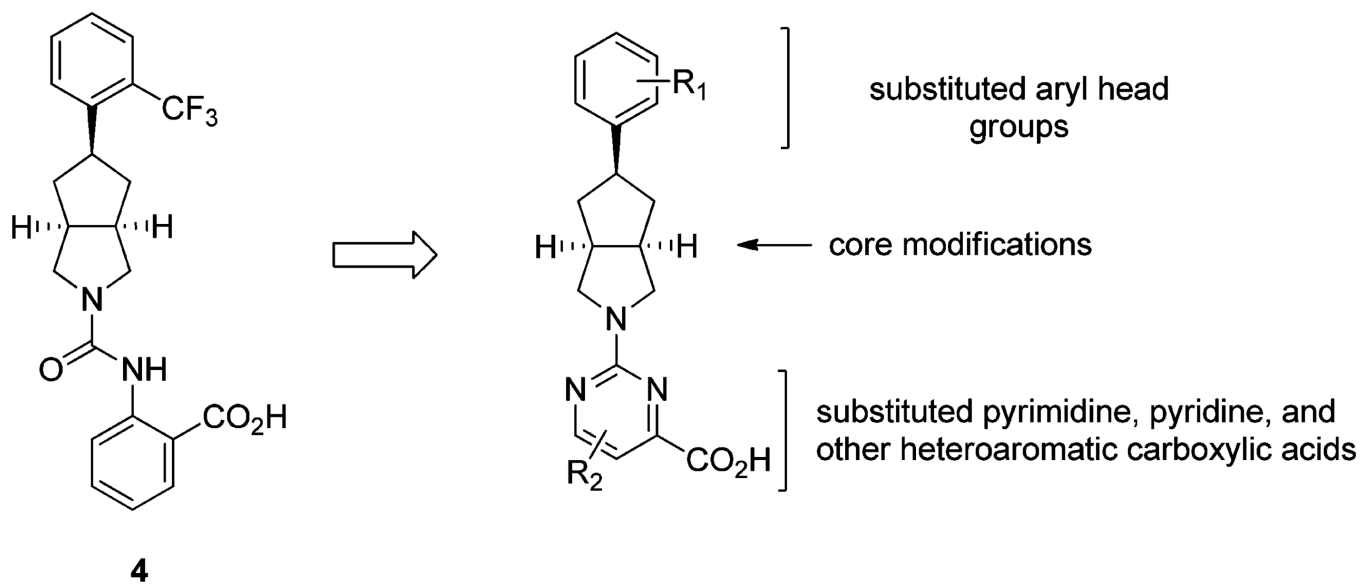


Figure 2. Medicinal chemistry work plan for pyrimidine-4-carboxylic acid containing antagonists of RBP4.

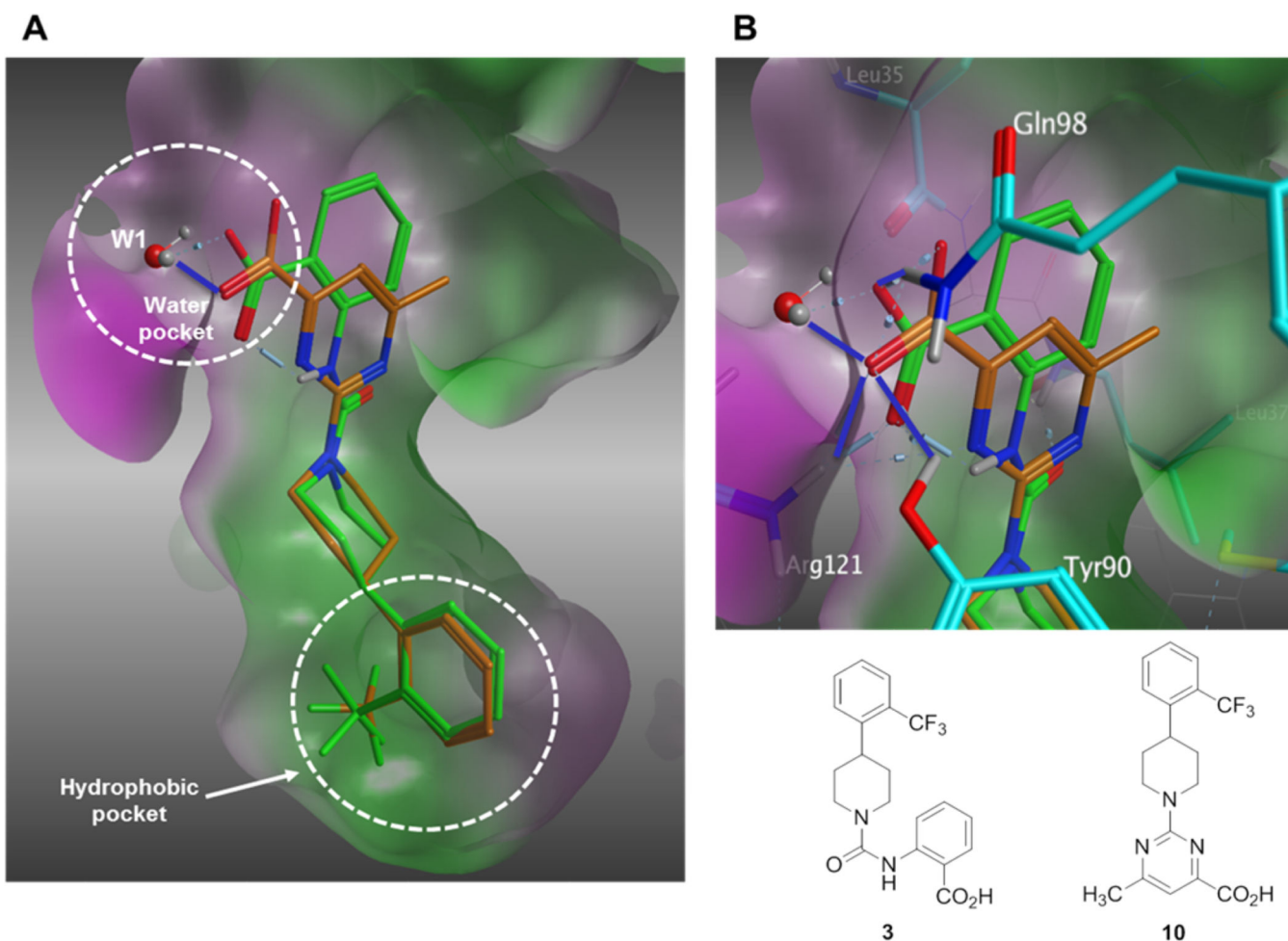


Figure 3.

(A) Overlay of minimized bound conformations of RBP4 antagonist **10** (orange) and **3** (green) within *3fmz*. (B) Expanded view of the anthranilic acid and 6-methylpyrimidine-4-carboxylic acid fragments of **3** and analogue **10**. Both moieties are shown engaging in H-bond interactions with Arg121, Gln98, and Tyr90. H-bond interactions to **10** are indicated with blue lines. Residues making contact with ligands are labeled and illustrated in stick format. Molecular surface is colored by hydrophobicity (green) and hydrophilicity (purple) using contact preferences (MOE, Chemical Computing Group, Inc., Montreal, CA).

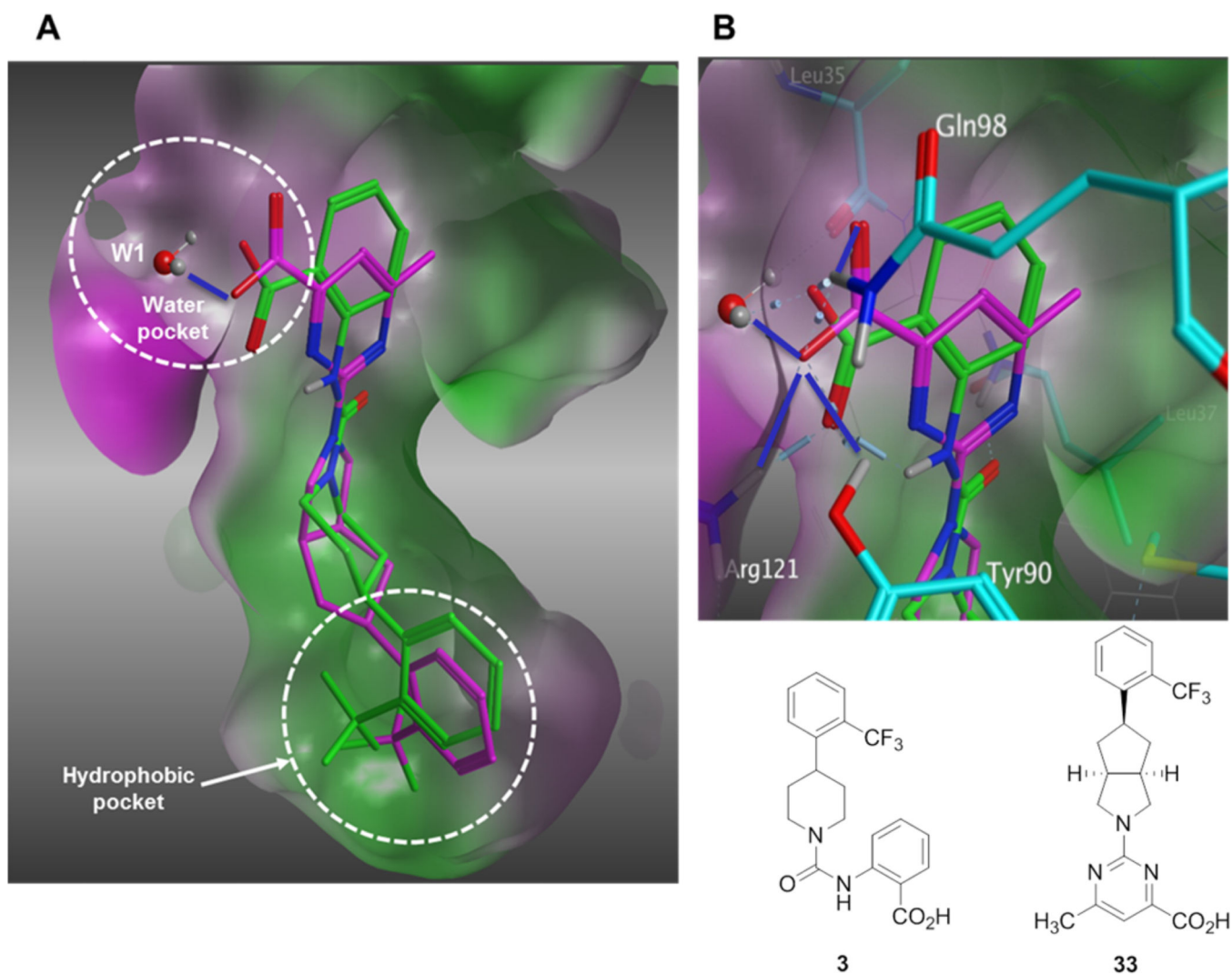


Figure 4.

(A) Overlay of minimized bound conformations of RBP4 antagonist **33** (magenta) and **3** (orange) within *3fmz*. (B) Expanded view of the anthranilic acid and 6-methylpyrimidine-4-carboxylic acid fragments of **3** (green) and analogue **33** (magenta). Both moieties are shown engaging in H-bond interactions with Arg121, Gln98, and Tyr90. H-bond interactions to **33** are indicated with blue lines. Residues making contact with ligands are labeled and illustrated in stick format. The molecular surface is colored by hydrophobicity (green) and hydrophilicity (purple) using contact preferences (MOE, Chemical Computing Group, Inc., Montreal, CA).

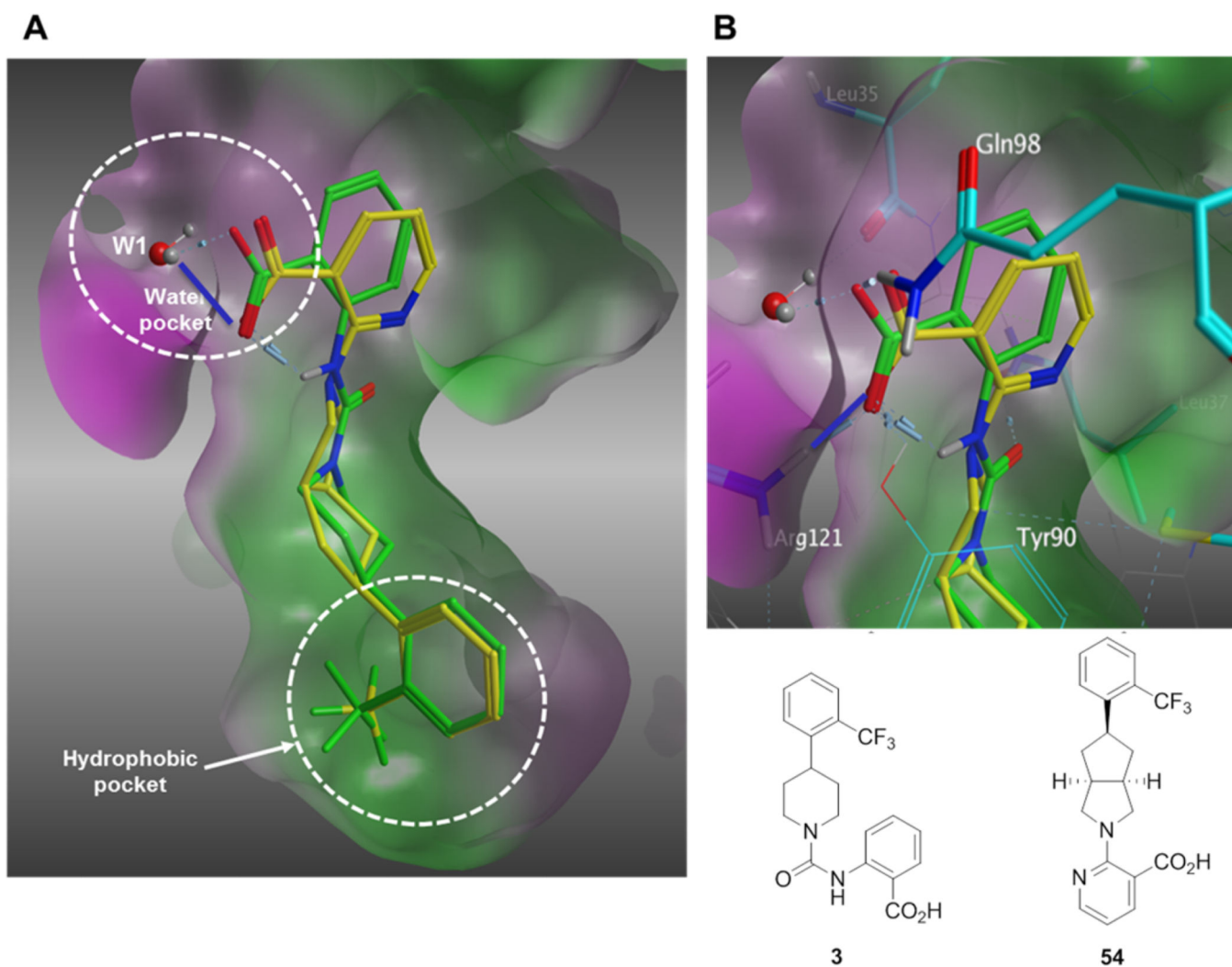
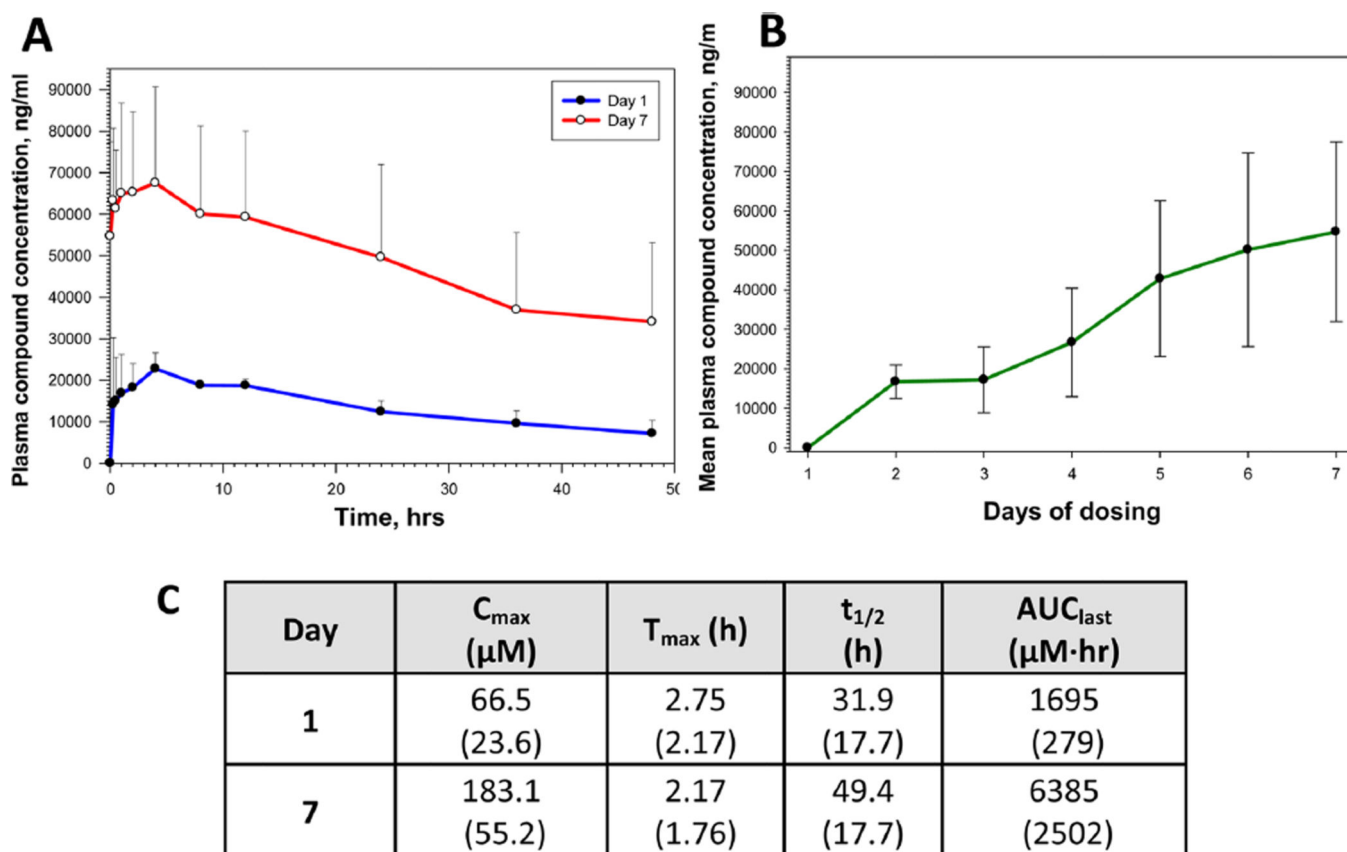


Figure 5.

(A) Overlay of minimized bound conformations of RBP4 nicotinic acid antagonist **54** (yellow) and **3** (A1120, green) within *3fmz*. (B) Expanded view of the anthranilic acid and nicotinic acid fragments of **3** (green) and analogue **54** (yellow). Both moieties are shown engaging in H-bond interactions with Arg121, Gln98, and Tyr90. H-bond interactions to **54** are indicated with blue lines. Residues making contact with ligands are labeled and illustrated in stick format. The molecular surface is colored by hydrophobicity (green) and hydrophilicity (purple) using contact preferences (MOE, Chemical Computing Group, Inc., Montreal, CA).

**Figure 6.**

(A) Plasma exposure levels of analogue **33** in Sprague–Dawley rats following a single (Day 1) and 7-day (Day 7) QD oral dose administration at 18.2 $\mu\text{mol/kg}$ (5 mg/kg). Data represented as the mean (SD). Each dosing group consisted of three drug naïve adult male Sprague–Dawley rats; the test article vehicle was 2% Tween 80 in 0.9% saline. The difference in plasma compound concentration between Day 1 and Day 7 samples was statistically significant at all time points studied ($P < 0.05$; two-tailed unpaired Student's t test). (B) Plasma concentration of analogue **33** at predose time points during the 7-day QD oral dose administration in three rats from Group 3. Data represented as the mean (SD). The predose compound concentration was statistically significantly increased at Day 7 in comparison to the Day 2 predose level ($P < 0.05$; two-tailed unpaired Student's t test). (C) Pharmacokinetic parameters for **33** in Sprague–Dawley rats after a single dose (Day 1) and seven QD oral doses (Day 7) at 18.2 $\mu\text{mol/kg}$. Data are represented as the mean with standard deviation shown in parentheses.

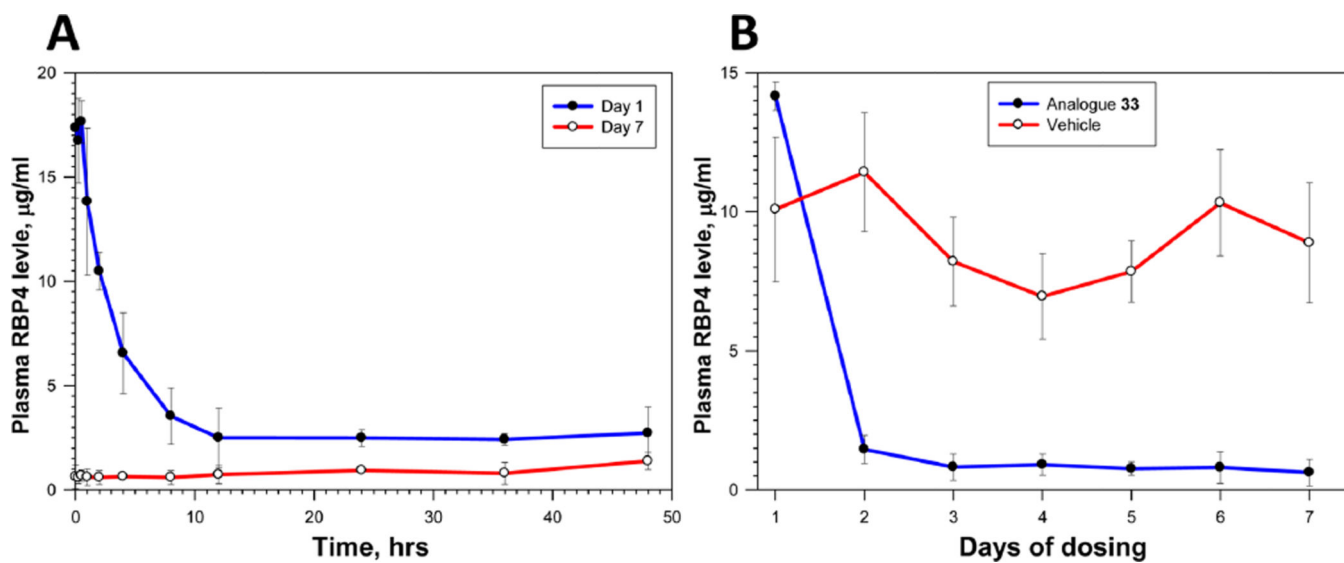
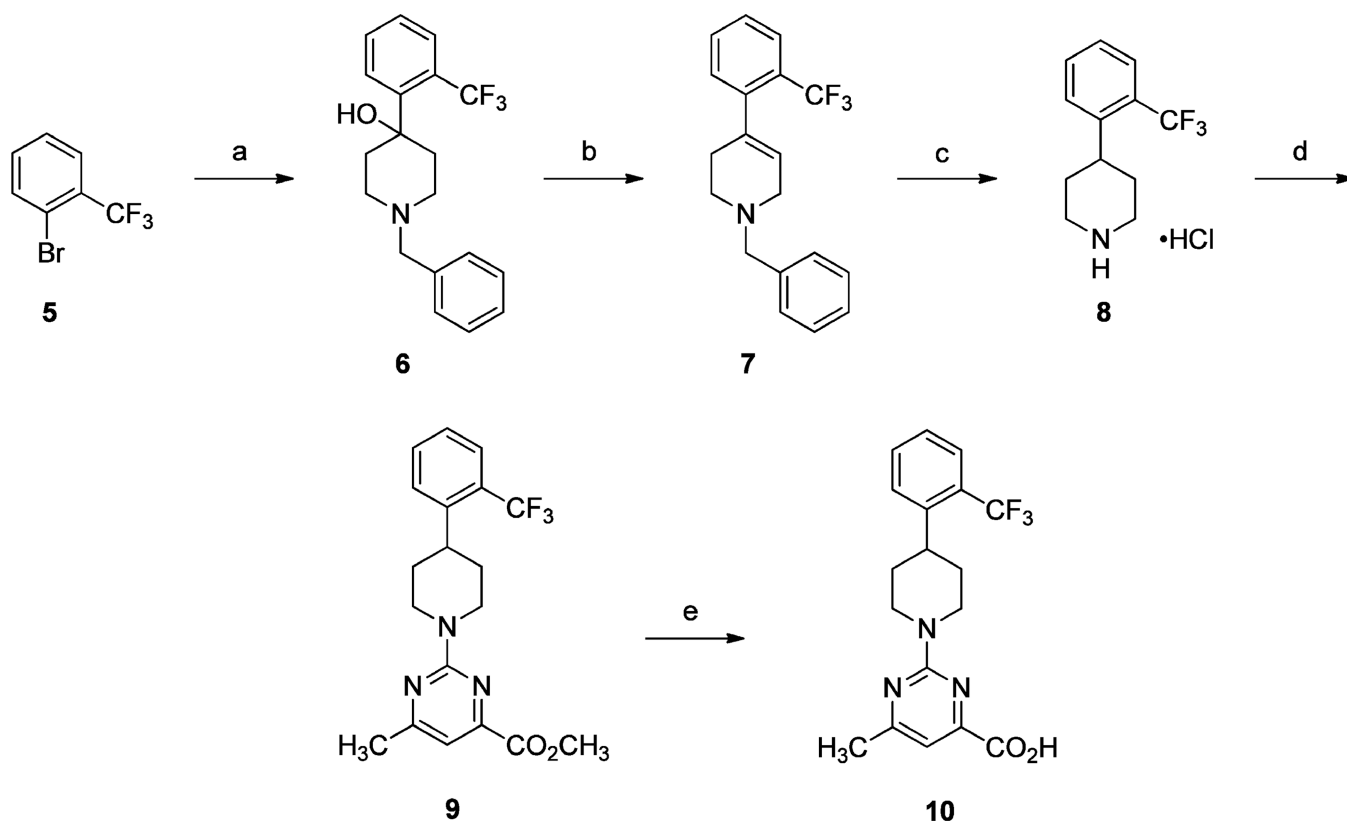
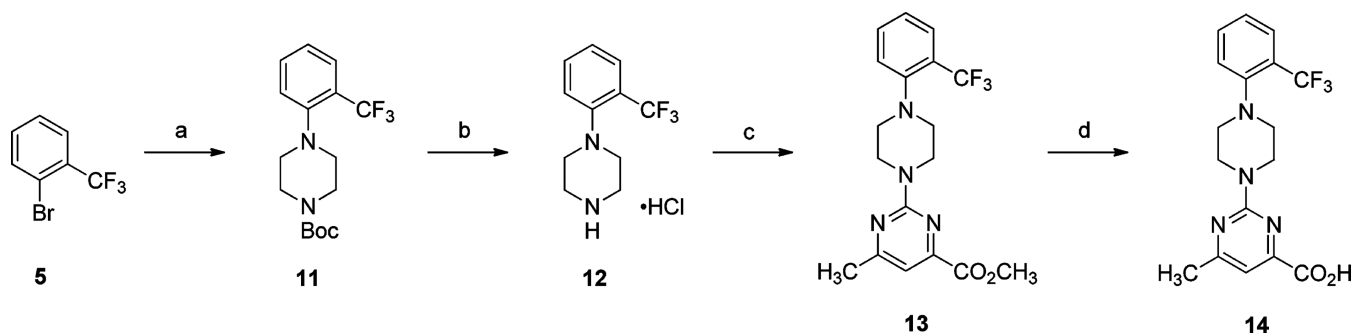


Figure 7.

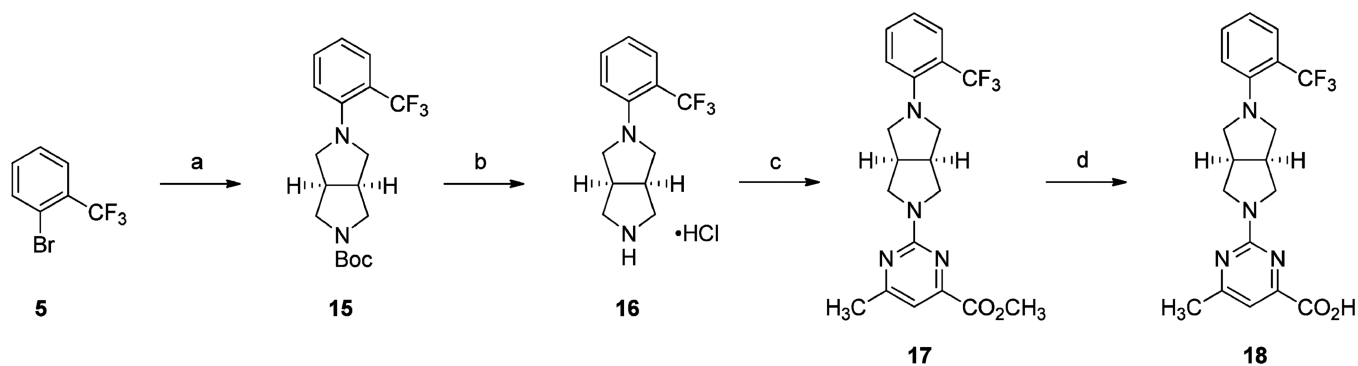
(A) Plasma RBP4 levels ($\mu\text{g/mL}$) in male Sprague–Dawley rats following single (Day 1, Group 1) and 7-day (Day 7, Group 3) $18.2 \mu\text{mol/kg}$ (5 mg/kg) QD dose administration of analogue **33**. Data represented as the mean (SD). (B) Plasma RBP4 levels ($\mu\text{g/mL}$) at predose time-points during the 7-day 5 mg/kg QD oral dose administration of analogue **33** (Group 3) or test article vehicle (Group 2) in Sprague–Dawley rats. Data represented as the mean (SD).

**Scheme 1^a**

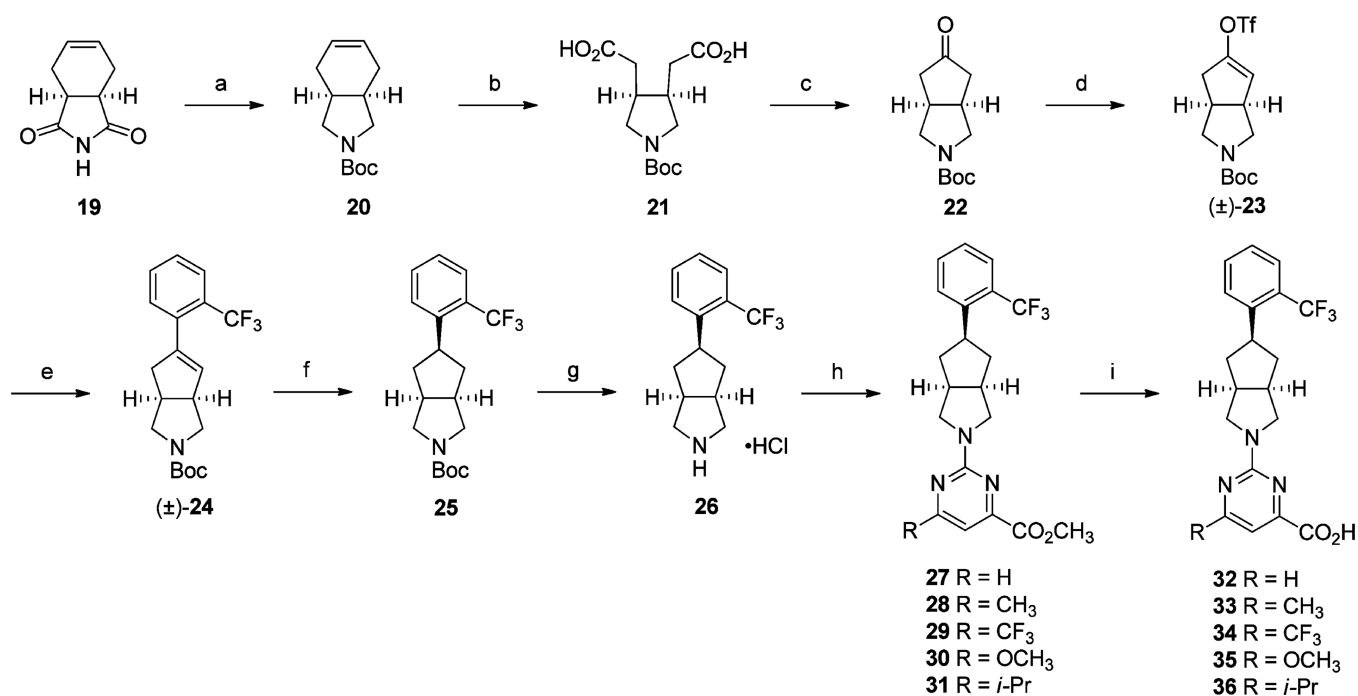
^aReagents and conditions: (a) (i) *n*-BuLi, THF, -78 °C, 40 min; (ii) 1-benzylpiperidin-4-one, THF, -78 °C; (b) SOCl₂, 0 °C, 2 h; (c) (i) HCO₂NH₄, 10% Pd/C, CH₃OH, reflux; (ii) 4.0 M HCl solution in 1,4-dioxane, CH₃CN, rt, 2 h; (d) methyl 2-chloro-6-methylpyrimidine-4-carboxylate, *i*-Pr₂NEt Et₃N, DMF, 60 °C, 16 h; (e) (i) LiOH·H₂O, H₂O, THF, rt, 16 h; (ii) 2 N aq HCl.

**Scheme 2^a**

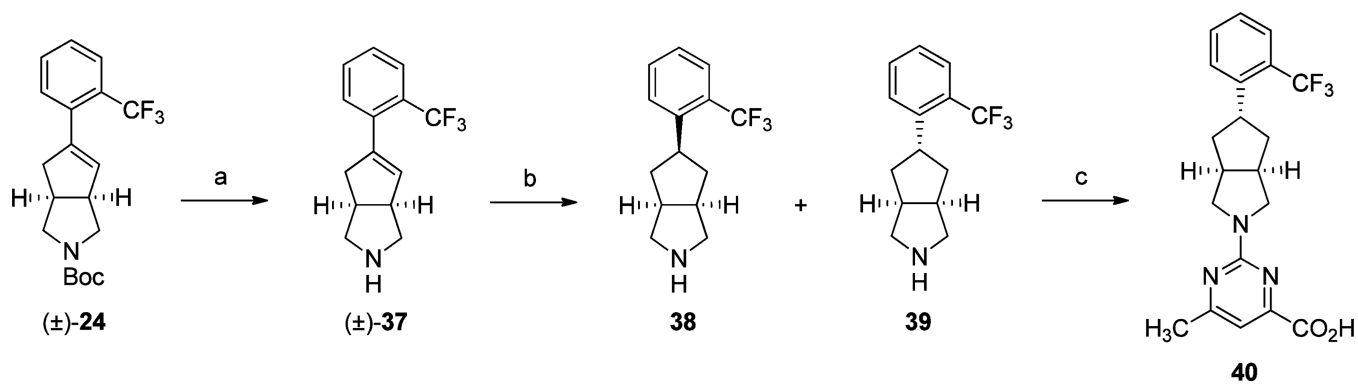
^aReagents and conditions: (a) *tert*-butyl piperazine-1-carboxylate, Pd(OAc)₂, BINAP, NaO*t*-Bu toluene, 110 °C, 16 h; (b) 2.0 M HCl solution in Et₂O, CH₂Cl₂, rt, 3 h; (c) methyl 2-chloro-6-methylpyrimidine-4-carboxylate, *i*-Pr₂NEt, DMF, 60 °C, 16 h; (d) (i) LiOH·H₂O, H₂O, THF, rt, 16 h; (ii) 2 N aq HCl.

**Scheme 3^a**

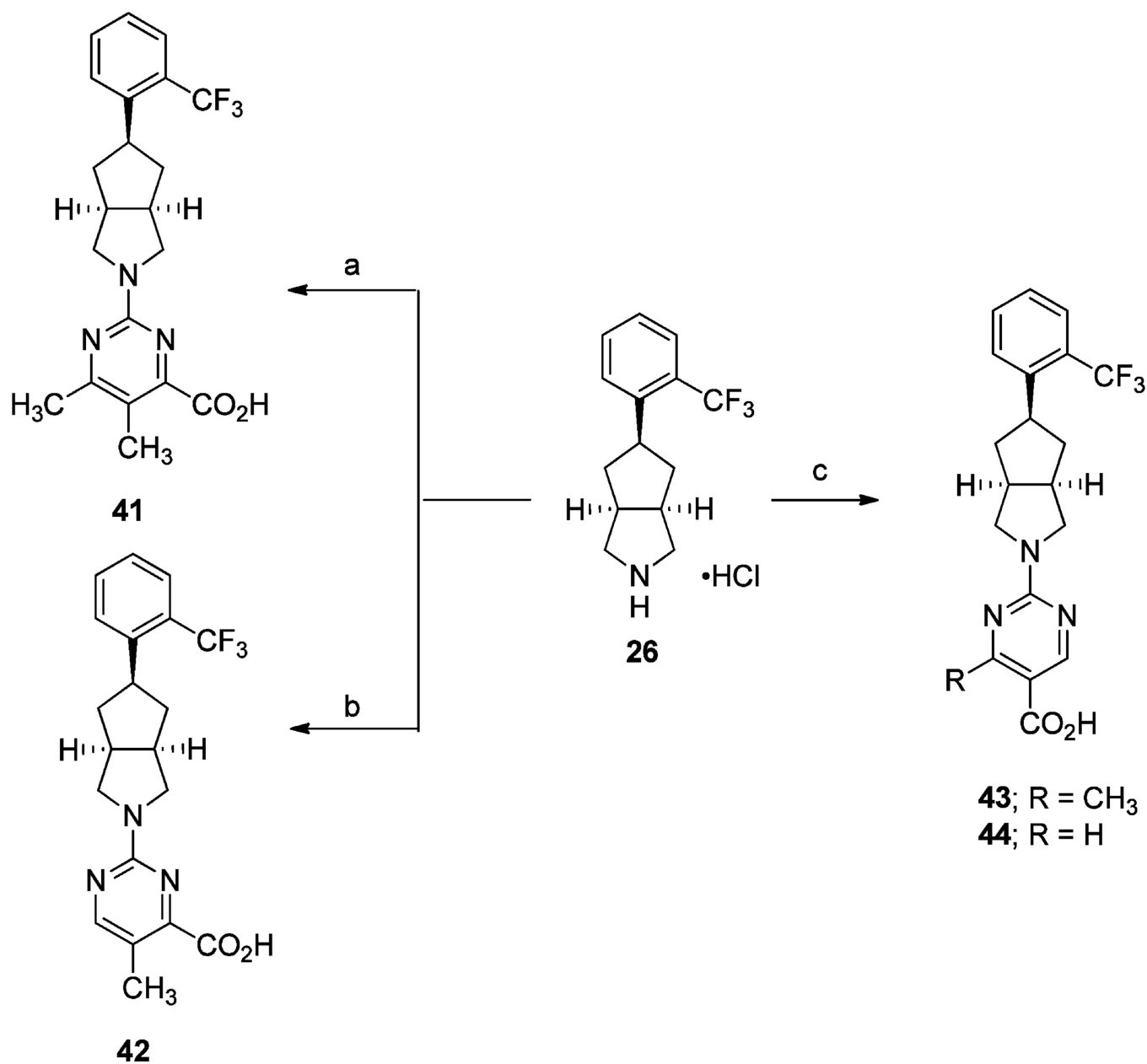
^aReagents and conditions: (a) (3*aR*,6*aS*)-*tert*-butyl hexahydropyrrolo[3,4-*c*]pyrrole-2(1*H*)-carboxylate, Pd(OAc)₂, BINAP, NaO*t*-Bu, toluene, 110 °C, 16 h; (b) 2.0 M HCl solution in Et₂O, CH₂Cl₂, rt, 3 h; (c) methyl 2-chloro-6-methylpyrimidine-4-carboxylate, *i*-Pr₂NEt, DMF, 60 °C, 16 h; (d) (i) LiOH·H₂O, H₂O, THF, rt, 16 h; (ii) 2 N aq HCl.

**Scheme 4^a**

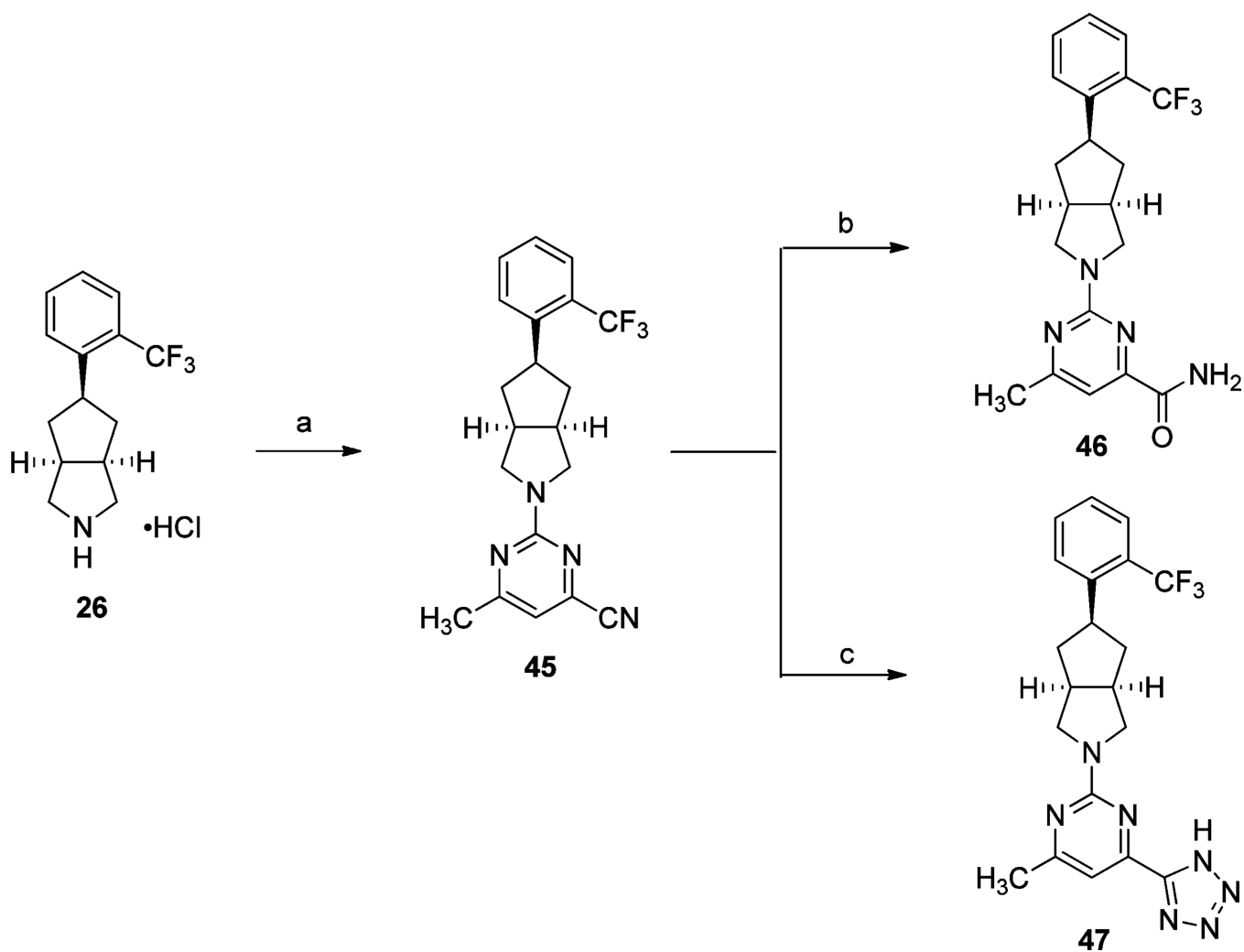
^aReagents and conditions: (a) (i) LiAlH₄ (1.0 M solution in THF), THF, 70 °C, 16 h; (ii) Boc₂O, CH₂Cl₂, rt, 16 h; (b) (i) NaIO₄, RuO₂·H₂O, CH₃CN, CCl₄, H₂O, rt, 24 h; (c) Ac₂O, NaOAc, 120 °C, 3 h; (d) (i) LiHMDS (1.0 M solution in THF), THF, -78 °C, 30 min; (ii), PhN(SO₂CF₃)₂, THF, -78 °C to rt, 3 h; (e) (2-(trifluoromethyl)phenyl)boronic acid, Pd(PPh₃)₄, 2 M Na₂CO₃, DME, 80 °C, 6 h; (f) H₂ (40 psi), 10% Pd/C, CH₃OH, rt, 16 h; (g) 2.0 M HCl in Et₂O, CH₂Cl₂, 0 °C to rt, 24 h; (h) 2-chloro-6-substitutedpyrimidine-4-carboxylic acid methyl ester, Et₃N, DMF, 60 °C, 16 h; (i) (i) 2 N aq NaOH, THF, CH₃OH, rt, 16 h; (ii) 2 N HCl.

**Scheme 5^a**

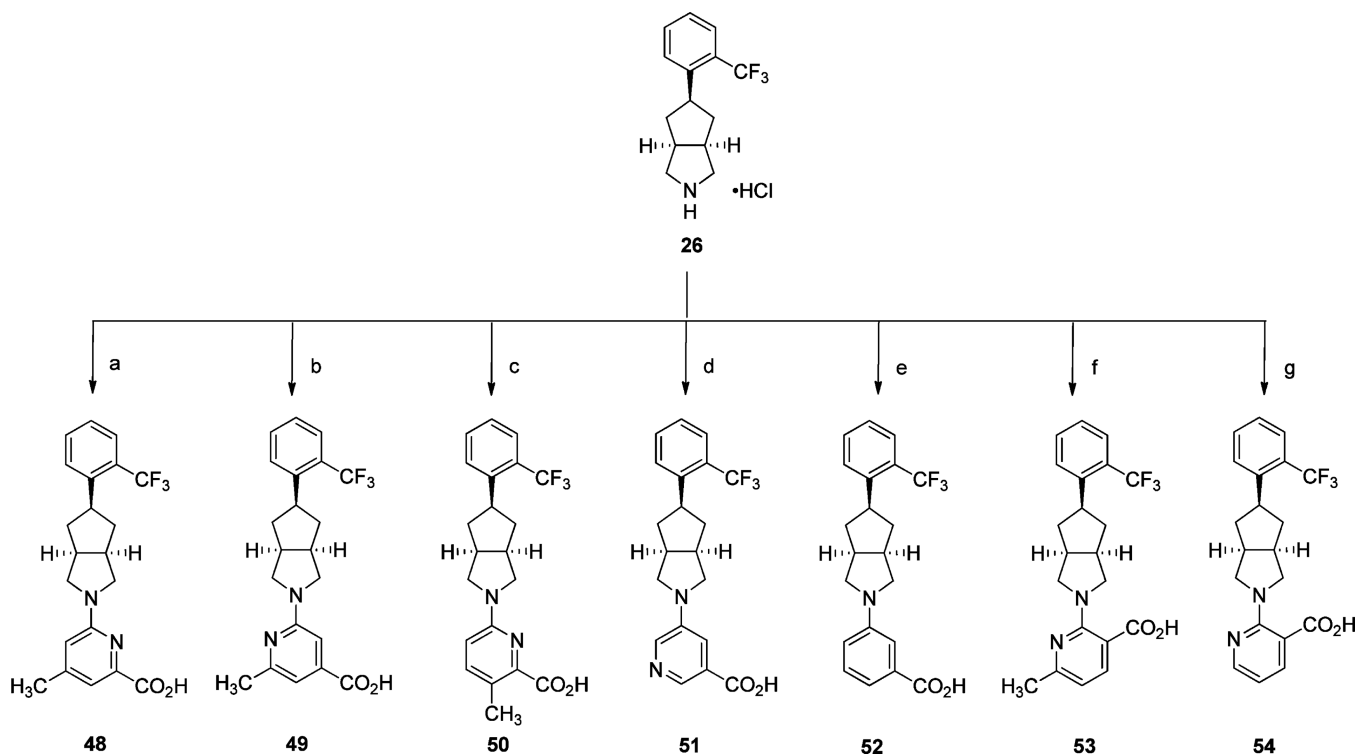
^aReagents and conditions: (a) TFA, CH₂Cl₂, rt, 3 h; (b) H₂ (50 psi), 10% Pd/C, CH₃OH, rt, 6 h; (c) (i) 2-chloro-6-methylpyrimidine-4-carboxylic acid, Et₃N, DMF, 60 °C, 16 h; (ii) 2 N aq NaOH, THF, CH₃OH, rt, 16 h; (iii) 2 N aq HCl.

**Scheme 6^a**

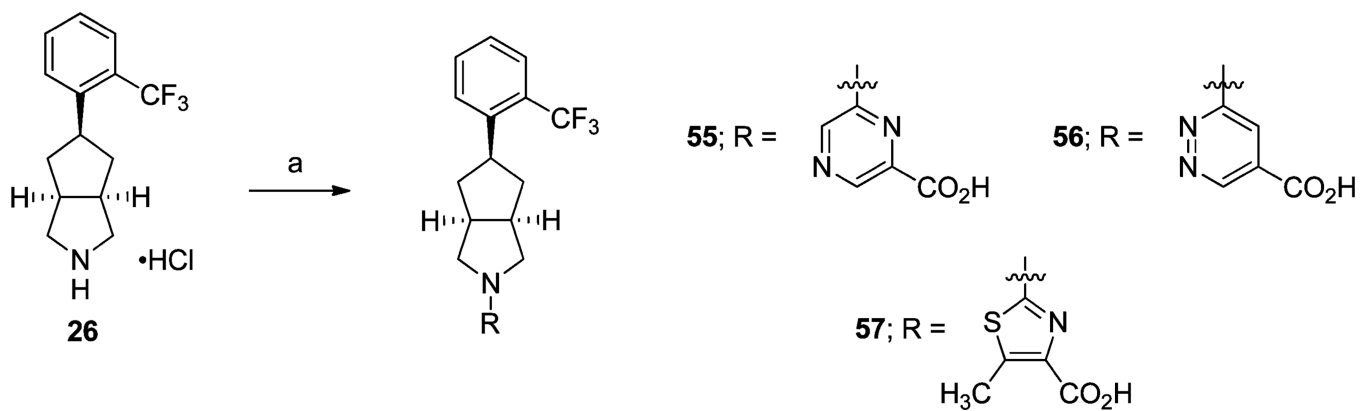
^aReagents and conditions: (a) (i) 2,4-dichloro-5,6-dimethylpyrimidine, Pd(OAc)₂, Cs₂CO₃, JohnPhos, toluene, reflux, 16 h; (ii) Mo(CO)₆, Pd(OAc)₂, BINAP, CH₃OH, CH₃CN, 80 °C, 16 h; (iii) LiOH·H₂O, THF, CH₃OH, H₂O, rt, 16 h; (b) (i) methyl 2-chloro-5-methylpyrimidine-4-carboxylate, Et₃N, DMF, 60 °C, 16 h; (ii) 2 N aq NaOH, THF, CH₃OH, rt, 16 h; (c) (i) methyl 2-chloro-4-methylpyrimidine-5-carboxylate or methyl 2-chloropyrimidine-5-carboxylate, *i*-Pr₂NEt, 70 °C (microwave irradiation), 1.5 h or Et₃N, DMF, 70 °C, 16 h; (ii) LiOH·H₂O, THF, H₂O, rt, 16 h or 2 N aq NaOH, THF, CH₃OH, rt, 16 h; (iii) 2 N aq HCl.

**Scheme 7^a**

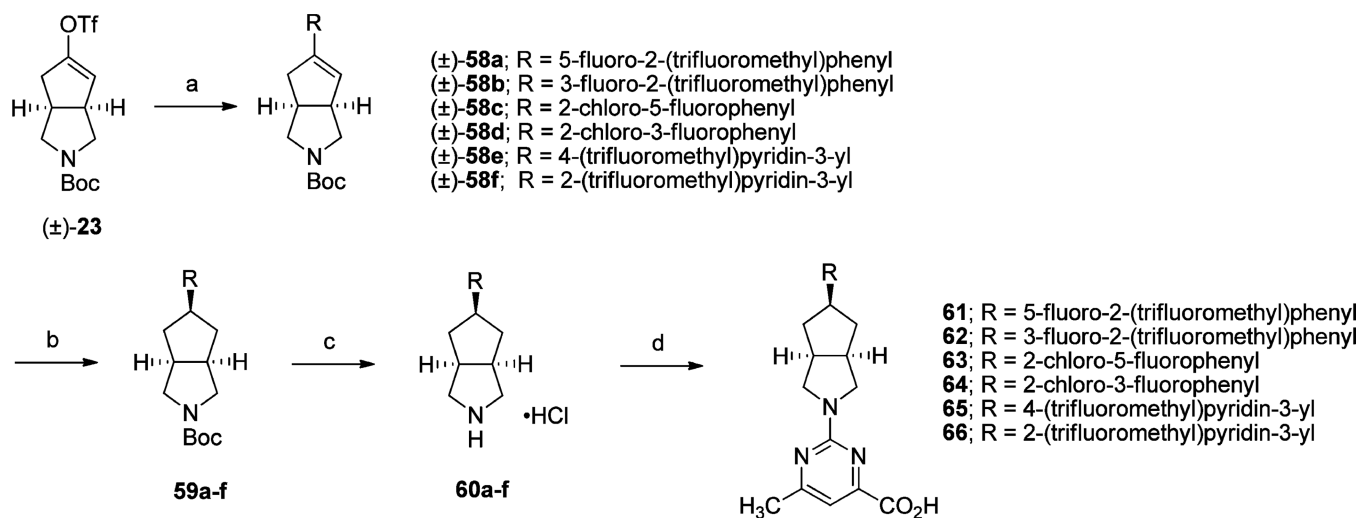
^aReagents and conditions: (a) (i) 2-chloro-6-methylpyrimidine-4-carbonitrile, *i*-Pr₂NEt, DMF, 60 °C, 16 h; (b) LiOH·H₂O, THF, H₂O, 70 °C, 18 h; (c) NaN₃, NH₄Cl, DMF, 130 °C (microwave irradiation), 1 h.

**Scheme 8^a**

^aReagents and conditions: (a) (i) methyl 6-chloro-4-methylpicolinate, Pd(OAc)₂, XantPhos, Cs₂CO₃, toluene, 110 °C, 16 h; (ii) 2 N aq NaOH, THF, CH₃OH, rt, 16 h; (iii) 2 N aq HCl; (b) (i) methyl 2-chloro-6-methylisonicotinate, Pd(OAc)₂, XantPhos, Cs₂CO₃, toluene, 110 °C, 16 h; (ii) 2 N aq NaOH, THF, CH₃OH, rt, 16 h; (iii) 2 N aq HCl; (c) (i) methyl 6-chloro-3-methylpicolinate, Pd(OAc)₂, JohnPhos, Cs₂CO₃, toluene, reflux, 14 h; (ii) LiOH·H₂O, THF, CH₃OH, H₂O, rt, 72 h; (iii) 2 N aq HCl; (d) (i) methyl 5-bromonicotinate, Pd₂(dba)₃, XantPhos, Cs₂CO₃, 1,4-dioxane, reflux, 16 h; (ii) LiOH·H₂O, THF, CH₃OH, H₂O, rt, 4 h; (iii) 2 N aq HCl; (e) methyl 3-bromobenzoate, Pd(OAc)₂, BINAP, NaO*t*-Bu, toluene, 110 °C, 16 h; (ii) LiOH·H₂O, THF, CH₃OH, H₂O, rt, 16 h; (iii) 2 N aq HCl; (f) (i) methyl 2-chloro-6-methylnicotinate, Pd₂(dba)₃, XantPhos, Cs₂CO₃, toluene, 100 °C, 16 h; (ii) LiOH·H₂O, THF, CH₃OH, H₂O, 50 °C, 30 min; (iii) 2 N aq HCl; (g) (i) methyl 2-chloronicotinate, Pd(OAc)₂, XantPhos, Cs₂CO₃, 1,4-dioxane, 110 °C, 16 h; (ii) LiOH·H₂O, THF, CH₃OH, H₂O, rt, 16 h; (iii) 2 N aq HCl.

**Scheme 9^a**

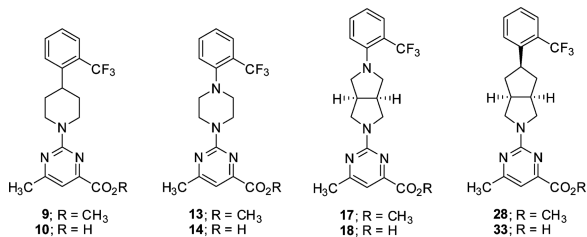
^aReagents and conditions: (a) (i) methyl 2-chloropyrazine-6-carboxylate or methyl 3-chloropyridazine-5-carboxylate or methyl 2-chloro-5-methylthiazole-4-carboxylate, Et₃N or *i*-Pr₂NEt, DMF, 60 °C, 16 h or *i*-Pr₂NEt, DMSO, 110 °C, 24 h; (ii) LiOH·H₂O, THF, CH₃OH, H₂O, rt, 30 min-16 h; (iii) 2 N aq HCl.

**Scheme 10^a**

^aReagents and conditions: (a) (i) substituted phenyl or pyridyl boronic acid, Pd(PPh₃)₄, 2.0 M Na₂CO₃, DME, 80 °C, 6 h; (b) H₂ (40 psi), 10% Pd/C, CH₃OH, rt, 16 h; (c) 2.0 M HCl in Et₂O, CH₂Cl₂, 0 °C to rt, 24 h; (d) (i) methyl 2-chloro-6-methylpyrimidine-4-carboxylate, Et₃N, DMF, 60 °C, 16 h; (ii) 2 N aq NaOH, THF, CH₃OH, rt, 16 h; (iii) 2 N aq HCl.

Table 1

RBP4 SPA Binding Affinity, RBP4 HTRF, and Liver Microsomal Stability Data for 6-Methylpyrimidine-4-carboxylic Acid and Methyl Ester Analogues



compd	RBP4 SPA ^a IC ₅₀ (nM) ^c	RBP4 HTRF ^b IC ₅₀ (nM) ^c	microsomal stability (% remaining)	
			HLM ^d	RLM ^e
3	15.0 ± 0.005	122 ± 0.035	3	85
4	72.7	294	100	75
9	4.1	132	ND	ND
10	35.3	188	68	96
13	9.7	1402	0.0	0.0
14	89.5	511	18	63
17	3.9	74.0	ND	ND
18	57.4	140	80	76
28	6.3	100	0.2	9.8
33	12.8 ± 0.4	43.6 ± 10.5	94	93

^aIC₅₀ values for the SPA assay obtained in the presence of a fixed, 10 nM concentration of ³H-retinol.

^bIC₅₀ values for the HTRF assay obtained in the presence of 1 μM concentration of retinol.

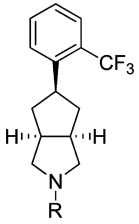
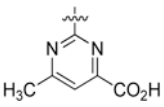
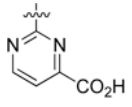
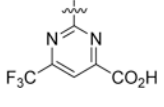
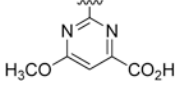
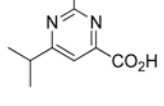
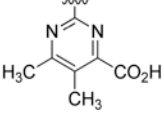
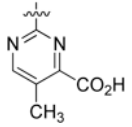
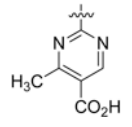
^cFor compounds tested multiple times (more than twice), the IC₅₀ data are represented as the mean ± standard deviation. For those compounds that were only tested twice, the IC₅₀ data are shown as the mean of two independent experiments and not as the mean ± standard deviation.

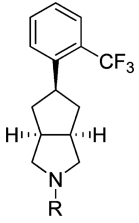
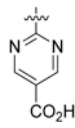
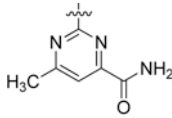
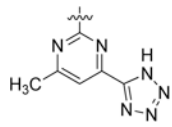
^dHLM = human liver microsomes.

^eRLM = rat liver microsomes. Compound concentration was 10 μM, and incubation time with either human or rat microsomes was 30 min. ND = not determined.

Table 2

RBP4 SPA Binding Affinity and RBP4 HTRF for Pyrimidine Carboxylic Acid Analogues

			
Compound	R	RBP4 SPA ^a IC ₅₀ (nM) ^c	RBP4 HTRF ^b IC ₅₀ (nM) ^c
33		12.8 ± 0.4	43.6 ± 10.5
32		20.8 ± 0.5	79.7
34		9.6	88.0
35		12.8 ± 1.6	81.2 ± 7.6
36		153 ± 0.6	202
41		48.8	123
42		90.1	595
43		40.8	523

			
Compound	R	RBP4 SPA ^a IC ₅₀ (nM) ^c	RBP4 HTRF ^b IC ₅₀ (nM) ^c
44		171	1864
46		3.3	248
47		7.5	175

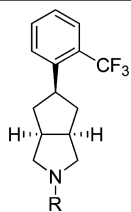
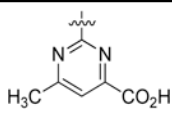
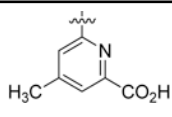
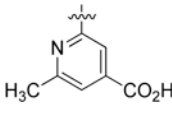
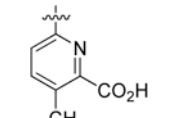
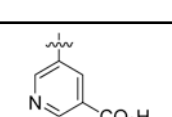
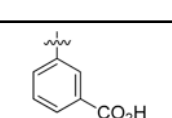
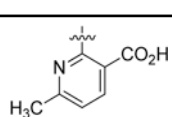
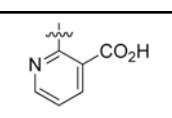
^aIC₅₀ values for the SPA assay obtained in the presence of a fixed, 10 nM concentration of ³H-retinol.

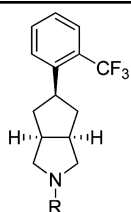
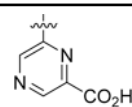
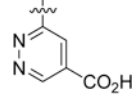
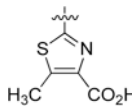
^bIC₅₀ values for the HTRF assay obtained in the presence of 1 μM concentration of retinol.

^cFor compounds tested multiple times (more than twice), the IC₅₀ data are represented as the mean ± standard deviation. For those compounds that were only tested twice, the IC₅₀ data are shown as the mean of two independent experiments and not as the mean ± standard deviation.

Table 3

RBP4 SPA Binding Affinity and RBP4 HTRF for Pyridine and Other Heteroaromatic Carboxylic Acid Analogues

			
Compound	R	RBP4 SPA ^a IC ₅₀ (nM) ^c	RBP4 HTRF ^b IC ₅₀ (nM) ^c
33		12.8 ± 0.4	43.6 ± 10.5
48		14.1	295
49		53.3	228
50		584	4908
51		>3000	ND
52		83.2	3956
53		68.4	2005
54		43.8	381

			
Compound	R	RBP4 SPA ^a IC ₅₀ (nM) ^c	RBP4 HTRF ^b IC ₅₀ (nM) ^c
55		166	ND
56		23.0	437
57		29.3	495

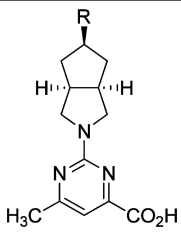
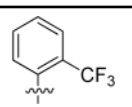
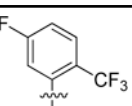
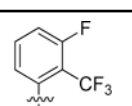
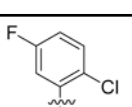
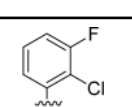
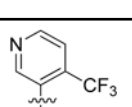
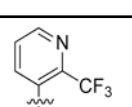
^aIC₅₀ values for the SPA assay obtained in the presence of a fixed, 10 nM concentration of ³H-retinol.

^bIC₅₀ values for the HTRF assay obtained in the presence of 1 μM concentration of retinol.

^cFor compounds tested multiple times (more than twice), the IC₅₀ data are represented as the mean ± standard deviation. For those compounds that were only tested twice, the IC₅₀ data are shown as the mean of two independent experiments and not as the mean ± standard deviation. ND = not determined.

Table 4

RBP4 SPA Binding Affinity and RBP4 HTRF for Pyridine and Other Heteroaromatic Carboxylic Acid Analogues

			
Compound	R	RBP4 SPA ^a IC ₅₀ (nM) ^c	RBP4 HTRF ^b IC ₅₀ (nM) ^c
33		12.8 ± 0.4	43.6 ± 10.5
61		46.3 ± 1.1	33.4 ± 1.8
62		196	ND
63		532 ± 198	347
64		137	504
65		51.8 ± 1.5	821 ± 142
66		31.1 ± 1.9	719 ± 22.4

^aIC₅₀ values for the SPA assay obtained in the presence of a fixed, 10 nM concentration of ³H-retinol.

^bIC₅₀ values for the HTRF assay obtained in the presence of 1 μM concentration of retinol.

^cFor compounds tested multiple times (more than twice), the IC₅₀ data are represented as the mean ± standard deviation. For those compounds that were only tested twice, the IC₅₀ data are shown as the mean of two independent experiments and not as the mean ± standard deviation. ND = not determined.

Table 5

In Vitro ADMET Profile for 33

solubility ^a	hepatic CL _{int} (μL/mL/min) ^b			cyno	CYP inhibition (IC ₅₀) 2C9, 2C19, 2D6, 3A4	hERG ^c (IC ₅₀)	% PPB ^d			MDCK-MDR1 permeability P _{app} (×10 ⁻⁶ cm/s)			class
	H	R	M				H	R	A-B	B-A			
>100 μM	<0.7	<0.7	<0.7	0.7	All >34 μM	>30 μM	99.9	99.4	74.7	82.2	82.2	high permeability	

^aKinetic solubility measured in PBS (pH 7.4).

^bHepatic intrinsic clearance; H = human; R = rat; M = mouse; cyno = cynomolgus monkey.

^c'Patch-Xpress' patch-clamp assay; compounds were tested (*n* = 3) in a five-point concentration-response on HE293 cells stably expressing the hERG channel.

^d% PPB = plasma protein binding.

Table 6

In Vivo PK Data for Analogue 33 Following IV and PO Administration in Rats^a

route	dose (μmol/kg)	C ₀ ^b (μM)	CL ^c (mL/h/kg)	t _{1/2} ^d (h)	V _{ss} ^e (mL/kg)	AUC _{last} ^f (μM·h)	AUC _{INF} ^g (μM·h)	%F ⁱ
IV	5.1	58.6 (1.8)	5.06 (0.49)	22.0 (3.0)	156 (9.0)	795 (48)	1017 (93)	NA
route	dose (μmol/kg)	C _{max} ^h (μM)	T _{max} ^h (h)	t _{1/2} ^d (h)	V _{ss} ^e (mL/kg)	AUC _{last} ^f (μM·h)	AUC _{INF} ^g (μM·h)	%F ⁱ
PO	12.7	62.2 (4.3)	2.67 (1.15)	38.8 (17.3)	NA	2011 (326)	3636 (1588)	143 (62.4)

^aData are represented as the mean with standard deviation in parentheses (mean (SD)). Dosing groups consisted of three drug naive adult male Sprague-Dawley rats. IV administration: the test article was administered at the 5.1 μmol/kg (2 mg/kg) dose; test article vehicle = 3% DMA/45% PEG300/12% EtOH/40% sterile H₂O; PO administration, test article was administered at the 12.7 μmol/kg (5 mg/kg) dose; vehicle = 2% Tween 80 in 0.9% saline. Bioavailability; $F = (\text{AUC}_{\text{INF}}^{\text{po}} \times \text{dose}_{\text{iv}}) \div \text{AUC}_{\text{INF}}^{\text{iv}} \times \text{dose}_{\text{po}}$.

^bObserved initial concentration of compound in plasma at time zero.

^cTotal body clearance.

^dApparent half-life of the terminal phase of elimination of the compound from plasma.

^eVolume of distribution at steady state.

^fArea under the plasma concentration versus time curve from 0 to the last time point that the compound was quantifiable in plasma.

^gArea under the plasma concentration versus time curve from 0 to infinity.

^hMaximum observed concentration of the compound in plasma.

ⁱTime of maximum observed concentration of the compound in plasma.